

ON THE USE OF TIME-DEPENDENT THROUGHFALL
CHEMISTRY DATA TO CALCULATE THE
DRY DEPOSITION FLUX

By

YUH-LING CHEN

Bachelor of Science
National Cheng-Kung University
Tainan, Taiwan
1980

Master of Science
University of Iowa
Iowa City, Iowa
1984

Submitted to the Faculty of the
Graduate College of the
Oklahoma State University
in Partial Fulfillment of
the requirements for
the Degree of
DOCTOR OF PHILOSOPHY
December, 1988

Thesis
1988D
C51850
cop. 2

ON THE USE OF TIME-DEPENDENT THROUGHFALL
CHEMISTRY DATA TO CALCULATE THE
DRY DEPOSITION FLUX

Thesis Approved:

Arund H. Johannes

Thesis Adviser

Eric M. Miller

Ruth C. Star

Darryl L. Fatch

Norman N. Durham

Dean of the Graduate College

ACKNOWLEDGMENTS

I would like to thank Professor Arland H. Johannes, my thesis adviser, for his continued support, patience and invaluable assistance throughout this study. The guidance he gave me during my stay at Oklahoma State University was always a valuable source of motivation.

Appreciation is expressed to Professor Gary L. Foutch, Professor Ruth C. Erbar and Professor Edwin L. Miller for their valuable discussions on every aspect of this research and for serving as members of the advisory committee.

I would also like to thank my friends in Chinese Bible Study, for their prayers for me during the frustrating days of this study.

Special thanks are extended to Johnny Huang, for his support, encouragement and understanding throughout my work.

Foremost, I would like to express my deepest gratitude to my parents, brother and sister for their love, encouragement and financial support which made the present study possible.

Finally, I must also give thanks to God for His sustaining power and grace manifested to me throughout this work.

TABLE OF CONTENTS

Chapter	Page
I. INTRODUCTION	1
Wet and Dry Deposition	2
Throughfall and Stemflow	3
Study Objective	7
II. LITERATURE REVIEW	9
Dry Deposition	9
Throughfall	17
Direct Approach	19
Indirect Approach	20
III. EXPERIMENTAL ANALYSIS	24
Description of the Tree	24
Description of Precipitation Network	26
Equipment Location	26
Equipment Description	26
Sampling Procedure	29
Data Analysis Procedure	32
IV. CONCEPTUALIZATION AND CONSTRUCTION OF THE MIXING MODEL	44
Conceptualization of the Model	44
Construction of the Model	52
Implementation	60
V. RESULTS AND DISCUSSIONS OF MIXING MODEL	61
Quality Control of Data	61
American Beech	61
Red Spruce	84
Performance of the Mixing Model	103
American Beech	104
Red Spruce	106
VI. DISSOLUTION OF DRY DEPOSITION	108
Formulation of the Problem	109
Method of Solution	116
Solution Procedures	118

Chapter	Page
Program Description	122
VII. RESULTS AND DISCUSSIONS OF DISSOLUTION MODEL	124
Model Verification	124
Results and Discussion	128
One Component System	128
Two Components System	133
Three Components System	136
Four Components System	140
VIII. SUMMARY AND RECOMMENDATIONS	147
BIBLIOGRAPHY	153
APPENDIX A - EXPERIMENTAL DATA	162
APPENDIX B - PROGRAM LISTING FOR MIXING MODEL	169
APPENDIX C - ERROR ANALYSIS OF EXPERIMENTAL DATA	186
APPENDIX D - MATHEMATICAL DERIVATION OF EQUATION (6.18) TO (6.20)	189
APPENDIX E - PROGRAM LISTING FOR DISSOLUTION MODEL	192

LIST OF TABLES

Table		Page
/ I.	Physical Characteristics of Tree Used	25
2 II.	Regression Parameters Used to Predict Canopy Characteristics	27
3 III.	Location of the Collectors	28
4 IV.	The Relationship Between Throughfall and Wetfall Volume (American Beech)	47
5 V.	Leaching Coefficients Obtained from Black Box Model (American Beech)	50
6 VI.	Material Balance for Event 1,2, and 7 without Leaching and Dry Deposition (American Beech)	63
7 VII.	Concentrations Versus Time for Event 2 without Dry Deposition and Leaching (American Beech)	68
8 VIII.	Leaching Coefficients Used in the Mixing Model (American Beech)	74
9 IX.	Throughfall Concentrations Versus Time in Event 2 with Dry Deposition and Leaching Coefficients (American Beech)	77
10 X.	Final Material Balance for Event 2 with Leaching and Dry Deposition (American Beech)	79
11 XI.	Material Balance for Event 2 without Leaching and Dry Deposition (Red Spruce)	85
12 XII.	Concentration Versus Time for Event 2 without Dry Deposition and Leaching (Red Spruce) ...	89
13 XIII.	Throughfall Concentration Versus Time in Event 2 with Dry Deposition and Leaching Coefficients (Red Spruce)	94
14 XIV.	Leaching Coefficients Used in the Mixing Model (Red Spruce)	96
15 XV.	Throughfall Concentrations Versus Time in Event 2 with Dry Deposition and Leaching Coefficients (Red Spruce)	100

Table	Page
16 XVI.	Final Material Balance for Event 2 with Dry Deposition (Red Spruce) 102
17 XVII.	Evaluation of Mixing Model for Throughfall Volume and Concentration of Ions (Event 2) .. 105
18 XVIII.	Parameters Used in the Dissolution Model 129
19 XIX.	Sulfate Replicate Analyses 186
20 XX.	Sulfate Analyses of EPA Laboratory-Prepared Standard Solutions 187
21 XXI.	Analytical Results for Laboratory-Prepared Standards and U.S. EPA Unknown Samples 188

LIST OF FIGURES

Figure	Page
1. Non-Winter Throughfall Collector	30
2. Volume Distribution in Event 1	33
3. Concentration Distribution for Sulfate Ion in Event 1	34
4. Concentration Distribution for Ammonium Ion in Event 1	35
5. Concentration Distribution for Potassium Ion in Event 1	36
6. Mass for Sulfate Ion in Event 1	37
7. Mass for Ammonium Ion in Event 1	38
8. Mass for Potassium Ion in Event 1	39
9. Cumulative Mass for Sulfate Ion in Event 1	40
10. Cumulative Mass for Ammonium Ion in Event 1	41
11. Cumulative Mass for Potassium Ion in Event 1 ...	42
12. The Relationship Between Throughfall and Wetfall Volume (American Beech)	46
13. Model Conceptualization	51
14. Flow Diagram for Mixing Model	53
15. Flow Diagram of Subroutine CHECK	57
16. Predicted and Measured Throughfall Volume in Event 2 (American Beech)	64
17. Concentration Distribution of Sulfate Ion in Event 2 (American Beech)	65
18. Concentration Distribution of Ammonium Ion in Event 2 (American Beech)	66

Figure	Page
19. Concentration Distribution of Potassium Ion in Event 2 (American Beech)	67
20. Concentration Distribution of Sulfate Ion in Event 2 with Dry Deposition (American Beech)	71
21. Concentration Distribution of Ammonium Ion in Event 2 with Dry Deposition (American Beech)	72
22. Concentration Distribution of Potassium Ion in Event 2 with Dry Deposition (American Beech) ..	73
23. Concentration Distribution of Potassium Ion in Event 2 with Dry Deposition and Leaching (American Beech)	75
24. The Throughfall Concentration of Sulfate Ion in Event 1 (American Beech)	80
25. The Throughfall Concentration of Potassium Ion in Event 1 (American Beech)	81
26. Throughfall Concentration of Potassium Ion in Event 7 (American Beech)	82
27. Throughfall Concentration of Sulfate Ion in Event 7 (American Beech)	83
28. Predicted and Measured Throughfall Volume in Event 2 (Red Spruce)	86
29. Throughfall Concentrations of Sulfate Ion in Event 2 (Red Spruce)	87
30. Throughfall Concentrations of Potassium Ion in Event 2 (Red Spruce)	88
31. Throughfall Concentration of Sulfate Ion in Event 2 with Dry Deposition and Leaching (Red Spruce)	92
32. Throughfall Concentration of Potassium Ion in Event 2 with Dry Deposition and Leaching (Red Spruce)	93
33. Throughfall Concentration of Sulfate Ion in Event 2 with Dry Deposition and Leaching (Red Spruce)	97
34. Throughfall Concentration of Potassium Ion in Event 2 with Dry Deposition and Leaching (Red Spruce)	98
35. Solid Dissolution into a Falling Liquid Film, with Fully Developed Velocity Profile	110

Figure	Page
36. Boundary Position in 2-Component Dissolution Process for Different Combinations of Solubilities and Diffusivity Parameters	125
37. Mass Fraction in 2-Components Dissolution Process for Different Combinations of Solubilities and Diffusivity Parameters	126
38. Dissolution of 2 Components for Differing Solubilities but Constant Premeabilities	127
39. Boundary Position for Single Component Dissolution	130
40. Effluent Concentration Profile at Different Location of y for Single Component Dissolution	.132
41. Mass Fraction for Two Components Dissolution	134
42. Effluent Concentration Profile for Two Components Dissolution	135
43. Mass Fraction for Three Components Dissolution ...	137
44. Concentration Distribution for Three Components Dissolution	138
45. Boundary Position Versus Time for One, Two and Three Components Cases	139
46. Boundary Position Versus Time for Four Components with Different Initial Mass Fraction	141
47. Variation of Mass Fraction Versus Time for Four Components Dissolution	142
48. Variation of Mass Fraction Versus Time for Four Components Dissolution	143
49. Effluent Concentration Profile for Four Components Dissolution	145

LIST OF SYMBOLS

a	thickness of the liquid film, Eq. (6.4)
ACR	anion/cation ratio, $\mu\text{eq}/\mu\text{eq}$
b_1, b_2	intercept of the Eqs. (4.1) and (4.2), liter
B_1	dimensionless variable, Eq. (6.10g)
BAI	branch area index, m^2/m^2
C	air concentration, Eq. (2.2)
C_i	concentration for the i th species in the liquid, $\mu\text{eq}/\text{l}$
\bar{C}_i	dimensionless concentration of the species i in the liquid, Eq. (6.10f)
C_{i1}	inlet wetfall concentration, Eq. (6.3)
d	diameter of the particle, μm
D_{bucket}	diameter of the collection bucket, 28.6 cm
D_{funnel}	diameter of the funnel, 19 cm
D_i	diffusivity of the i th component, Eq. (6.1), cm^2/sec
DBH	diameter at breast height, m
DC_i	concentration of the dry deposition flux for the i th ion, $\mu\text{eq}/\text{l}$
DD_i	dry deposition flux for the i th ion, μeq
DR	dilution ratio, DR = 4 in this study
ϵ_i	relative error, Eq. (5.5)
ϵ_m	mean relative error
F	dry deposition flux, Eq. (2.2)
F_c	time average vertical flux, Eq. (2.1)

f_1	dimensionless variable of diffusivity parameter, Eq. (6.10b)
g_1	mass fraction of component i in the solid layer
g_{10}	initial mass fraction, Eq. (6.9)
H_1	parameter characterizing the solubility of component 1
HOLDUP	holdup volume of the tree, liters
L	simulation distance in Z-direction, length
LAI	leaf area index, m^2/m^2
m	slope of Eq. (4.3)
N	number of tanks
$N_1(T)$	dimensionless variable, Eq. (6.10h)
O_1	observed value, Eq. (5.3)
O_m	mean observed value, Eq. (5.3)
P_1	predicted value from model, Eq. (5.2)
P_m	mean predicted value, Eq. (5.2)
r	correlation coefficient, Eq. (5.1)
R	dimensionless variable of $s(t)$, Eq. (6.10d)
R_a	aerodynamic resistance to mass transfer, Eq. (2.3)
R_b	diffusive boundary layer resistance to mass transfer, Eq. (2.3)
R_c	canopy resistance, Eq. (2.3)
R_t	total resistance to mass transfer, Eq. (2.3)
S_0	initial thickness of solid layer, Eq. (6.9)
$s(t)$	interface position at time= t
t	time variable, minutes
T	dimensionless variable of time, Eq. (6.10a)
t_c	time required for complete dissolution, minutes

V_d	deposition velocity, cm/sec, Eq. (2.4)
V_z	volume flux of rainwater in Z-direction, Eq. (6.1)
w	vertical wind speed, Eq. (2.1)
x, z	space variable
X, Z	dimensionless variables of x and z , respectively. Eq. (6.10c) and Eq. (6.10e)
y	transformation coordinate, Eq. (6.17)
ρ_a	air density, g/cm ³
ρ_s	mass density of solid phase, g/cm ³
ϵ_1	relative error, Eq. (5.5)
ϵ_m	mean relative error

CHAPTER I

INTRODUCTION

Acid rain has become an environmental concern of global importance within the last decade. This concern is well documented in terms of lake acidification and resulting fish mortality in the eastern portion of North America and Europe. Deterioration of building materials, along with damage to forests, have also been noted (Drablos and Tollan, 1980; Hutchinson and Havas, 1980; Johnson et al., 1982; Likens and Bormann, 1974; Linthurst, 1984; National Research Council of Canada, 1981; Overrein et al., 1980). This incidence and severity of acid precipitation has increased significantly within the last twenty-five years.

Acid precipitation is associated with emission of oxides of sulfur and nitrogen, and gaseous hydrogen chloride resulting from the combustion of fossil fuels (Gorham, 1981). These air pollutants may remain in the atmosphere for several days, during which they may transport large distances, before being deposited on water or land surfaces (OECD, 1977).

Wet and Dry Deposition

Atmospheric pollutants are returned to the earth's surface through wet or dry deposition. The term wet deposition encompasses all processes by which atmospheric pollutants are transported to the earth's surface in one of the many forms of precipitation: rain, snow, fog, etc. Wet deposition, therefore, involves attachment of pollutants to atmospheric water and includes chemical reactions in the aqueous phase as well as the precipitation process itself. Ionic compounds such as H_3O^+ , SO_4^{2-} , NO_3^- , Cl^- , NH_4^+ , Na^+ , and K^+ occur in varying concentrations depending on time of the year, type of precipitation, type of storm event and the geographical location. Moreover, the concentrations and precipitation amounts, within geographic regions, vary temporally and spatially. The collection and measurement of wet deposition is accurate and reliable, even with all these complications, in large field studies.

Dry deposition is conveniently defined as the aerodynamic transfer of trace gases and aerosols from the air to the surface, and the gravitational settling of particles. The processes depend on concentrations of the pollutants, small-scale meteorological effects near the surface, as well as on the characteristics of the receiving surface. Usually dry deposition includes three subcomponents: dry fallout, large particles ($d > 2 \mu\text{m}$) that are affected mainly by gravity; impacted aerosols, small particles ($d < 2 \mu\text{m}$) that are removed from the atmosphere by

inertial impaction, interception or diffusion; gaseous deposition, gases or vapors, which are transported to a surface and adsorbed or absorbed. In the context of acid deposition assessment, dry deposition is generally acknowledged to be about as significant as wet deposition (Galloway et al., 1980) primarily as a consequence of efficient transfer of trace gases to transpiring foliage (Hicks, 1986).

Throughfall and Stemflow

Water falling on the forest is called incident precipitation. Precipitation which passes through the canopy and falls to the ground is called throughfall. An additional portion of precipitation reaches the ground by running down the branches and trunk. This portion is called stemflow. The sum of throughfall and stemflow is called net precipitation or net rainfall (Zinke, 1966). Incident precipitation that does not appear on the forest floor by either of these routes is called interception loss (Kittredge, 1948). While incident precipitation is the largest nutrient input to many forests, throughfall and stemflow fluxes are important flux pathways in the internal nutrient dynamics of forest.

The quality of precipitation falling on forests is altered during a brief but significant interaction with the surfaces of plants, resulting in the transfer of additional mineral matter to the forest (Eaton et al., 1973). These

alterations in nutrient concentrations involve numerous processes and combined materials originating both within and outside of the forest ecosystems (Tamm, 1951). It is known that at least four distinct processes are capable of changing concentrations and amounts of precipitation. These are: (i) evaporation of intercepted water; (ii) washing, by precipitation, of deposits accumulated upon the canopy between events; (iii) leaching of material from internal plant tissues; and (iv) uptake, sorption or permanent attachment of solutes, gases or particles by foliage (Clesceri and Vasudevan, 1980; Cronan and Reiners, 1983; Eaton et al., 1978; Fowler, 1980; Hoffman et al., 1980).

Although the potential contributions of a given process to throughfall quality is described by Parker (1983), controversy still exists as to which mechanism is dominant and whether competing mechanisms exist for different chemical species.

Stemflow transports a smaller amount of material to the forest floor than throughfall (Cole et al. 1967). Elemental concentrations in stemflow are distinctly higher than those of throughfall (Iwatsubo and Tautsumi, 1967), by up to an order of magnitude. Stemflow has a pH characteristically much lower than that of throughfall (Mahendrappa, 1974) and has high concentrations of Ca, K, S, and Mg and of particulate organic matter (Mina, 1967; Mahendrappa, 1974).

To evaluate the effects of the deposition of acidifying

substances to the ecosystem the atmospheric input must be known qualitatively and quantitatively, together with the pathways by which the deposition takes place. It has been long recognized that chemical change in throughfall is a mixture of at least two major processes: washoff of deposited particles and gases (dry deposition) as well as uptake and release of substances by the plants. As neither dry deposition nor canopy exchange is easily quantified, separating their respective contributions to total chemical deposition in throughfall is difficult.

However, several attempts have been made. Direct methods for separating the leaching and dry-deposition usually involve the collection of bulk precipitation under an inert surface to imitate the canopy (Hoffman et al. 1980; Lindberg et al. 1986; White and Turner, 1970). In these cases, actual rainwater impinges on the 'canopy'. Occasionally, such inert surfaces are exposed to dry deposition, retrieved and washed in the laboratory. In any case, the materials mobilized from such surfaces estimate the washoff contribution to net throughfall. The remaining portion is taken as the amount due to canopy leaching. Such methods suffer from the uncertainty in relating deposition on an artificial collector to that on natural vegetation.

Another approach involves the controlled washing of plant parts (Dasch, 1986; Lindberg and Lovett, 1983; Sickles et al. 1983). Leaf washing is common in tracer experiments estimating the portion of known deposition which cannot be

mobilized by water.

Recently, the deposition of different air pollutants was estimated by sampling and analyzing the throughfall beneath the tree canopy (Eaton et al., 1973; Hoffman et al., 1980; Lindberg et al., 1979; Lovett and Lindberg, 1984; Miller et al., 1976). Miller et al. (1976) used the intercept of the regression of bulk incident deposition on bulk throughfall as an estimate of canopy exchange of K, Ca, Mg and Na. Lakhani and Miller (1980) used a more complicated regression approach. This resulted in an intercept term representing the mean value of canopy exchange for the collection periods, 28 days in their case.

Event throughfall data while providing information about net changes, masks details on the initial portion of an event where washoff of dry deposition is most likely to have the greatest effect. A multiple regression analysis to single-event sample of throughfall to separate the contributions of dry deposition and canopy exchange has been made (Lovett and Lindberg, 1984). It is found that the sources of ions in throughfall vary considerably between chemical species. They also concluded that in the cases of SO_4^{2-} and NO_3^- , throughfall was dominated by wet deposition. Potassium in the throughfall was dominated by canopy exchange, while calcium was dominated by dry deposition. As a method for measuring dry deposition, this technique avoids the expensive equipment and strict site limitations characteristic of micrometeorological methods.

It also gives a clearer indication of deposition to the entire canopy than do artificial surface methods.

In spite of the large amount of research work has been done, however, little work has been done to determine the fate of dry deposition mass in trees and to model its movement in the water-tree system. The objectives of this research is to develop a mathematical model that can reasonably represent the dry deposited material transport process and predict throughfall concentration profile as a function of time and space.

Study Objectives

The purpose of this study is to estimate the spatial and temporal variation of throughfall concentrations for determining the impact of dry deposition. The objectives are as follow:

1. to develop a mixing model based on the time-averaged field data.
2. to develop a dissolution model which can simulate the canopy response at the beginning of the rainfall event. A second-order partial differential equation together with a set of boundary and initial conditions to describe the transport phenomenon is constructed. Finite difference methods are derived to solve the mathematical equations. The system of difference equations is solved on an IBM-3081 computer based on a simplified Gaussian elimination technique for tridiagonal matrices. It is

hoped that examining this dissolution process in detail will lead to a better understanding of dry deposition effects on acid precipitation.

CHAPTER II

LITERATURE REVIEW

Dry Deposition

Dry deposition, which combines all the input processes between storms, is an important mechanism for the removal of certain reactive gases and large particles from the atmosphere (Droppo, 1979). The process of dry deposition is mainly determined by the two mechanisms. First, the aerosols transport from the free atmosphere to the laminar boundary layer of air close to surfaces of objects. Second, the gases or particles transport through this layer by Brownian diffusion and/or sedimentation are adsorbed, captured or otherwise entrained by the surface (Droppo, 1976).

As a consequence of these complex processes and the variety of possible interactions among them, the rate of transfer of pollutants between the air and exposed surfaces is controlled by a wide range of chemical, physical and biological factors. Presently, the existing abilities to study the effects of dry deposition are limited.

A great variety of experimental methods has been used to obtain data on dry deposition. These range from studies of the rate of accumulation on natural surfaces

(Lindberg and Lovett, 1985), to studies of deposition to surrogate surfaces (Davidson et al, 1985) and to a wide range of methods that derive the surface flux from measurements made elsewhere (Hicks, 1984; Hicks et al. 1986; Mayer and Ulrich, 1978, 1980).

All of the many available methods have special characteristics that make them especially attractive in some circumstances. Collecting vessels, for example, have been used to investigate deposition of atmospheric particulate pollutants during the 1950's and early 1960's. Experience obtained in studies of radioactive fallout suggested that such wet/dry samplers yielded results which agreed with known inputs and measured atmospheric inventories. However, exploratory application to these technique to non-radiative particulate pollutants has severe limitations due to contamination by birds, wind-blown dusts, etc (Feely et al, 1985).

Such wet/dry collectors are but one of many forms of artificial collection devices used to measure the deposition of atmospheric particles. Flat plates and shallow pans of various configurations are presently in use in monitoring program (Sickles et al., 1983).

In 1983, Dasch presented comparisons between deposition data obtained using several different surrogate surfaces, mounted with both upward- and downward-facing exposures. The results indicate that gravitation settling was the most important removal mechanism to most surfaces. It also

showed there is a large range of collection efficiencies between surrogate surfaces, as is the case for natural surfaces (Dasch, 1983).

Another intercomparison between different kinds of surrogate surfaces and collection vessels has been made by Dolske and Gatz (1982). They found fluxes derived from exposing dry buckets are more than those obtained using small dishes, which in turn exceeds values obtained using rimless flat plates.

All such methods assume that the collection characteristics of some artificial surface are the same as those of the natural surface of interest. In general, these collection devices provide accurate measures of surface deposition for particles large enough that their sedimentation velocity exceeds the turbulent velocity. However, in most studies, investigators must worry not only about large, gravitationally settling particles but also about small particles that are formed in the air from gaseous precursors and about trace gases themselves.

The conceptual difficulties concerning the use of buckets is their inability to reproduce the detailed physical, chemical and biological characteristics of natural surfaces, which are believed to have strong influence on pollutant uptake in most instances (Hicks and Wesely, 1980). The inability to simulate the intricacies of gas exchange between the atmosphere and biological systems has focused attention on alternative deposition measurement methods in

recent years.

Since dry deposition is a related turbulent exchange process, many of the methods initially developed to measure the meteorological fluxes are now being used to measure atmosphere/surface exchange of trace gases and small particles.

Eddy correlation methods, using tower-mounted instruments with a time response on the order of one second, provide direct measurements that evaluate instantaneous products of the vertical wind speed, w , and pollutant concentration, c , in order to derive the time-average vertical flux F_c as

$$F_c = \overline{w' * c' * \rho_a} \quad (2.1)$$

where ρ_a is air density and the primes denote deviations from mean values. The over-bar indicates a time average. Eddy-correlation methods have been used in field experiments addressing the fluxes of ozone (Eastman and Stedman 1977), sulfur oxides (McMillen et al. 1987; Wesely et al. 1983), nitrogen oxides (Wesely et al. 1982), carbon dioxide (Desjardins and Lemon 1974), and small particles (Wesely et al. 1983).

The stringent site uniformity requirement for use of eddy-correlation approaches has been emphasized (Droppo and Doran, 1983). Additionally, the measurement of flux to the surface by eddy correlation is limited to chemical species which have no sources or sinks between the point of

measurement and the surface.

A variation on conventional eddy correlation methods is the so-called eddy accumulation technique (Desjardins, 1977). A fast-response sampling system which accumulates an air sample at a rate proportional to the measured vertical velocity is employed. Practically, the technique has two major limitations. First, the sampling system must operate with rapid response over a wide dynamic range. Second, very small difference in concentration must be measured with accuracy (Hicks and McMillen, 1984). In practice, the technique appears most suitable for studies of rapidly-deposited particles.

The gradient method can also be used to estimate the dry deposition of several rapidly depositing species to relatively short vegetations, providing the appropriate eddy diffusivity is known. It has the advantage that it can measure fluxes of those species whose concentrations can only be measured using slow techniques such as filterpacks or real-time continuous monitors in multi-level sampling arrangement. The technique places extreme requirements on the precision of the measurement system. Unfortunately, the vertical concentration differences are exceedingly small which makes it very difficult to measure with the accuracy necessary to determine fluxes. Thus, the gradient method should only be used when alternatives are not practical (Hicks, 1986).

None of the various micrometeorological methods has yet

been developed to the extent necessary for routine application. They are more suitable for investigating the processes that control dry deposition rather than for monitoring the flux itself. Nevertheless, some techniques that might be appropriate for dry deposition monitoring are under development. The so-called "modified Bowen Ratio" method which removes much of the uncertainty involved in the specification of an appropriate diffusivity might permit an accurate determination of vertical fluxes (Hicks and Wesely, 1980).

Due to the lack of a suitable method for measurement of dry deposition for small particles and trace gases on a routine basis, concentration-monitoring procedures provide a partial solution. In 1979, the Environmental Protection Agency sponsored a workshop (Hicks et al., 1980) to determine the best method for dry deposition measurement. Their recommendation was to base deposition calculations on estimates of deposition velocity (V_d) and measurements of air concentration (C) (the so-called inferential approach). The dry deposition rates of interests are then evaluated as the product

$$F = V_d * C \quad (2.2)$$

Although the concept of deposition velocity, V_d , is very useful for applications involving modeling and monitoring of dry deposition, the limitations of the method have been emphasized. First, the techniques are essentially inferential, relying heavily on the accurate measurement of

air concentrations and on the evaluation of accurate deposition velocities. Second, concentration-monitoring techniques suitable for routine use at remote locations are not yet well developed.

In much earlier work, estimates of the deposition flux were derived by applying an assumed-constant deposition velocity to concentration data. Most information on gas transfer either deals with average uptake in laboratory conditions (chamber, wind-tunnel), or is derived from short-term micrometeorological measurements at carefully selected field sites (Clough, 1975).

For particles in the range of 0.05 to 1 μm diameter the wind tunnel results indicates a minimum of V_d with values in the range of 0.003 to 0.05 cm s^{-1} . Field observations give variable results and often indicate deposition velocities larger than 0.1 cm s^{-1} . The large difference between some estimates of V_d obtained in field experiments and in the wind tunnel suggests that there may be an important difference between the mechanisms of deposition in the two circumstances (Garland, 1982).

Successful flux estimation via concentration monitoring requires the ability to infer V_d accurately from meteorological data, pollutant properties, and observations of local surface conditions and vegetations. Most efforts to model and parameterize V_d employ a 'big-leaf', multiple-resistance analog model (Baldocchi et al. 1986; Hicks, 1984; Hicks et al. 1985). Such big-leaf models are one-

dimensional and are most applicable over relatively flat, horizontally homogeneous terrain. The total resistance to mass transfer, R_t , is given by the sum of three terms: an aerodynamic resistance to turbulent atmospheric transfer, R_a , which is controlled by wind speed, surface roughness, and atmospheric stability; a diffusive boundary layer resistance, R_b , which is determined by surface friction and a molecular diffusivity of the substance in question; and a resistance to uptake by vegetation, soil, and other receptors, R_c , which is a function of environmental and physiological conditions, surface wetness and chemistry, leaf area index, and diffusivity of the pollutants (Sehmel, 1980; Unsworth, 1980),

$$R_t = R_a + R_b + R_c \quad (2.3)$$

and

$$V_d = 1/R_t \quad (2.4)$$

In comparison, the aerodynamic(R_a) and quasi-laminar(R_b) components are relatively simple products of factors not strongly influenced by the physiology of the surface. It is the uncertainty surrounding specification of the canopy resistance, R_c , which limits the ability to infer dry deposition rates from air concentration data. A considerable amount of measurements of canopy resistance to gaseous deposition is available in the literature (Fowler and Unsworth, 1979; Hicks et al., 1982; Lenschow et al.,

1982).

Since, deposition velocities are complicated functions of meteorological and surface properties, errors can arise by using the average fluxes which are estimated from inaccuracies or inadequacies to infer V_d . Moreover, particles whose atmospheric transfer is different from that of trace gases cannot be considered in this way. Further, estimating appropriate deposition velocities that are site specific and species dependent constitutes a major difficulty in the application of inferential methods to derive deposition rates from concentration data.

As an extension of dry deposition research programs, a trial network has been set to test the inferential method (Hicks et al., 1986).

Although researchers have used a variety of techniques to measure dry deposition, no one method has gained universal acceptance. In the absence of simple direct monitoring methods, it is necessary to infer dry deposition from quantities that can be measured easily.

Throughfall

The alteration of the composition of water in contact with plant tissue has been recognized since 1804 (Tukey, 1970). The chemistry of the throughfall can be drastically different from that of the incident precipitation. Its ion content can be enriched or depleted by many factors. These factors include; dryfall accumulated on the canopy during

the between-event dry period, the intercepted wetfall, ion transformation reactions, wetfall retained on the canopy during the present and previous event, leaching material from internal plant tissue and foliar uptake, deposition or attachment of solute (Eaton et al. 1973; Hoffman et al., 1980; Parker, 1983; Reiners and Olson, 1984). The effects of these processes may vary with the specific characteristics of the canopy, incident precipitation, preceding dry period and ambient ion concentration. Several investigations have made attempts to characterize throughfall and estimate the significance of its components (Mayer and Ulrich, 1974; Lakhani and Miller, 1980; and Miller and Miller, 1980).

Although foliar uptake can be most important for nutrients in low supply such as nitrogen, it has long been recognized that washoff and leaching are the dominant processes in throughfall enhancement. Numerous approaches have been employed to separate the washoff and leachate portions of net throughfall. Most methods are indirect and applicable only under certain unique conditions. Only a few direct evaluations have been obtained in field situations. A discussion of the various approaches and their assumptions and their limitations as general methods will be presented in the following section.

Direct Approach

Usually, direct methods for separating leaching and washoff involve the estimation of dry deposition to inert surfaces intended to simulate canopy filtering potential. Actual precipitation is collected both under and adjacent to such surfaces. Regardless of sophistication, questions always remain as to the ability of a surrogate surface to simulate the action of an actual leaf whose shape, wetness and microstructure may all be important to the process of dry deposition.

The controlled washing of plant parts is another direct approach. Increases in wash water concentration are presumed to be due to dry deposition, if the leaching contribution is constant (Lindberg et al., 1979). White and Turner (1970) washed leaves and branches of several tree species exposed to known aerosol loads to calibrate the trapping efficiency of wind-vane mounted filter papers. The inputs to actual canopies were then estimated as the product of ambient concentrations sampled by the filter paper and the estimated trapping efficiency. Since leaf washings contain leachates in addition to dry deposits, the efficiencies reported are probably an overestimate.

In 1983, Chen et al., developed a canopy model based on canopy properties and field observations. The model simulates the biogeochemical processes (processes which can moderate and change atmospheric inputs and affects biogeochemical flux by its output within/between ecosystems,

e.g. biological uptake, mineralization, throughfall etc.) (Likens et al. 1977) which alter the chemistry of the rainwater as it travels through the watershed. The results are considered accurate (Chen et al, 1983).

Indirect Approaches

Net throughfall sources may also be partitioned with methods that do not estimate dry deposition directly (Eaton et al. 1978; and Lindberg et al. 1979). Mayer and Ulrich (1974) suggested that the washoff rate in a deciduous forest is equal to the rate of net throughfall flux during the leafless period assuming that the leafless forest would neither differ in filtering ability from the extensive summer canopy nor be appreciably leached.

Eaton et al. (1978) calculated the dry deposition input to a Northern hardwood forest as the difference in system inputs and outputs, assuming negligible sulfur storage. Bache (1977) asserted that the net throughfall enrichment of sulfur approximately balances the contribution arising from dry deposition. Raybould et al. (1977) also suggested that gaseous deposition could account for all net throughfall sulfur. By using a combination of artificial collection surfaces, leaf washing, and ambient aerosol measurement, Lindberg et al. (1979) determined that 26% of the net throughfall sulfate deposition at the Walker Branch Watershed was due to deposition of particulate sulfate to foliage and stems.

Alternatively they imply that the partitioning of net throughfall sulfate can truly vary from primarily atmospheric input to wholly internal nutrient cycles. All of the above estimates are limited in their applicability to other forest systems.

A linear regression of weekly throughfall deposition and incident wet deposition was proposed to estimate the leaching fraction as the positive y-intercept of the relation by Miller et al. (1976). This suggests that a very small storm will consist largely of leachate. However, for most ions, the relation is probably not linear (Parker, 1982) and leaf washing studies have shown that soluble deposits are quickly released on wetting of the canopy (Little, 1973, 1977). Therefore, a refinement of regression approach has been proposed (Lakhani and Miller, 1980). Additional incident precipitation sampling under screened collectors and the assumption that additional deposition in screened collectors are proportional to aerosol inputs to forest canopies are required. The study of sequential sampling of throughfall was undertaken trying to gain a better understanding of the processes involved in throughfall by detailing the change in throughfall chemistry during an event. Throughfall quality measurements within a storm are few and show a variety of patterns. Wide oscillations without a clear trend, especially in small storms (Richter and Granat, 1978), or patterns which roughly mimic those of incident precipitation (Sollins and Drewry,

1970) or a regular, nearly exponential decline with successive amounts of precipitation (Yawney and Leaf, 1971) are observed.

Lovett and Lindberg (1984) describe a method for determining dry deposition rates by regression analysis of net deposition. In this technique, net deposition for individual storm events is regressed against the length of the antecedent dry period (the dry period preceding the event) and the amount of rainfall in the storm. Because the dry-deposition flux is correlated with the amount of precipitation, this technique can separate these two components of net deposition. However, there are several caveats to this approach, the most important of which is the case that the canopy may irreversibly absorb dry-deposited nitrate, and results in an underestimate of the dry-deposition rate. Clearly, characterization of pollutant concentrations above and throughout canopies should be a key research objective.

Recently, sequential throughfall data and sequential wetfall data, collected from Adirondack Mountains of New York by Dackson (1983), suggested that highest ion concentrations occurred during the initial portion of an event and decreased during the event. This enrichment and subsequent decay conceptually supports dissolution and washoff of dry deposition. Since all data is time dependent, it is impossible to compare the result without the use of a mathematical model. Therefore, this data

combined with a mathematical model, should help to characterize the complex interactions occurring between precipitation and a forested canopy.

CHAPTER III

EXPERIMENTAL ANALYSIS

Data was collected at Woods Lake watershed, located in the Adirondack Mountains of New York State in September and early October 1981. The characteristics of the watershed, collector designs, sampling procedures, and field and laboratory analysis has been discussed by Dackson (1983), therefore, the details are omitted where possible.

Description of the Trees

The dominant deciduous species in the study area is the American Beech while the dominant coniferous species is the Red Spruce (Vasudevan, 1982). Two trees of similar diameter were chosen so comparisons between deciduous and coniferous species could be made. The physical characteristics of the trees are summarized in Table I.

Diameter at breast height (DBH) is measured at a height of 150 cm off the ground. Height is measured by triangulation. Land surface covered by the canopy is determined by measuring the radius of the canopy in four directions, averaging these measurements, and calculating the area. Leaf and branch surface area are determined indirectly from regression equations (Whittaker et al.,

TABLE I
PHYSICAL CHARACTERISTICS OF TREES USED

<u>Variable</u>	<u>American Beech</u>	<u>Red Spruce</u>
Diameter breast height (cm.)(DBH)	24.3	21.0
Height(m.)	10.3	13.6
Leaf surface area covered by canopy(m ²)	44.0	12.0
Leaf surface area(m ²)	120.0	71.0
Leaf area index(LAI)	2.7	5.9
Branch surface area(m ²)	66.0	39.0
Branch area index(BAI)	1.5	3.3

1974). These equations are summarized in Table II. Leaf area index (LAI) is defined as leaf surface area per unit land area covered by canopy. Branch area index (BAI) is similarly defined as branch surface area per unit land area covered by canopy.

Description of Precipitation Network

Equipment Location

A standard sampling site is set up include a wedge type rain gauge, a total event collector and a sequential throughfall collector. Collectors were placed in the open, under a deciduous tree and under a coniferous tree. The opening to each piece of equipment was one meter off the ground. In order to minimize splash-off of stemflow into the throughfall collectors, collectors were placed away from the tree trunks.

The location of the throughfall and total collectors under each tree species are summarized in Table III. A wedge gauge was placed 114 centimeters away from the trunk. A third set of collectors, including a sequential collector, a total event collector, a wedge gauge, a totalfall collector and a dryfall collector, was located in an opening 19 meters from the Red Spruce tree.

Equipment Description

Throughfall collectors consisted of two 19 cm diameter

TABLE II
 REGRESSION PARAMETERS USED TO PREDICT
 CANOPY CHARACTERISTICS
 (Whittaker, 1974)

$$\text{Log}(\text{Area}) = a + b * \text{Log}(\text{DBH})$$

where DBH in centimeter

	<u>American Beech</u>	<u>Red Spruce</u>
Leaf	a = 3.8398	a = 3.6898
Surface		
Area(cm ²)	b = 1.6169	b = 1.6359
Branch	a = 3.3673	a = 2.9252
Surface		
Area(cm ²)	b = 1.7718	b = 2.0170

TABLE III
LOCATION OF THE COLLECTORS

<u>Collector type</u>	<u>Red Spruce</u>	<u>American Beech</u>
sequential throughfall collector	74 (cm.)	142 (cm.)
total event collector	41 (cm.)	150 (cm.)
distance between these two collectors	48 (cm.)	71 (cm.)

distance was measured away from the tree trunk

(567 cm²) polyethylene funnels connected with Tygon tubing to a 500 ml polyethylene collection bottle. A Whatman 500 filter paper was placed inside each funnel to remove any canopy debris before collection. A schematic representation of a non-winter throughfall collector is shown in Figure 1. Total event collectors were similar to the throughfall collectors. The major differences being that the total event collectors used a 1000 ml polyethylene bottle, and there was only one funnel-crosspiece assembly. The totalfall collector consisted of a polyethylene bucket with a tightly fitting lid that is placed on it during sample transport. The bucket is 28.6 cm in diameter (641 cm²) and 24.8 cm deep with a slight taper from top to bottom. Dryfall collectors consisted of a plastic bucket with an automatic cover controlled by a rain sensor, which directed the cover over the bucket at the beginning of a rain event and uncovered it during a dry period. The problem with this collector is that very often the sensing device does not work fast enough, with the initial fraction of the precipitation ending up in the dryfall bucket. Therefore, when the dryfall bucket was collected, the volume of precipitation, if any, was recorded to adjust the dryfall loading calculations.

Sampling Procedure

Sequential samples were collected approximately every 60 ml on an event basis. During the later part of a low

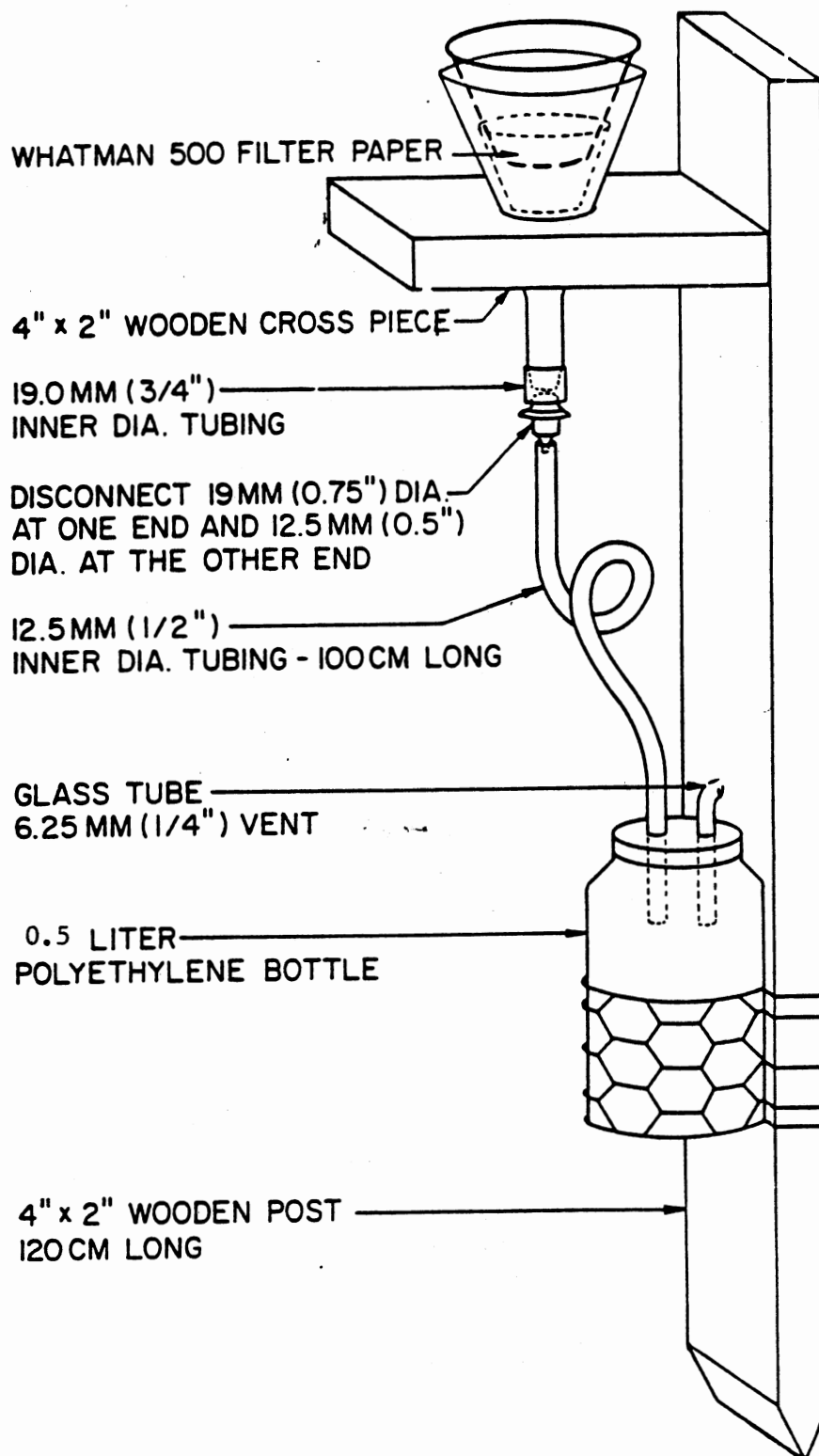


Figure 1. Non-Winter Throughfall Collector
(from Vasudevan and Clesceri, 1981)

intensity event, the collection frequency dropped to hourly intervals. A complete description of the sample processing procedure is given by Ierardi (1981), Vasudevan (1982), and Dackson (1983). A very brief description is given here:

- Wetfall, totalfall, and throughfall samples were processed as soon as possible upon returning to the field laboratory where sample volume, field pH and conductivity were measured.
- The remainder of the sample was filtered through a 0.4 micron Nucleopore polycarbonate filter and stored in a clear polyethylene bottle. Samples were refrigerated at 4°C without preservatives until chemically analyzed at the main analytical laboratory.
- Dryfall samples were extracted with 250 ml of demineralized water and processed in the same manner as wetfall samples.
- Upon arrival at the main analytical laboratory, samples were analyzed for pH, sulfate, nitrate, chloride, ammonium, calcium, magnesium, sodium and potassium and for conductivity. The cations (except ammonium) were measured using a Perkin-Elmer Model 403 Atomic Absorption Spectrophotometer. Ion concentrations were determined spectrophotometrically using Perkin-Elmer lamps. Anions (except sulfate) and ammonium were analyzed using a Technicon Auto Analyzer and a colorimetric procedures. Sulfate

analysis was performed on a Technicon Auto Analyzer according to the method of Lazrus et al. (Technicon Corporation). Specific details of the chemical analysis are given elsewhere (Dackson, 1983).

Data Analysis Procedure

Rain data was collected for nine events (Dackson, 1983). Analysis in this work is done using events 1, 2 and 7 only (Appendix A), as the data in the other events are incomplete. General temporal trends, including volume versus time, concentrations versus time, mass loading versus time, and cumulative mass loading versus time were noted and example results are plotted in Figures 2 through 11 for event 1.

A general trend worthy of note is that higher concentrations are usually observed for all species during the earlier collections in an event. As time progresses, these concentrations decrease, then increase near the end of an event.

Viewing Figures 2 through 11 as a comparison among coniferous, deciduous, and open loadings, it is observed that American Beech exhibited lower volume, and ammonium concentration, greater potassium concentration, and about the same sulfate loading as in the open. Also, compared with American Beech, Red Spruce exhibited similar volume, and ammonium, and greater loadings for potassium and sulfate ions.

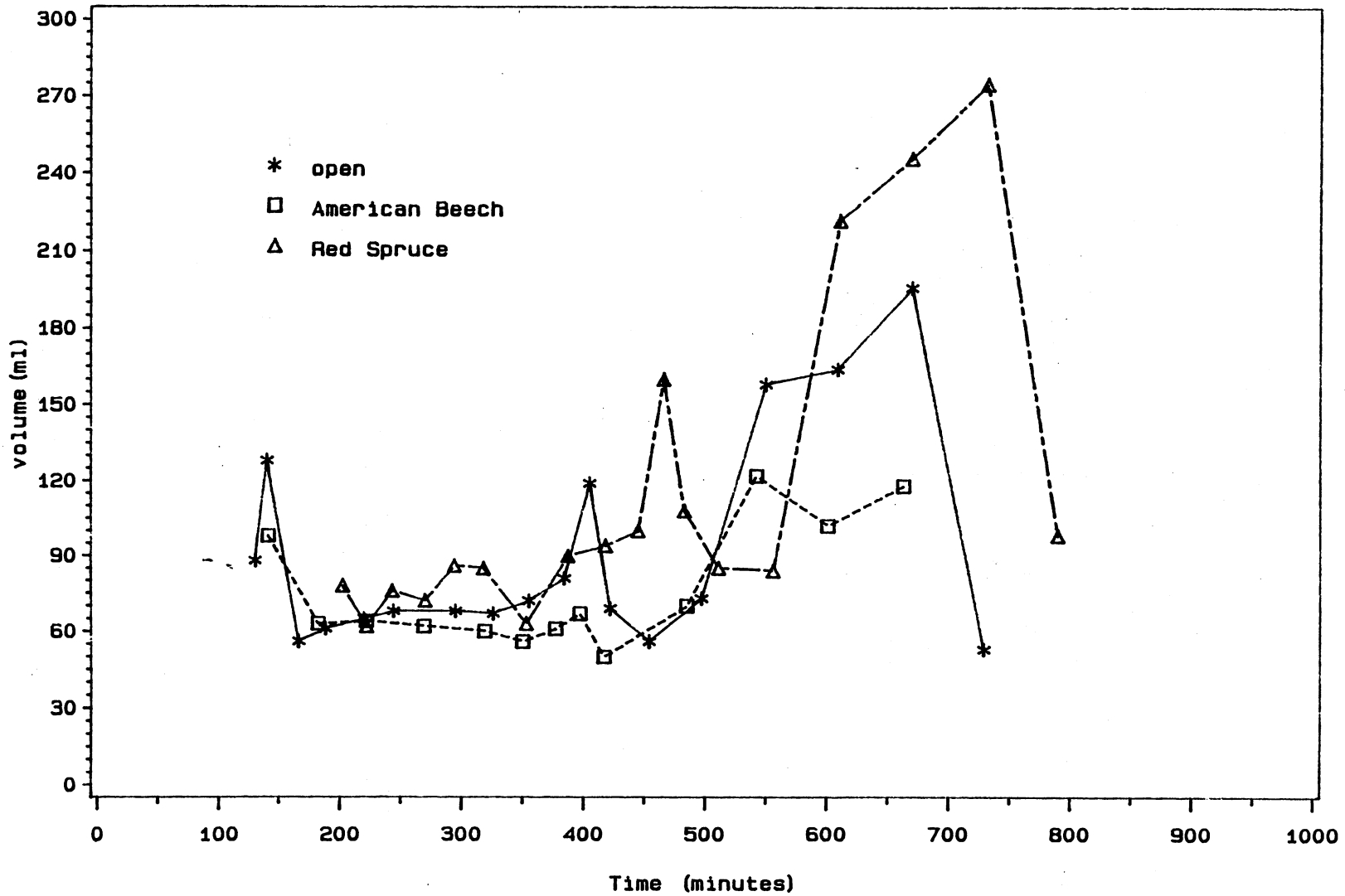


Figure 2. Volume Distribution in Event 1

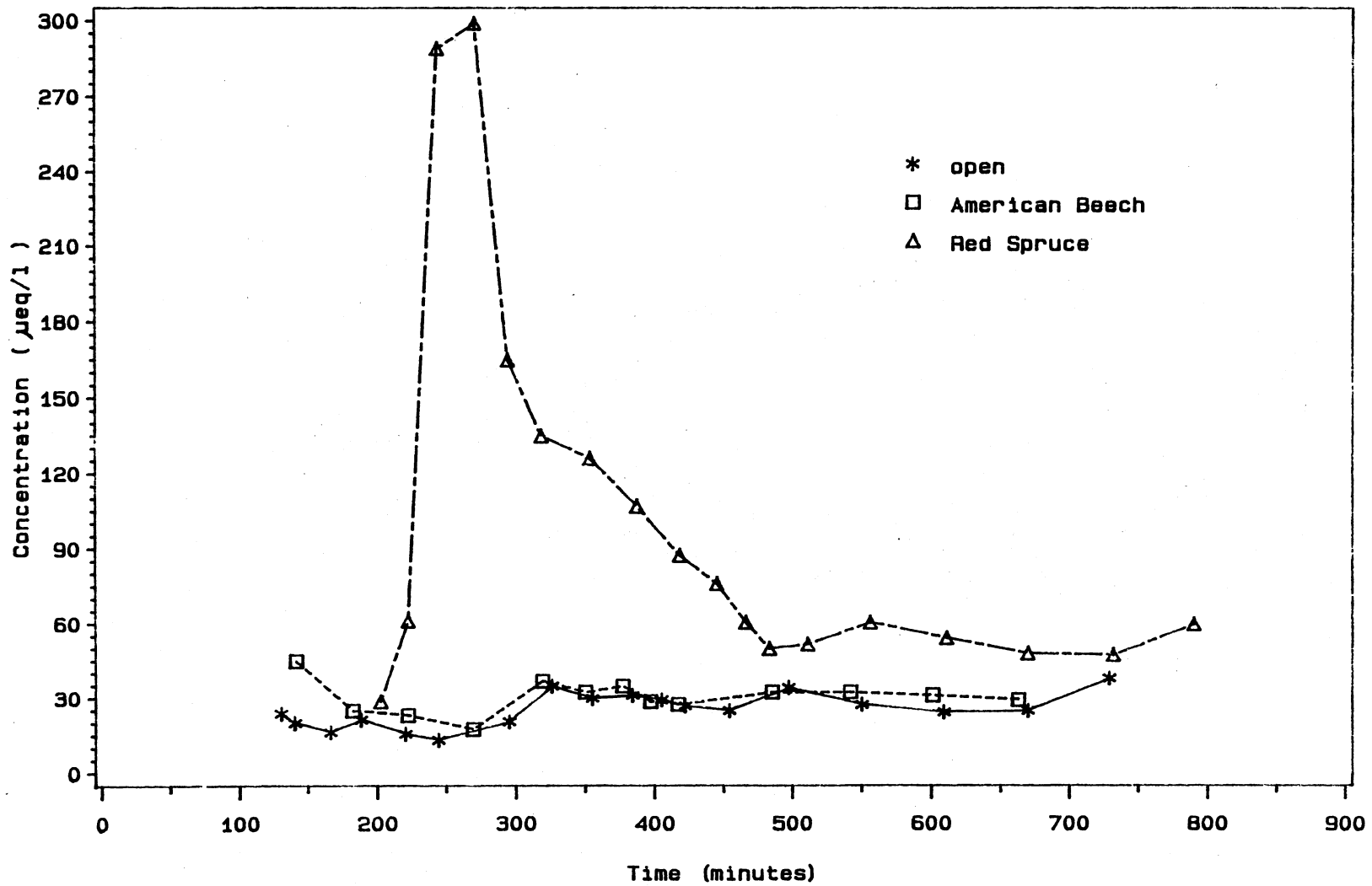


Figure 3. Concentration Distribution for Sulfate Ion in Event 1

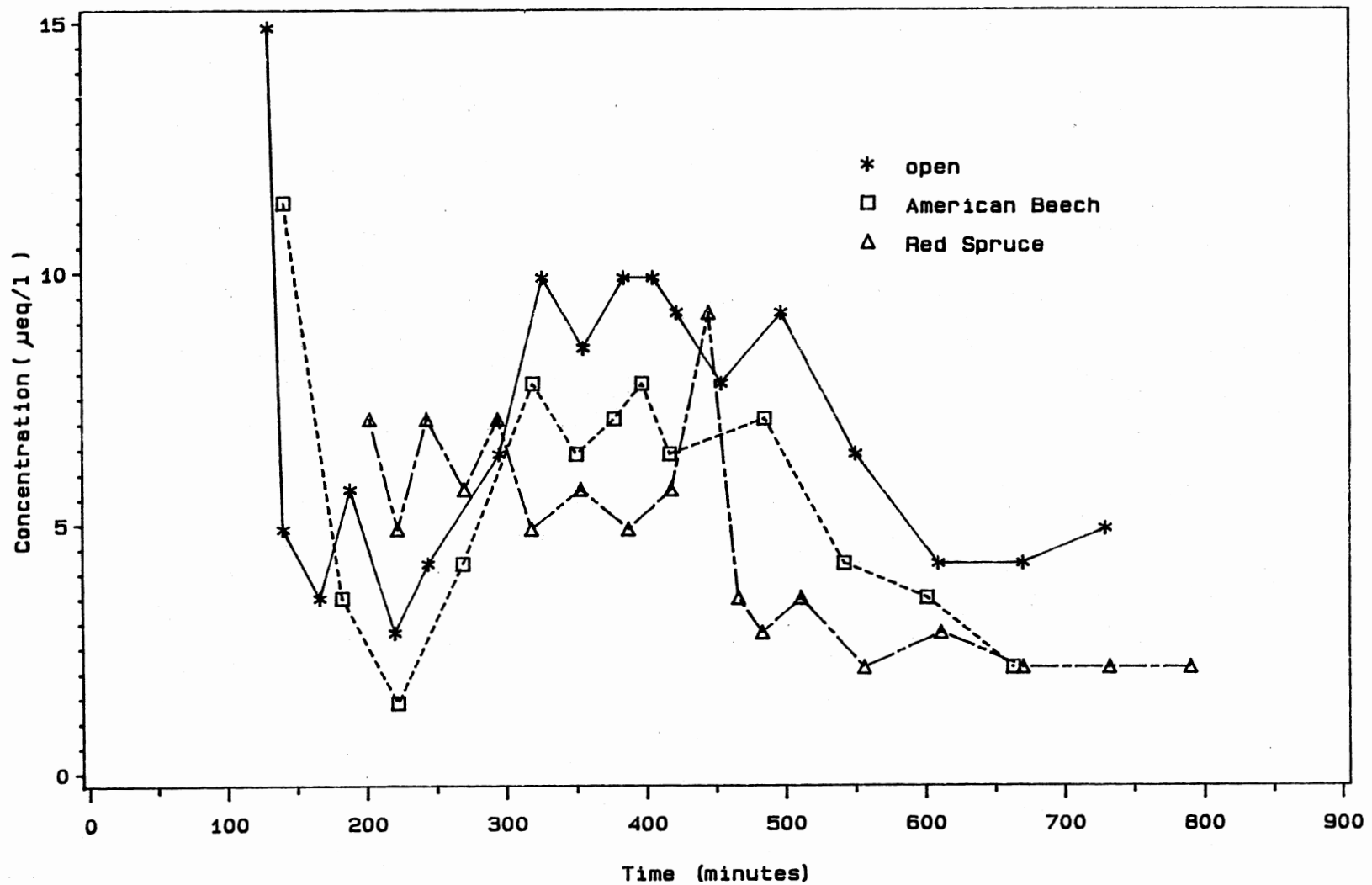


Figure 4. Concentration Distribution for Ammonium Ion in Event 1

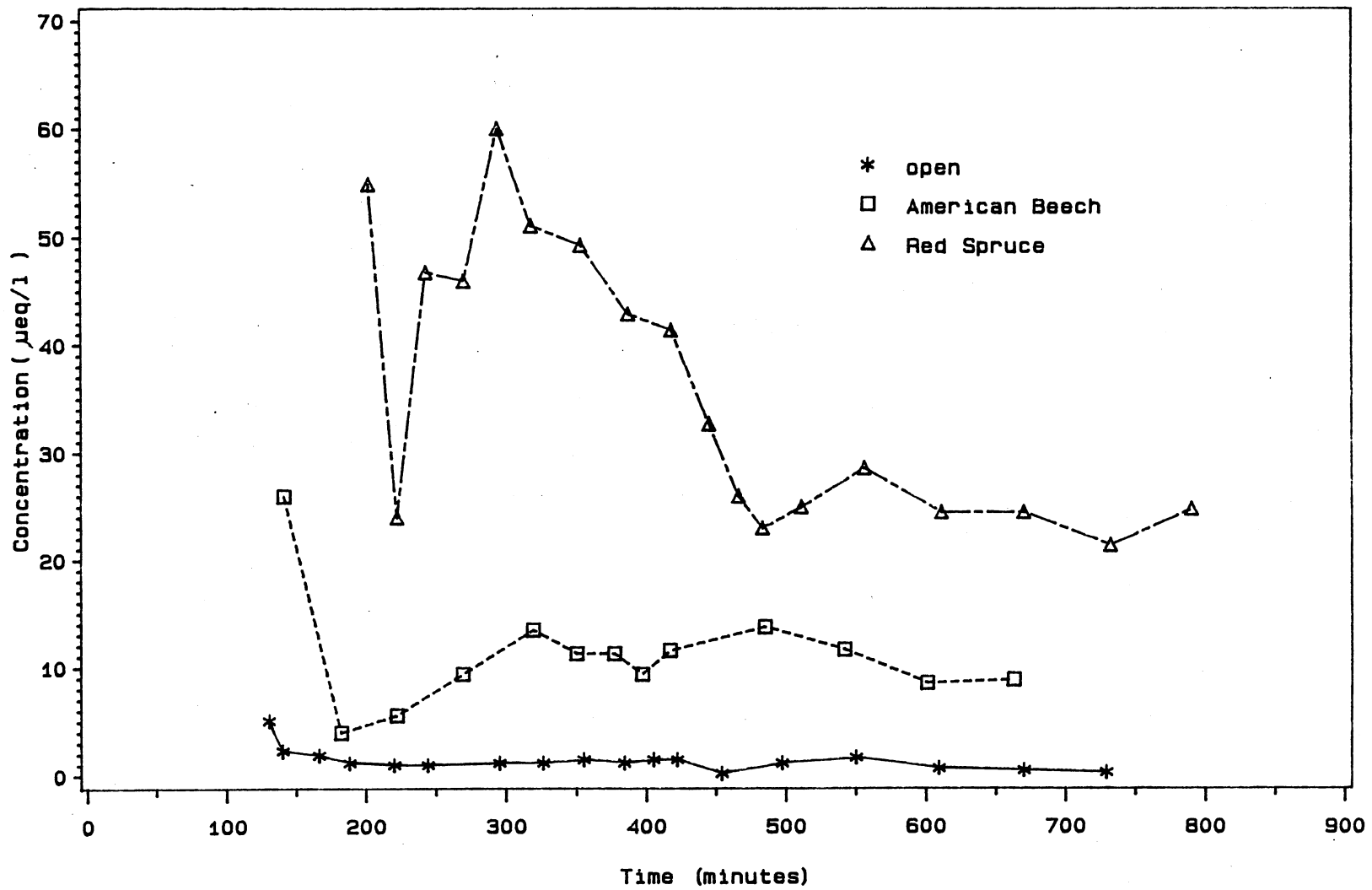


Figure 5. Concentration Distribution for Potassium Ion in Event 1

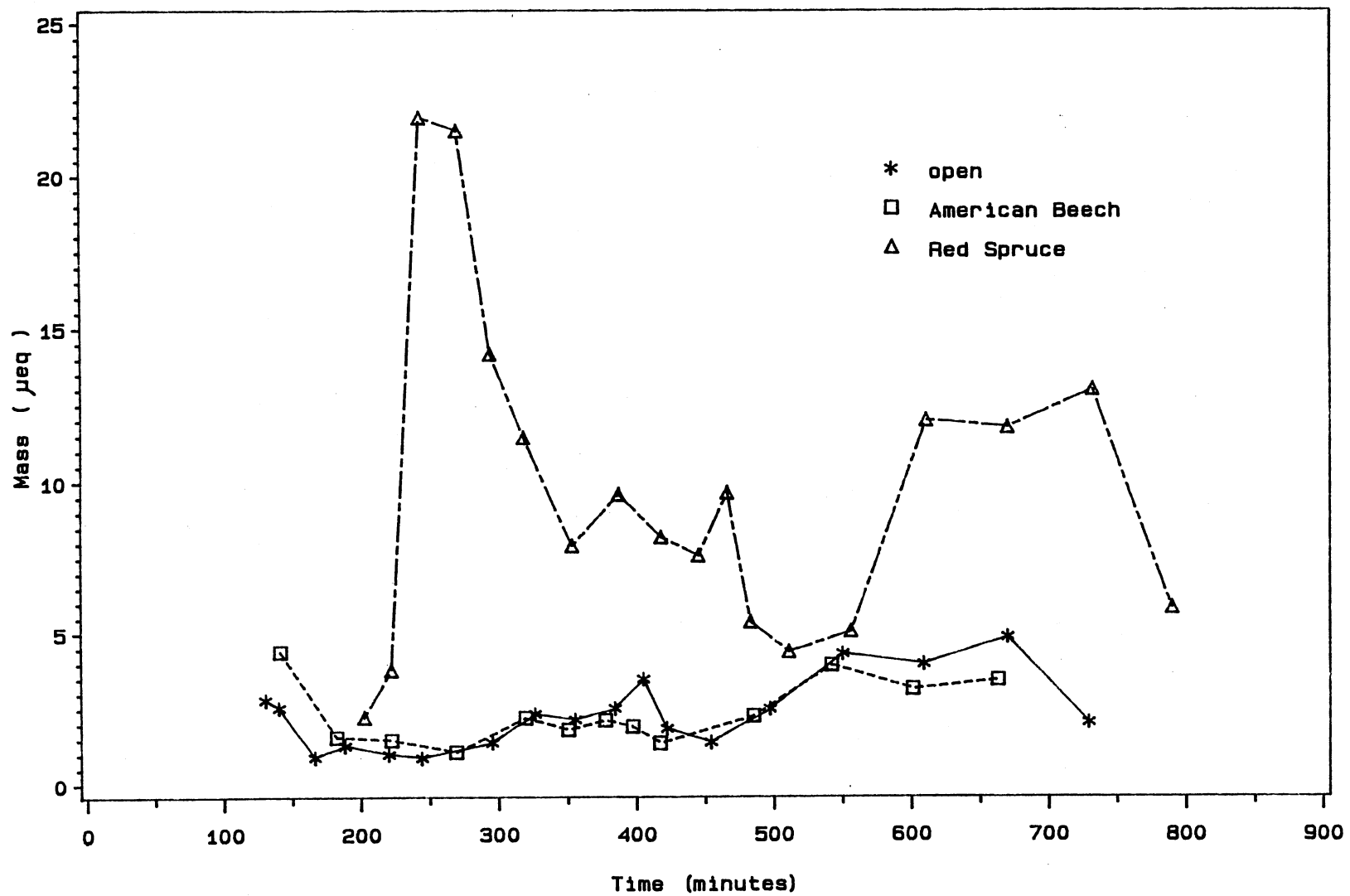


Figure 6. Mass for Sulfate Ion in Event 1

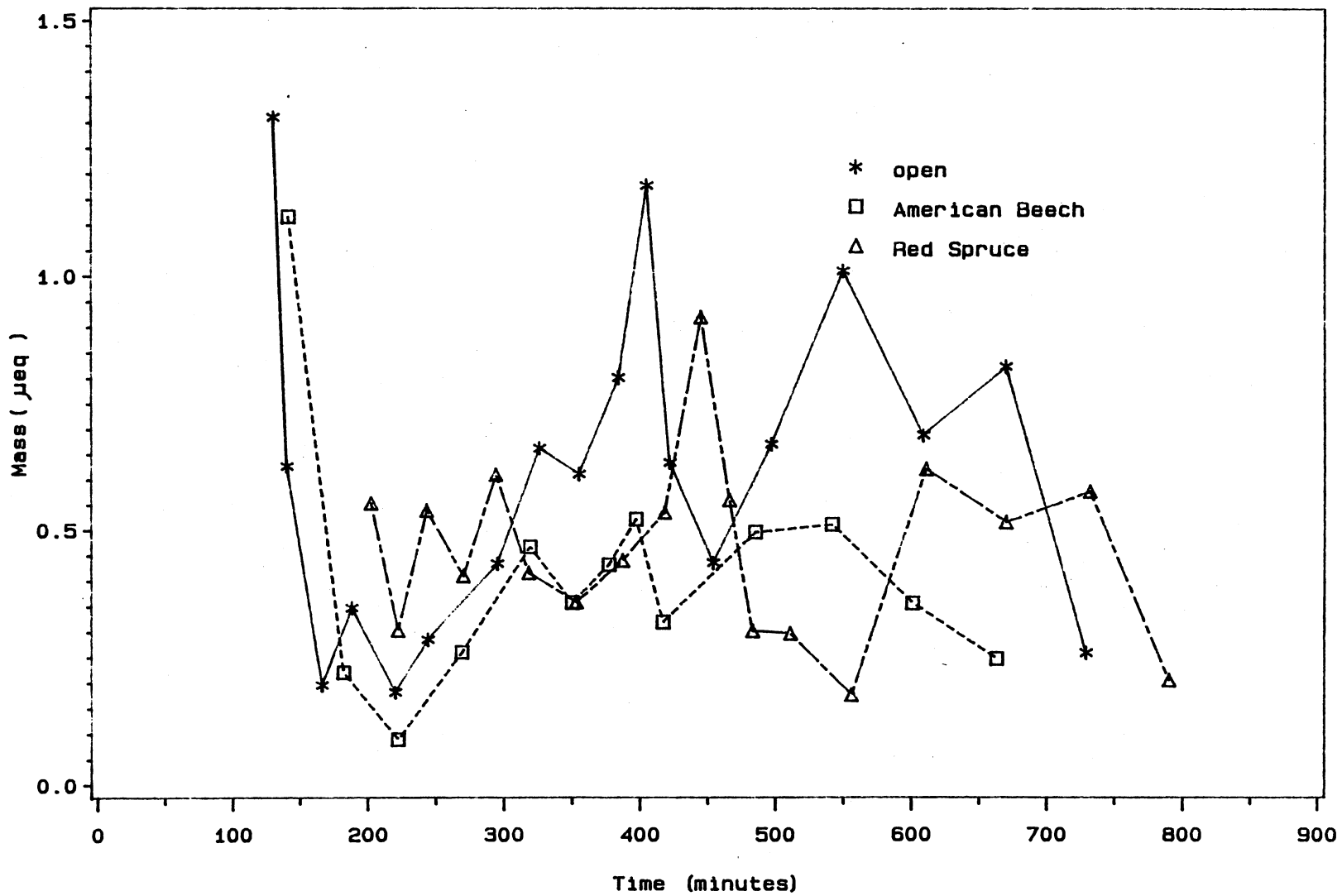


Figure 7. Mass for Ammonium Ion in Event 1

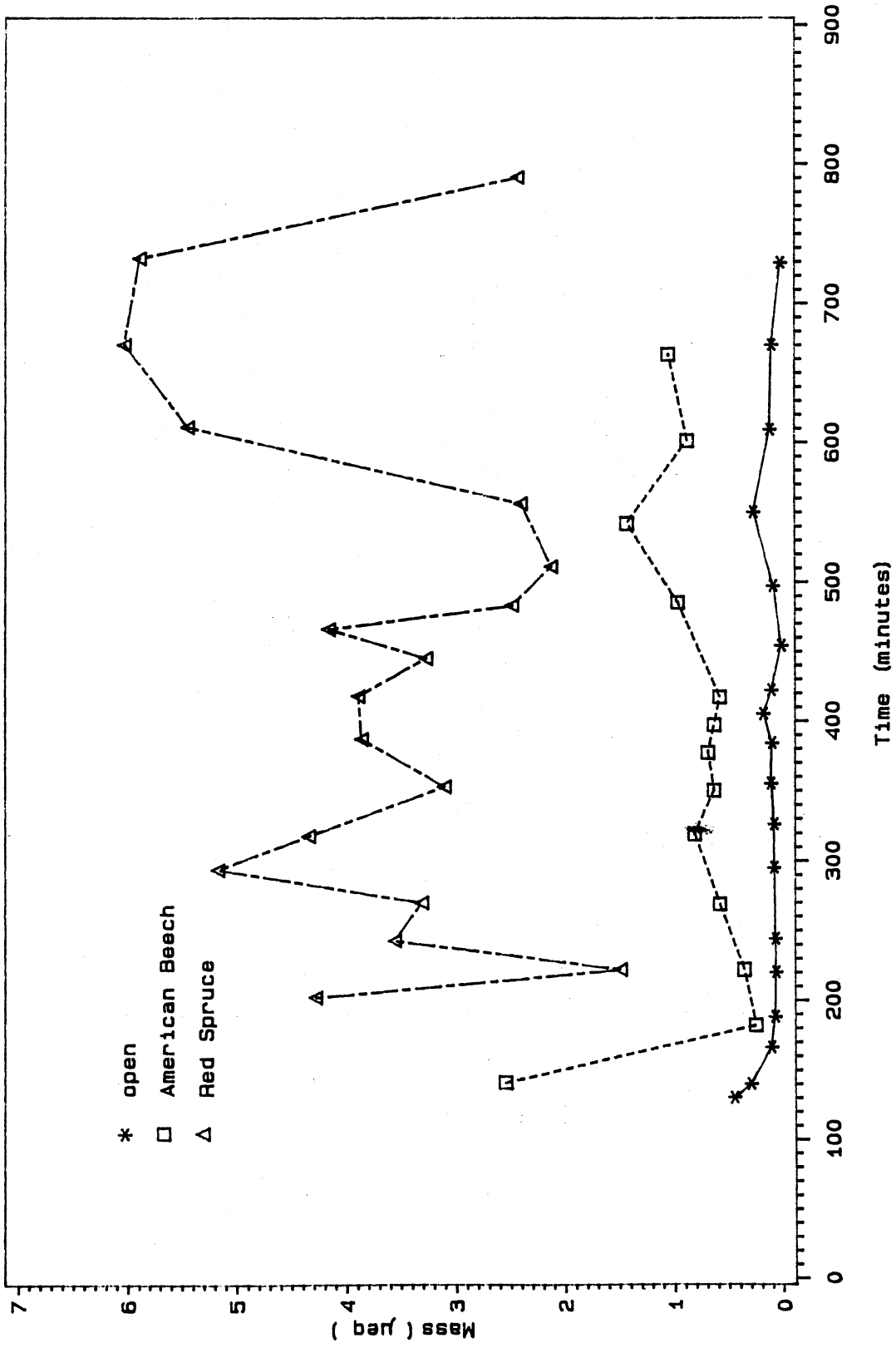


Figure 8. Mass for Potassium Ion in Event 1

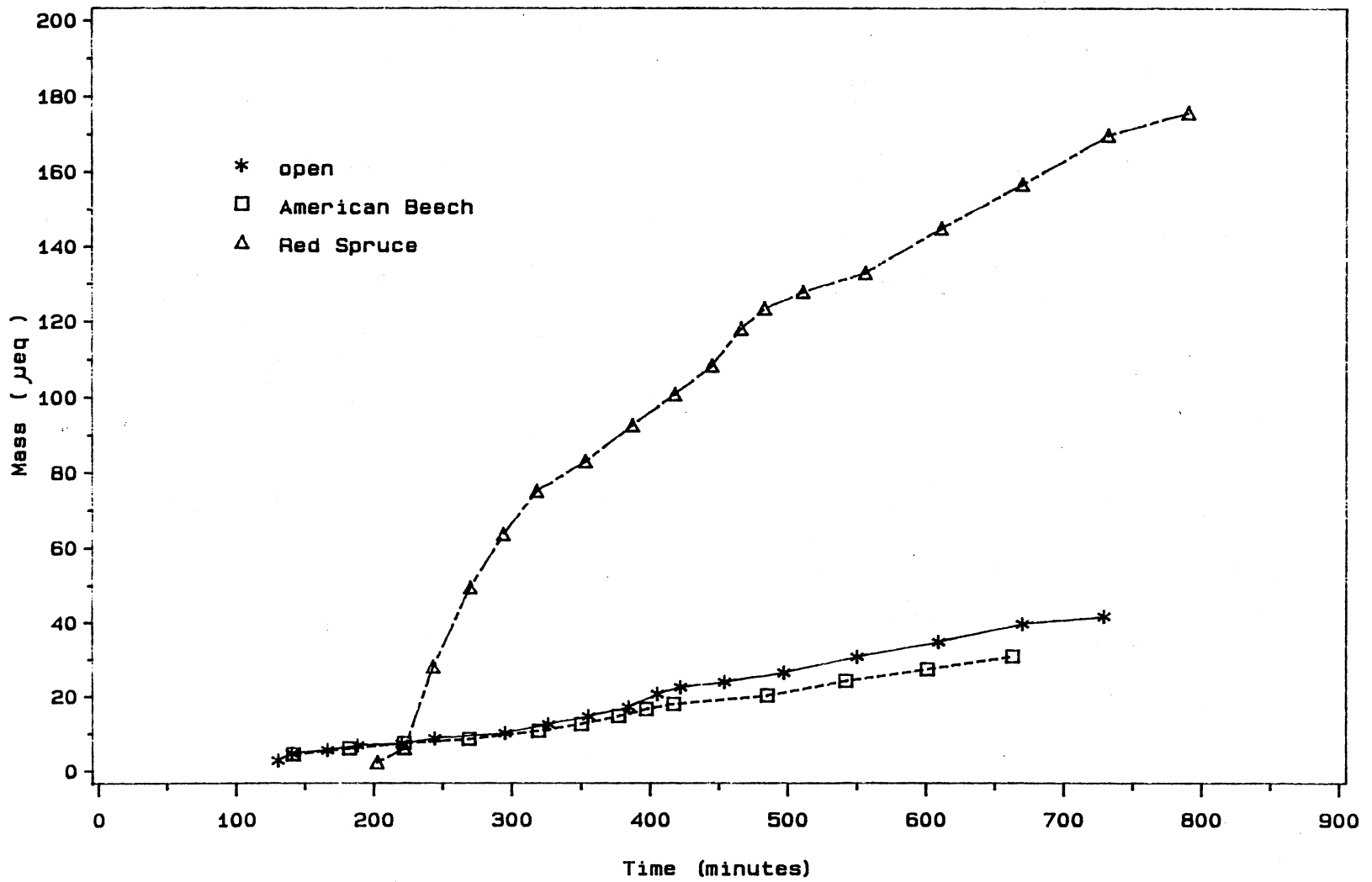


Figure 9. Cumulative Mass for Sulfate Ion in Event 1

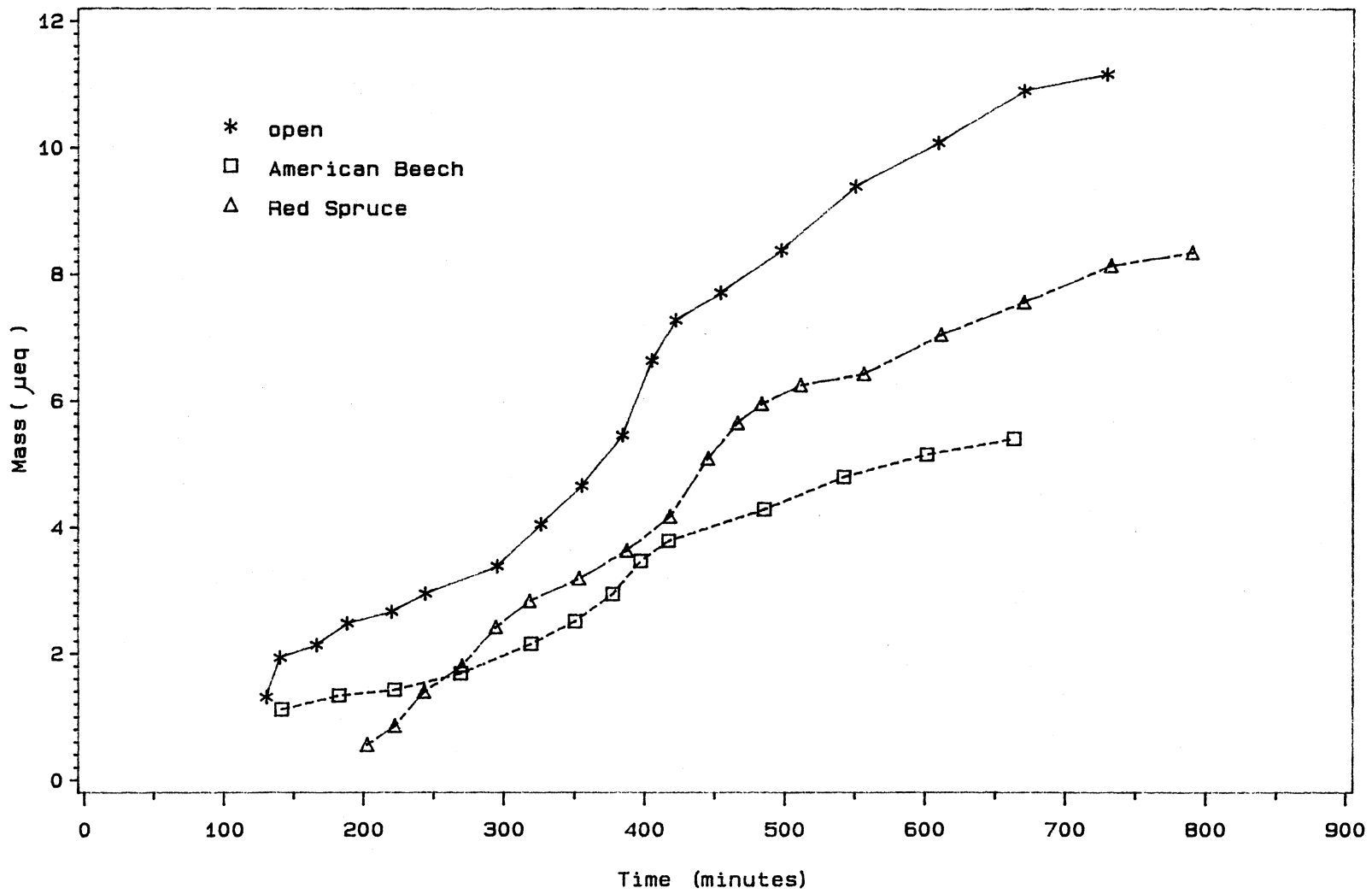


Figure 10. Cumulative Mass for Ammonium Ion in Event 1

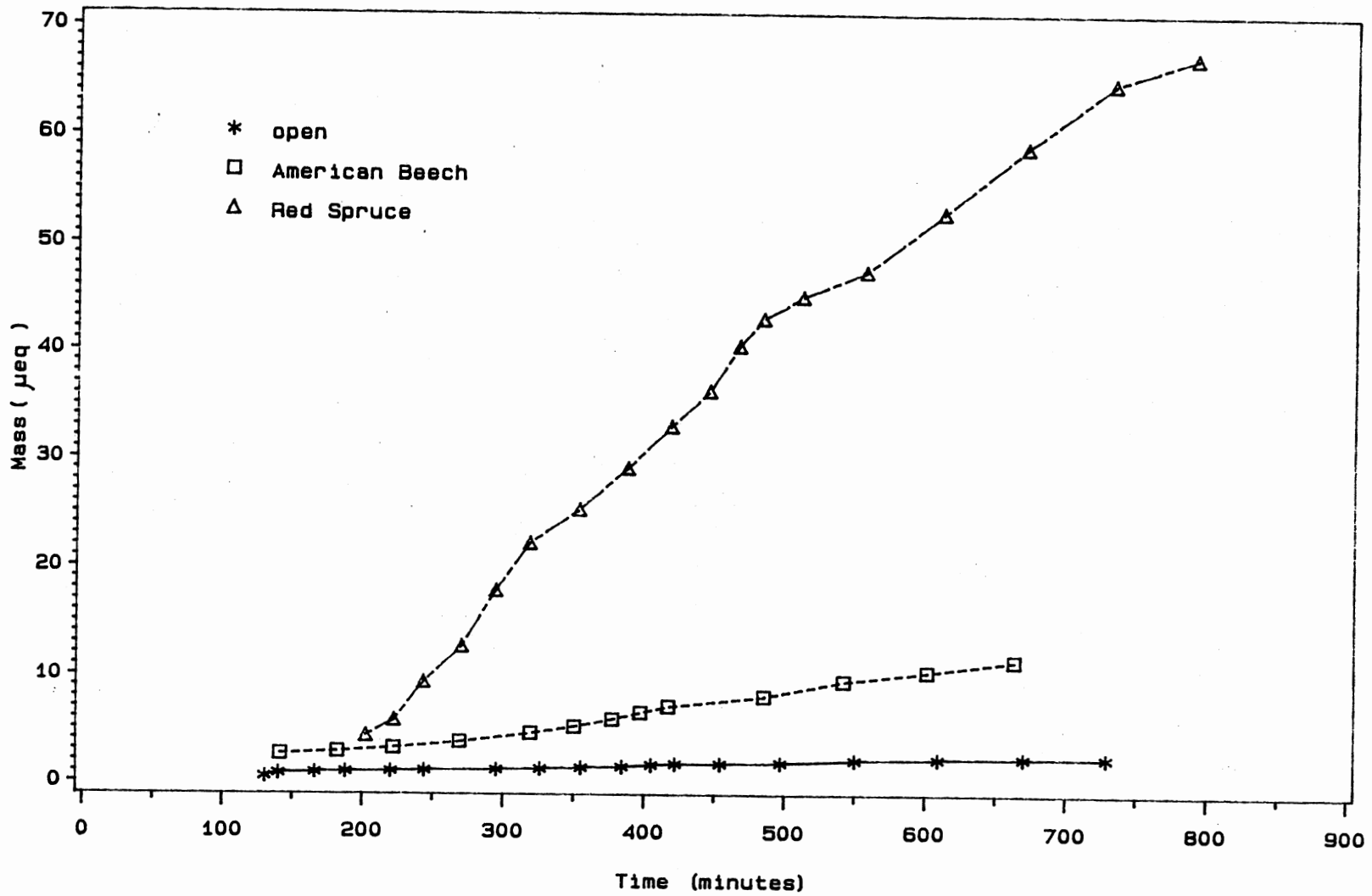


Figure 11. Cumulative Mass for Potassium Ion in Event 1

The anion/cation ratios (ACR) were computed as the sum of all of the cations collected to a corresponding value for all of the anions. Within a sample, ACR is a measure of the actual ionic balance, while between events, ACR is a measure of the consistency of the effect of plant type on throughfall. Values in the range of 0.8 to 1.2 are accepted to be within the limits of experimental precision. Due to the presence of organic acids leaching from the plant system, which are not accounted for in the analysis of the samples, the ACR value of throughfall is usually not within the acceptable range.

CHAPTER IV

CONCEPTUALIZATION AND CONSTRUCTION OF THE MIXING MODEL

Conceptualization of the Model

During a non-precipitation period, gases (CO_2 , NH_3 , and SO_2) and total suspended particles are transported to the canopy surfaces. Gases are transported mainly through diffusional processes while particles are transported to the surfaces by impaction, interception and sedimentation. When precipitation begins, it first strikes the surface of the vegetation. Many drops of rain are caught and retained by the foliage and stem. Gradually, the whole upper surface of the foliage is wetted to its saturation or storage capacity. As rain continues, the upper parts of the plant can hold no more water, and water dripping begins (throughfall), or water runs down the stem (stemflow), wetting lower parts of the vegetation. As the rainwater cascades through the canopy, a unit of water interacts with numerous plant surface. This situation can be represented by a simple mixing model (Ritchit and Togby, 1974), with each level represented by an ideally mixed tank. Further, material may pass through the walls of the tank. This represents the leaching of the material from the plant system. Also, undissolved dry material is assumed to be in each tank

previous to the start of an event. The tree was therefore conceptualized as a series of ideally stirred tanks where dissolution, leaching and mixing occurred (Dackson, 1983; Johannes et al., 1986). The total number of tanks for each tree is based on a leaf area index (LAI) and rounded to integer value.

In the absence of stemflow volume and holdup data in this study, a regression approach was employed in order to determine the relationship between wetfall and throughfall volume. After plotting a total of 52 data points from events 1, 2 and 7 for American Beech, as shown in Figure 12, a linear relationship between wetfall and throughfall volume was found. A least square fit of the sequential data (see Table IV) yielded the equation

$$[\text{throughfall volume}] = 0.685 [\text{wetfall volume}] - b_1 \quad (4.1)$$

where volume is given in liters, and the value b_1 is equal to 0.00475.

Table IV also includes the least square analysis for each event. The R^2 value in Table IV is called the coefficient of determination. This provides a measure of the proportion of the variability in one of the variables which may be explained by the linear relationship it has with the other variable. A value of R , square root of R^2 , equal to -1 or +1 indicates perfect linear relationship and implies good correlation between the two variables (throughfall volume and wetfall volume, in this case).

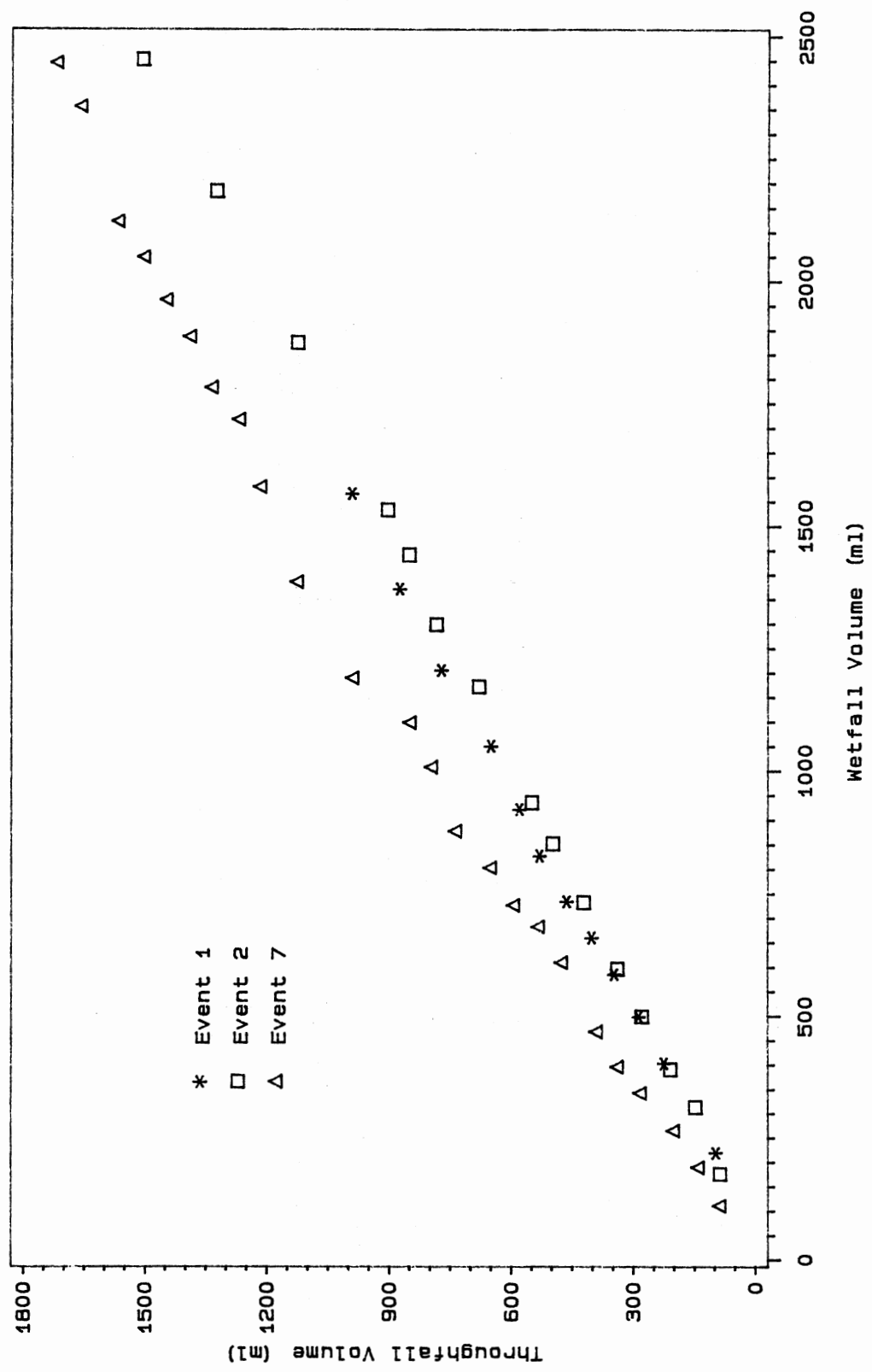


Figure 12. The Relationship between Throughfall and Wetfall Volume

TABLE IV
 THE RELATIONSHIP BETWEEN THROUGHFALL AND WETFALL VOLUME
 (Volume in Liters)

American Beech				
Dependent Variable: THR				
Event	1,2,7	1	2	7
Total Observations	52	13	16	23
F value	1142.0	19295.5	45589.4	6874.6
Parameter				
Estimated				
Intercept	-0.0048	-0.039	-0.039	0.062
Slope(wetfall)	0.685	0.67	0.63	0.71
R ²	0.958	1.0	1.0	0.99
Red Spruce				
Dependent Variable: THR				
Event	1,2,7	1	2	7
Total Observations:	52	17	14	21
F Value	410.1	1470.5	6078.5	2156.2
Parameter				
Estimated				
Intecept	0.019	-0.41	-0.25	0.12
Slope	0.70	1.36	0.73	0.63
R ²	0.81	0.98	1.0	0.98

An interpretation of Eq. (4.1) is that a certain volume of wetfall must fall before any throughfall is observed. This required storage capacity is generally termed as interception or holdup. A holdup parameter may be derived by setting the throughfall volume equal to zero and solving for the wetfall volume required. In this study, the holdup is equal to 0.007 liters. An estimate of stemflow volume based on RPI/ILWAS study was used to satisfy the water balance requirement (Johannes et al., 1981).

The procedure was repeated for the Red Spruce. The least squares fit of the sequential data for event 2 yielded:

$$[\text{throughfall volume}] = 0.732 [\text{wetfall volume}] - b_2 \quad (4.2)$$

where b_2 is equal to 0.250.

The holdup volume of Red Spruce is equal to 0.342 liters, which is much higher than the holdup volume of American Beech. The result is reasonable since a general increase in interception capacity with increasing leaf area is expected.

In order to calculate the throughfall volume from one stage to the next, a modified version of Eq. (4.1) is used:

$$TF_{\downarrow}^k = m^{1/N} * (TV^{k-1} - \text{HOLDUP}/N) \quad (4.3)$$

where TF_{\downarrow}^k is the throughfall volume entering the k^{th} tank; TV^{k-1} is the total volume in the $k-1^{\text{st}}$ tank; m is the slope of Eqs. (4.1) or (4.2); N is the number of tanks and HOLDUP

is the holdup volume under investigation.

Predictions of throughfall chemistry were made by a simple mixing model superimposed on a hydrology model. That is, the incoming throughfall (or wet deposition in the first tank) enters a stage and completely mixes with any water already present. Stages must be completely filled before any stemflow or overflow to the next compartment occurs. Further, while the water is on any given stage, the plant system may either take up (uptake) or give off (leaching) nutrients from the water.

During the model development, the system was treated as a black box with known inputs and output. The difference between inputs and output should yield the leaching parameters, if done on a mass basis. Since the system is assumed to leach material constantly, one may expect that the difference between output and input will increase based on a cumulative mass basis. In the absence of field evaluation of the foliar uptake rate, the variables of uptake and leaching are combined as the net leachate. The leaching coefficients for the American Beech based on this black box model are presented in Table V. In examining the leaching coefficients, one notes that some are positive, indicating leaching; while others are negative, indicating absorption by the plant system.

A conceptualization framework of the simulation of throughfall model is illustrated in Figure 13. The model calculates the throughfall volume and ion concentrations

TABLE V
LEACHING COEFFICIENTS OBTAINED FROM BLACK BOX MODEL
(American Beech)

<u>Ion</u>	<u>Leaching Coefficient</u> ($\mu\text{eq}/\text{min}$)
Hydrogen	-0.022
Sulfate	-0.004
Nitrate	-0.004
Chloride	-0.001
Ammonium	-0.005
Calcium	0.007
Magnesium	0.0007
Sodium	0.007
Potassium	0.016

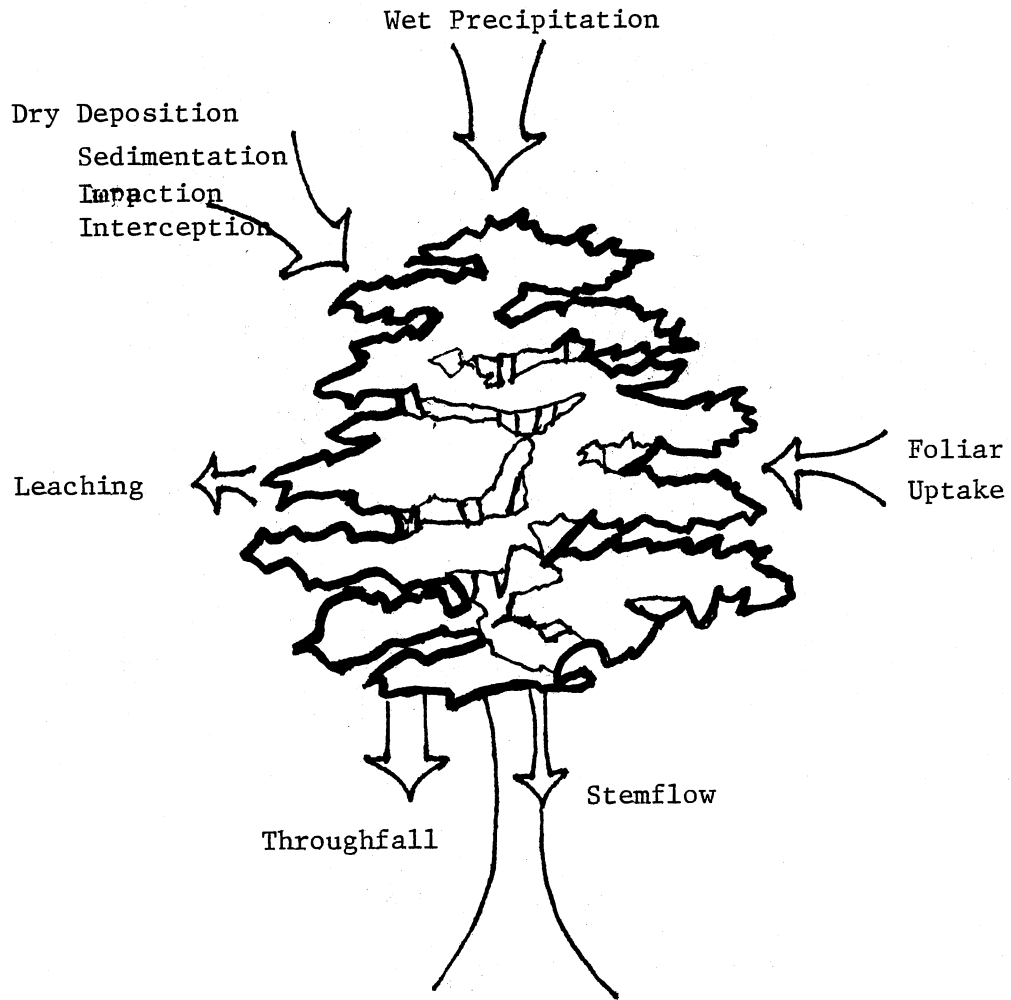


Figure 13. Model Conceptualization

with respect to time. A Fortran program was written and is documented in Appendix B.

Construction of the Model

A flow diagram of computer simulation program is presented in Figures 14 and 15. The model reads in the following data:

- * Vegetation data (canopy characteristics)
 - Holdup of the tree (HOLDUP)
 - Leaf area index (LAI)
 - Slope of the Eq. (4.1) or (4.2)
 - Intercept of the Eq. (4.1) or (4.2)
- * Incident precipitation chemistry within an event
- * Throughfall chemistry within an event
- * Leaching coefficients and dry deposition

Canopy data was presented in Table I, and incident precipitation chemistry and sequential throughfall data are taken directly from Appendix A.

One important subject in the study of forested area is that of Leaf area index (LAI). As stated previously, the LAI is defined as the ratio of canopy leaf surface area to its covered ground surface area. It is actually a dimensionless measure of the amount of vegetative cover there is over the ground. Knowledge of leaf area and its distribution is essential for estimating photosynthesis, transpiration, respiration and canopy interception (Gholz et al., 1976).

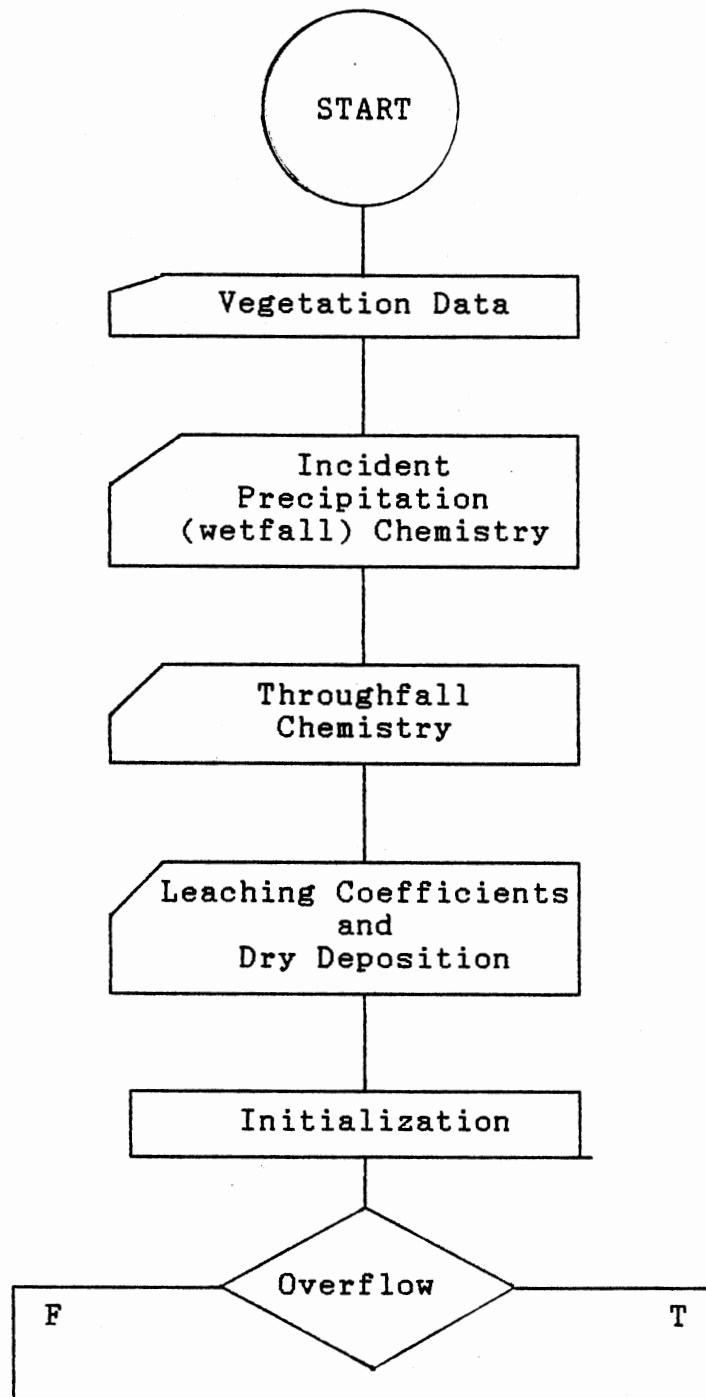


Figure 14. Flow Diagram for Mixing Model

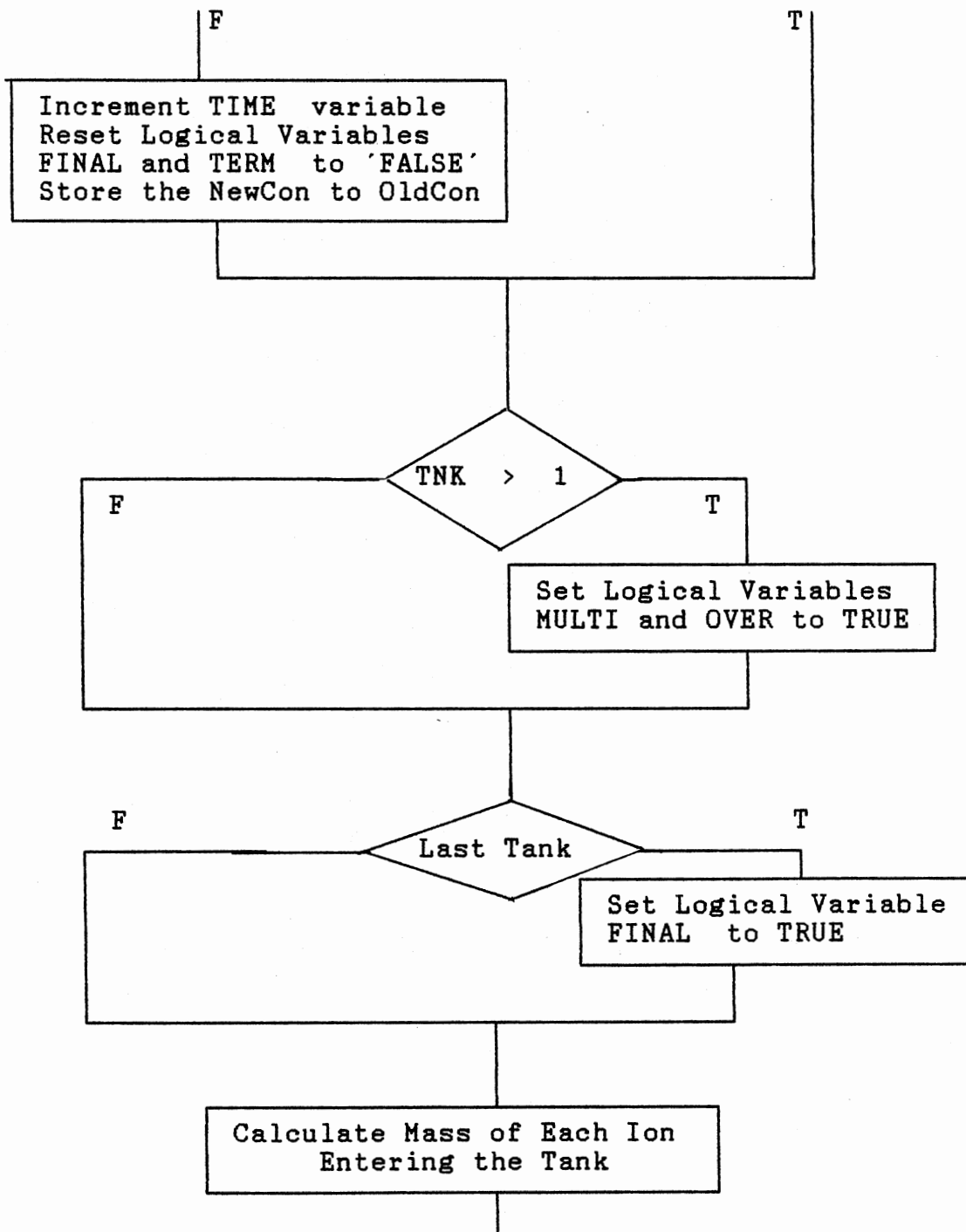


Figure 14. (Continued)

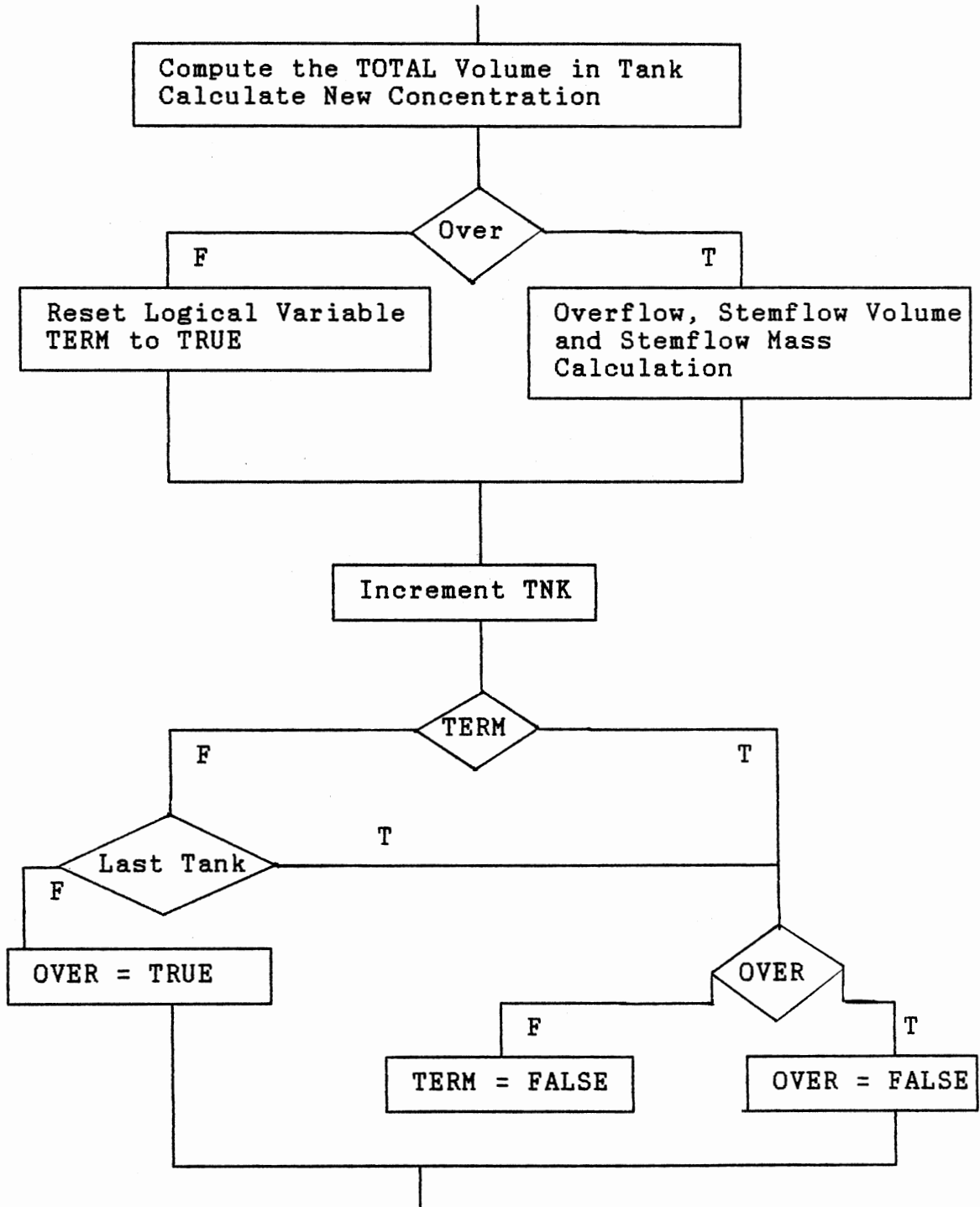


Figure 14. (Continued)

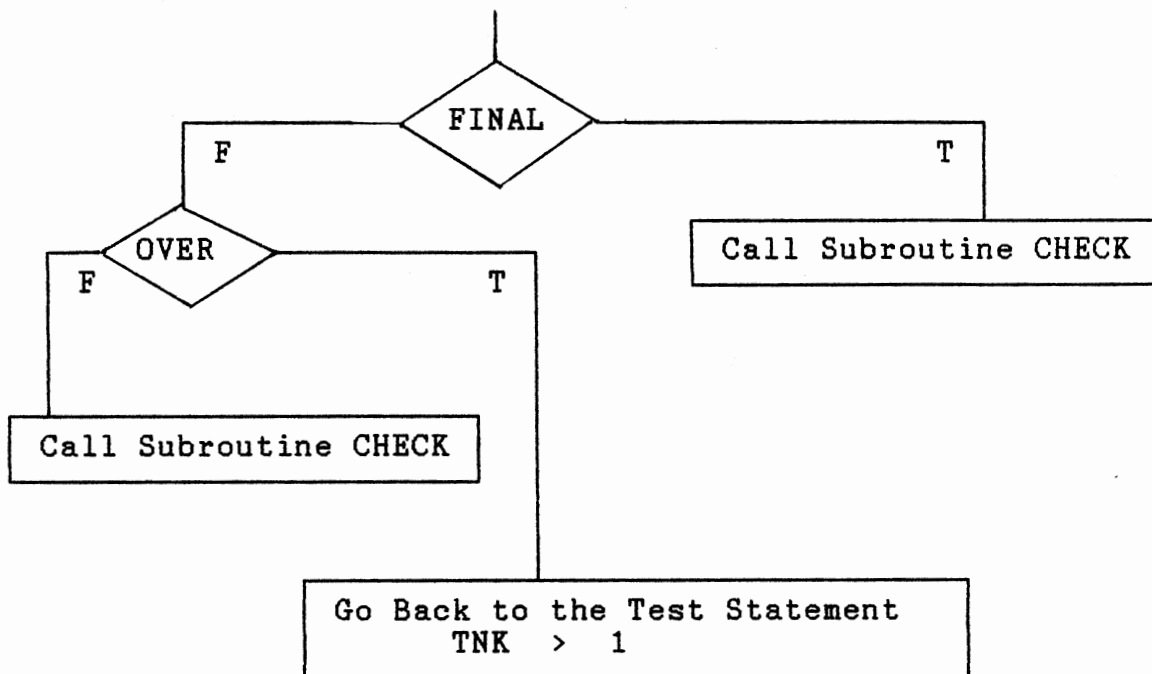


Figure 14. (Continued)

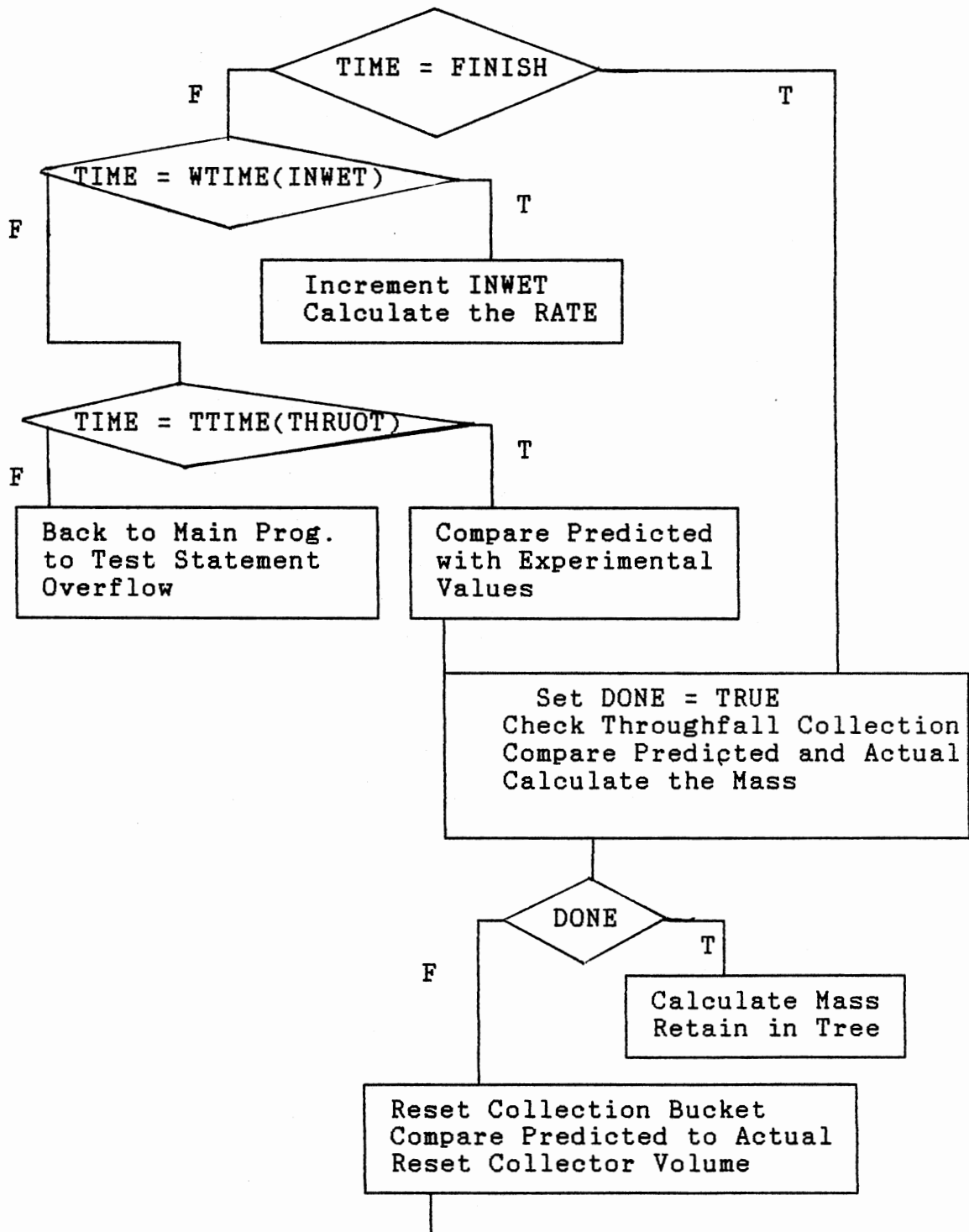


Figure 15. Flow Diagram of Subroutine CHECK

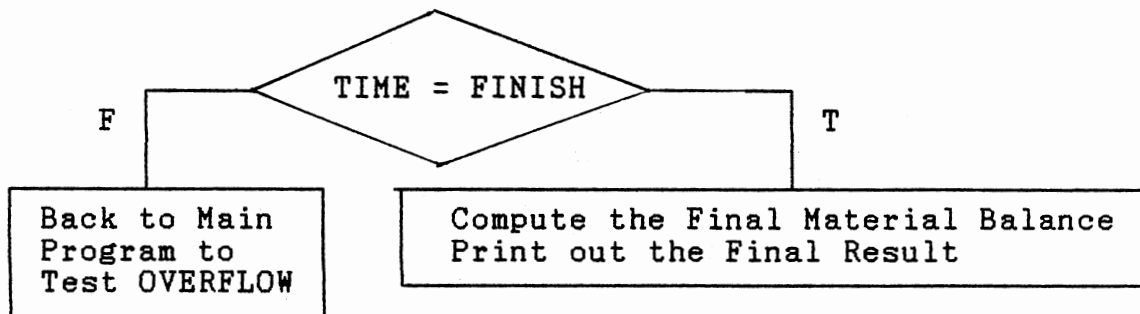


Figure 15. (Continued)

Event throughfall concentrations are calculated by initially setting dry deposition values for each ion in each compartment. When a compartment is wetted, the dry material within that compartment is totally dissolved and the dry deposition value is ignored for the rest of the run for that compartment. Adjustment of the collection area with respect to the wetfall collection in the calculation of dryfall loadings are summarized below:

$$\begin{aligned}
 DD_1 &= \frac{DC_1}{DR} * \frac{\text{Collection area of funnel}}{\text{Collection area of open bucket}} \\
 &= \frac{DC_1}{DR} * \frac{2 * \frac{\pi}{4} * D_{\text{funnel}}^2}{\frac{\pi}{4} * D_{\text{bucket}}^2} \\
 &= 0.2212 * DC_1
 \end{aligned}$$

where DD_1 is the value of the dry deposition for the 1st ion (μeq); DC_1 is the dry concentration of the 1st ion ($\mu\text{eq/l}$); D_{funnel} is the diameter of the funnel (19 cm); D_{bucket} is the diameter of the dryfall bucket (28.6 cm) and DR is dilution ratio, in this study, DR=4.

The leaching coefficients listed in Table V were used as input data. New chemical concentrations were calculated for the stored water and this concentration was assigned to the throughfall generated by the model.

Implementation

In order to keep the model simple, a 'focus until finish' philosophy was adopted. For example, if a rain drop enters compartment 1, only the drop is followed until it either cascades into a subsequent compartment or it enters the collector as throughfall. It is also noted that the time scale we are dealing with is very long. An appropriate time interval, 1 minute in this case, has been chosen to reflect the accuracy of the temporal data.

Finally, the wetfall and throughfall collections rarely occur at the same time. A logical flow was designed to first check for new wetfall data, then for the throughfall collection. If throughfall collection is indicated, current values of predicted throughfall concentrations are printed for comparison with measured values. The collection is then reset, and a check for program termination is made. For no throughfall collection, control is directed to the top of cascade for the next time interval.

The model was set up to simulate the throughfall quality and quantity. Results were compared to the throughfall data listed in Appendix A and are presented in the following chapter.

CHAPTER V

RESULTS AND DISCUSSIONS OF MIXING MODELS

Quality Control of Data

In order to make valid estimates of parameters, experimental error in the data on which the estimates are based must be known. A quality control program is therefore necessary to ensure the accuracy of the sampling technique and the analytical methods. Although it is very difficult to estimate the magnitude of the sampling and analytical error, a quality control procedure which included analysis of replicates, standard additions, U.S. EPA unknowns and laboratory prepared standards was employed by Johannes et al. (1984). The results (summarized in Appendix C) showed that the precision of the instrumental methods was generally within five percent. At very low concentrations, fifteen percent errors can be encountered. Thus, the experimental data collected by Dackson (1983) provides representative data for calibration and testing of the mixing model.

American Beech

The model is run using the base case with no leaching or dry deposition, as a first trial. A check of simple material balances is shown for water, sulfate, and potassium

for events 1 , 2 and 7 in Table VI. Although the measured throughfall volume was often less than predicted, the calculated water balance showed excellent agreement with the measured values for event 2 (Figure 16). Predicted sulfate, and ammonium concentrations, shown in Figures 17 and 18, were closely matched except for the first two data points. Figure 19 showed the difference between the predicted throughfall concentrations of potassium ion and the measured data. Concentrations versus time for all other ions appear in Table VII.

Several important differences between the predicted and measured data, on an individual ion basis, were noted. In the case of NO_3^- , no apparent net release of NO_3^- by the canopy has been indicated. Although nitric acid vapor is an extremely reactive vapor and may deposit readily to external surfaces, it is believed that canopies can take up NO_3^- from incident precipitation. Therefore, we may conclude that the nitrate budget is complete and no leaching and uptake of nitrate will take place. Similar observations are made for chloride and magnesium ions for event 2. The model underpredicts throughfall concentrations of metallic cations and hydrogen ion.

Dry deposition was introduced next. Lindberg and Lovett (1985) have demonstrated that dissolution of most surface-deposited material occurs within 3-4 minutes after leaves are wetted. Thus, we expect that any dry deposition effect to be manifested only in the first time interval of

TABLE VI
 MATERIAL BALANCE FOR EVENT 1, 2 AND 7
 WITHOUT LEACHING AND DRY DEPOSITION
 (American Beech)

<u>Water Balance (ml.)</u>	<u>Event1</u>	<u>Event2</u>	<u>Event7</u>
Total Input Volume	1589.0	2526.0	3003.0
Total Thrufall Volume			
Predicted	1067.0	1724.0	2050.6
Measured	988.0	1568.0	2068.0
Total Stemflow Volume			
Predicted	492.0	795.0	946.0
Volume Retained(Holdup)	7.0	7.0	7.0
Total In-Out-Holdup	23.0	0.0	0.0
<u>Sulfate</u>			
Input Wet Mass	40.0	31.0	92.0
Total Dry Mass	0.0	0.0	0.0
Total Mass Leached	0.0	0.0	0.0
Total Thrufall Mass	27.0	21.0	63.0
Total Stemflow Mass	12.0	10.0	29.0
Total Mass Retained	0.0	0.0	0.0
Total In-Out-Holdup	1.0	0.0	0.0
<u>Potassium</u>			
Input Wet Mass	2.0	2.0	10.0
Total Dry Mass	0.0	0.0	0.0
Total Mass Leached	0.0	0.0	0.0
Total Thrufall Mass	2.0	2.0	7.0
Total Stemflow Mass	1.0	1.0	3.0
Total Mass Retained	0.0	0.0	0.0
Total In-Out-Retained	0.0	0.0	0.0

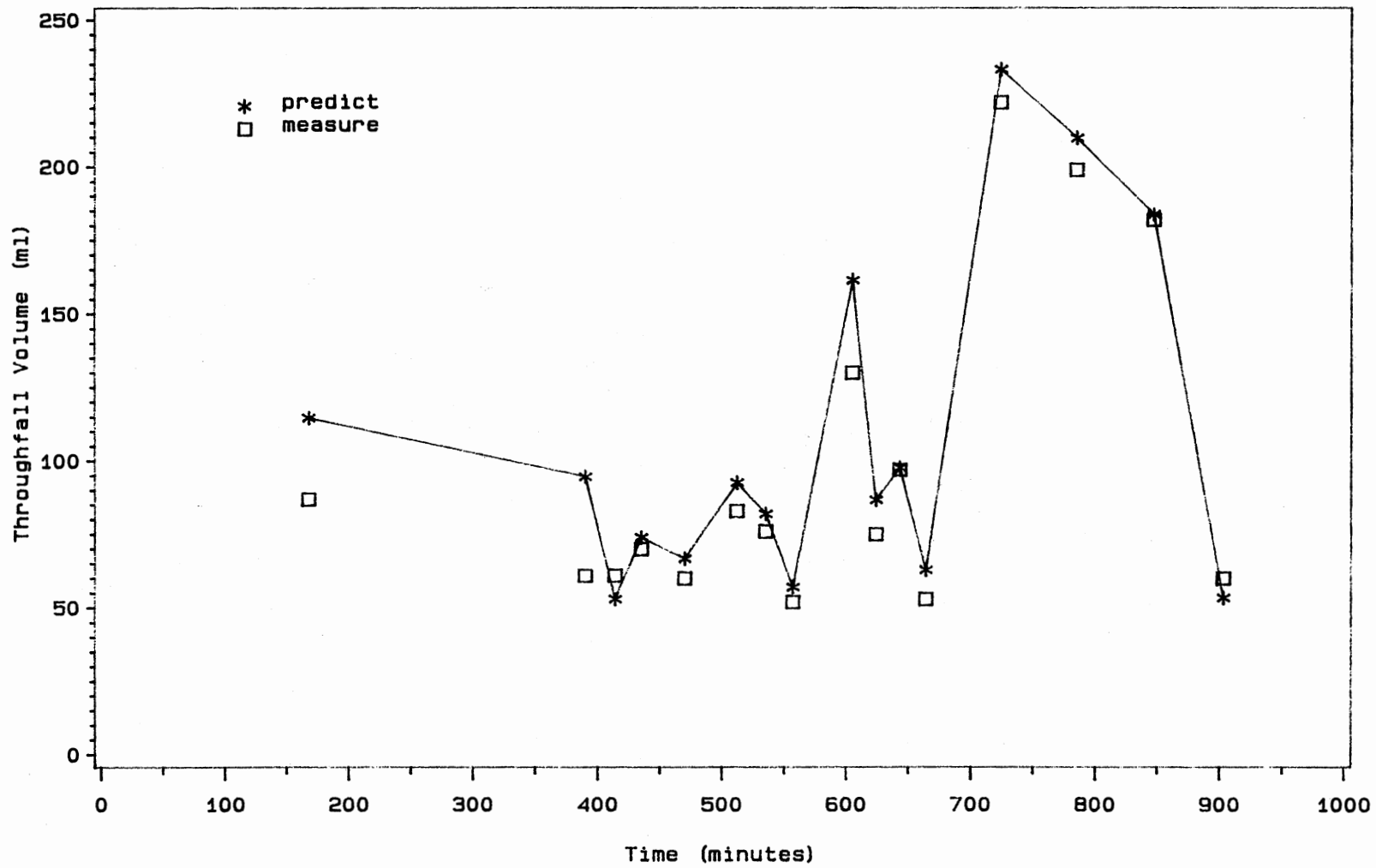


Figure 16. Predicted and Measured Throughfall Volume in Event 2

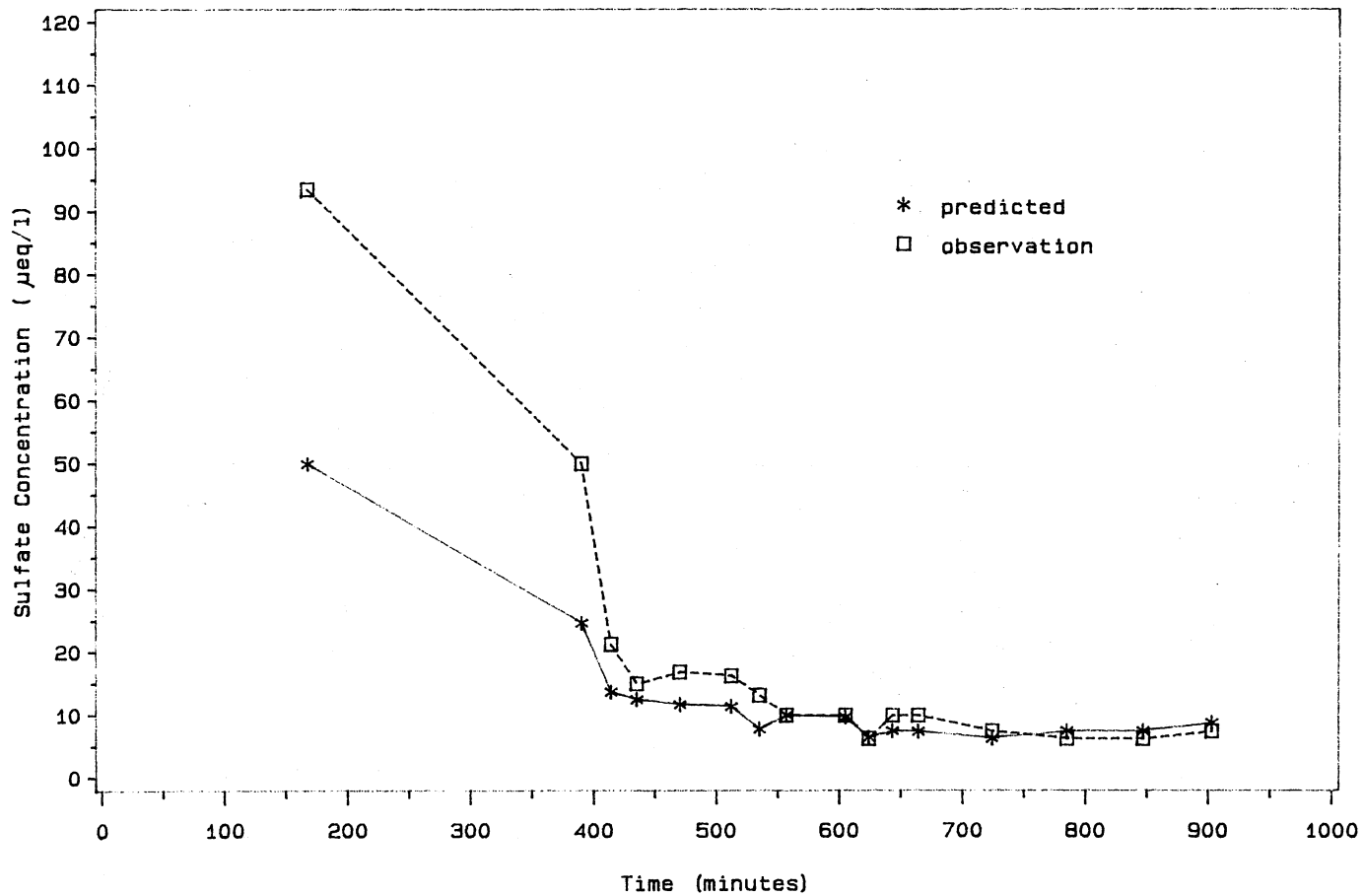


Figure 17. Concentration Distribution of Sulfate Ion in Event 2 (American Beech)

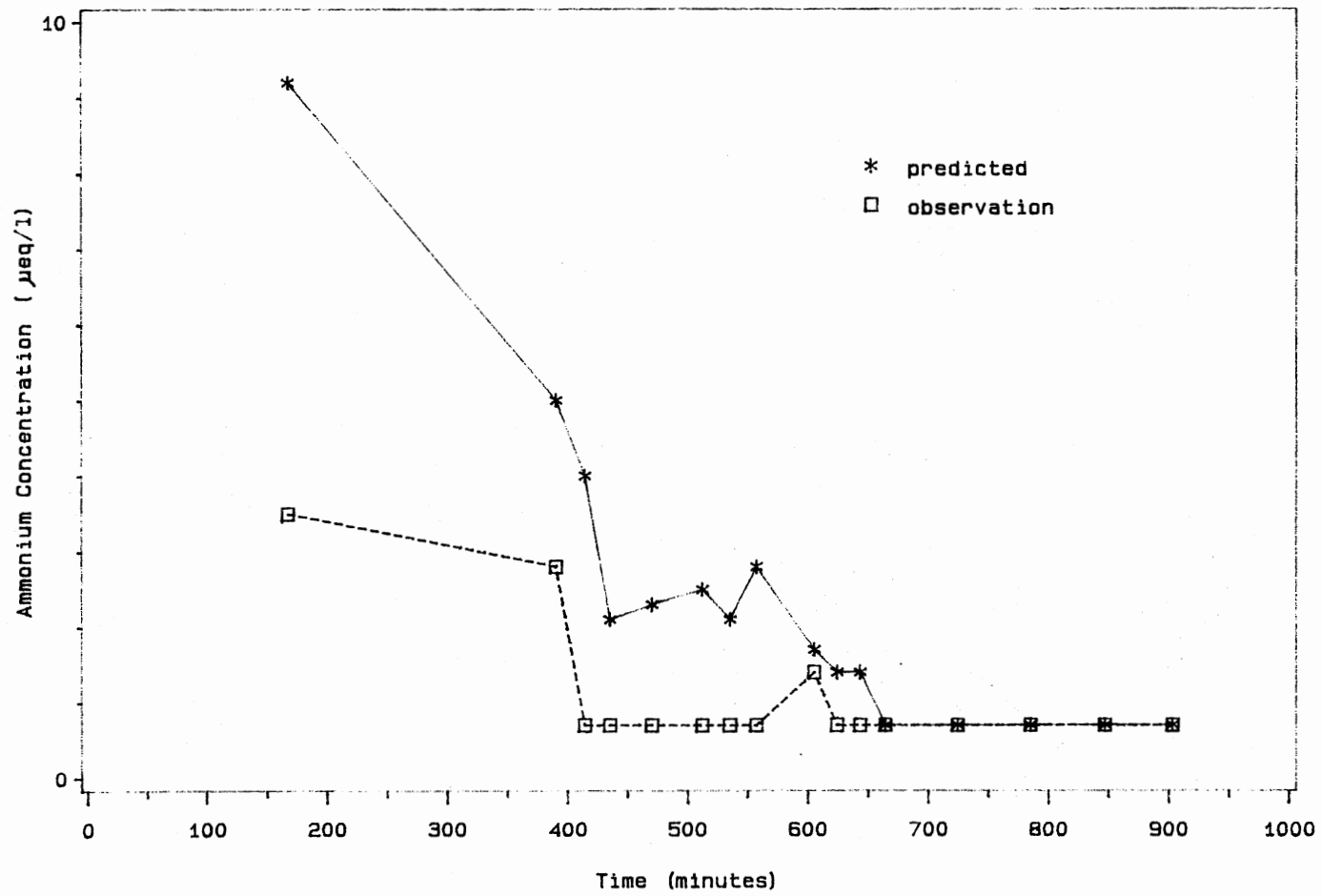


Figure 18. Concentration Distribution of Ammonium Ion in Event 2 (American Beech)

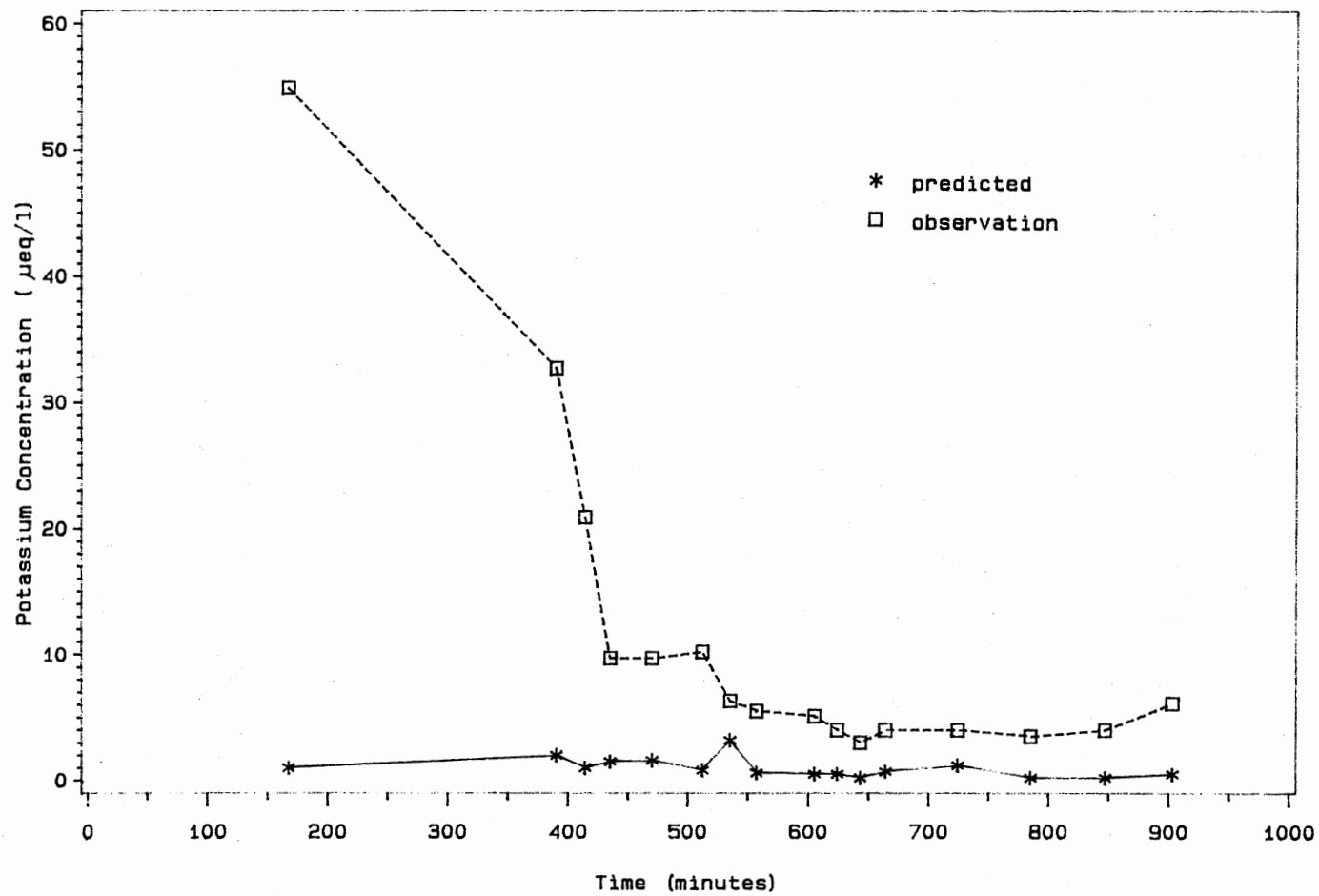


Figure 19. Concentration Distribution of Potassium Ion in Event 2 (American Beech)

TABLE VII
 CONCENTRATIONS VERSUS TIME FOR EVENT2
 WITHOUT DRY DEPOSITION AND LEACHING
 (American Beech)

Time (mins)	concentrations ($\mu\text{eq/l}$)					
	H ⁺		NO ₃ ⁻		Cl ⁻	
	<u>Pred.</u>	<u>Meas.</u>	<u>Pred.</u>	<u>Meas.</u>	<u>Pred.</u>	<u>Meas.</u>
167	35.9	33.1	32.1	37.1	2.8	9.0
390	16.7	18.6	7.2	17.8	4.7	5.6
414	8.1	9.5	3.8	5.7	2.9	3.3
435	5.4	11.0	2.1	2.8	1.6	1.4
470	6.8	11.2	2.0	3.5	1.4	1.6
512	7.9	9.8	3.2	3.5	1.9	1.6
535	1.6	7.4	2.2	2.1	1.5	0.8
557	6.5	6.8	2.8	2.8	1.9	1.6
605	8.1	9.3	3.0	2.8	1.4	0.5
624	3.1	4.6	0.7	1.4	1.1	0.8
643	4.8	3.8	0.7	0.7	1.1	0.8
664	3.2	4.5	1.3	1.4	1.5	1.9
724	3.0	4.1	0.7	0.7	0.5	0.8
785	4.2	2.9	0.7	0.7	0.5	0.8
847	4.0	4.0	0.7	0.7	0.5	0.8
903	6.6	4.8	2.1	1.4	1.4	2.2

TABLE VII (Continued)

concentrations ($\mu\text{eq/l}$)

Time (mins.)	Ca ⁺²		Mg ⁺²		Na ⁺	
	<u>Pred.</u>	<u>Meas.</u>	<u>Pred.</u>	<u>Meas.</u>	<u>Pred.</u>	<u>Meas.</u>
167	34.9	3.4	1.2	14.8	2.6	3.9
390	5.0	17.9*	1.0	7.4	6.8	2.1
414	2.4	8.9	0.9	3.2	3.9	2.8
435	4.3	5.4	0.8	1.6	1.9	8.9
470	2.1	6.4	0.8	1.5	1.3	10.9
512	0.8	1.5	1.9	12.6*	0.8	10.2
535	1.5	3.4	1.2	1.5	1.8	2.3
557	1.9	0.4	0.8	1.4	2.1	125.0*
605	1.8	2.2	0.8	1.0	1.1	1.3
624	1.4	3.4	0.8	0.8	1.0	1.9
643	0.9	2.4	0.8	0.8	1.0	1.0
664	2.3	2.1	0.8	0.8	2.4	2.8
724	0.9	1.9	0.8	0.8	0.8	1.3
785	1.4	1.9	0.8	0.8	1.3	0.8
847	0.4	2.4	0.8	0.8	2.6	1.0
903	1.9	2.4	0.8	1.6	1.7	3.9

* : indicates the experimental data might be inaccurate

sulfates, ammonium, and potassium ions versus time are presented in Figures 20 through 22.

Good agreements between predicted sulfate concentrations and observed values. Temporal variation of predicted and observed ammonium ion is presented in Figure 21. It is observed from this figure that predicted values follow similar trends of observed values except for first few collection points. As before, the predicted concentrations of potassium ion were significant lower than the measured values. The only major difference is at the first collection point, when initial washoff of dry deposition takes place.

Leaching coefficients shown in Table V were used as inputs along with dry deposition. Negative concentration values for nitrate, chloride, and ammonium were obtained at some collection points. The possible interpretation is that leaching does not occur at a constant rate during the event.

Next, suitable values for leaching parameters were obtained by trial and error, so that the predicted concentration was within the acceptable range. The leaching coefficients listed in Table VIII were used so that the best fit can be obtained. Figure 23 shows the result for potassium by using both leaching parameter and dry deposition. A significant improvement for the fit of potassium curve is noted. Therefore, very good estimates of measured values can be obtained by adding in the leaching

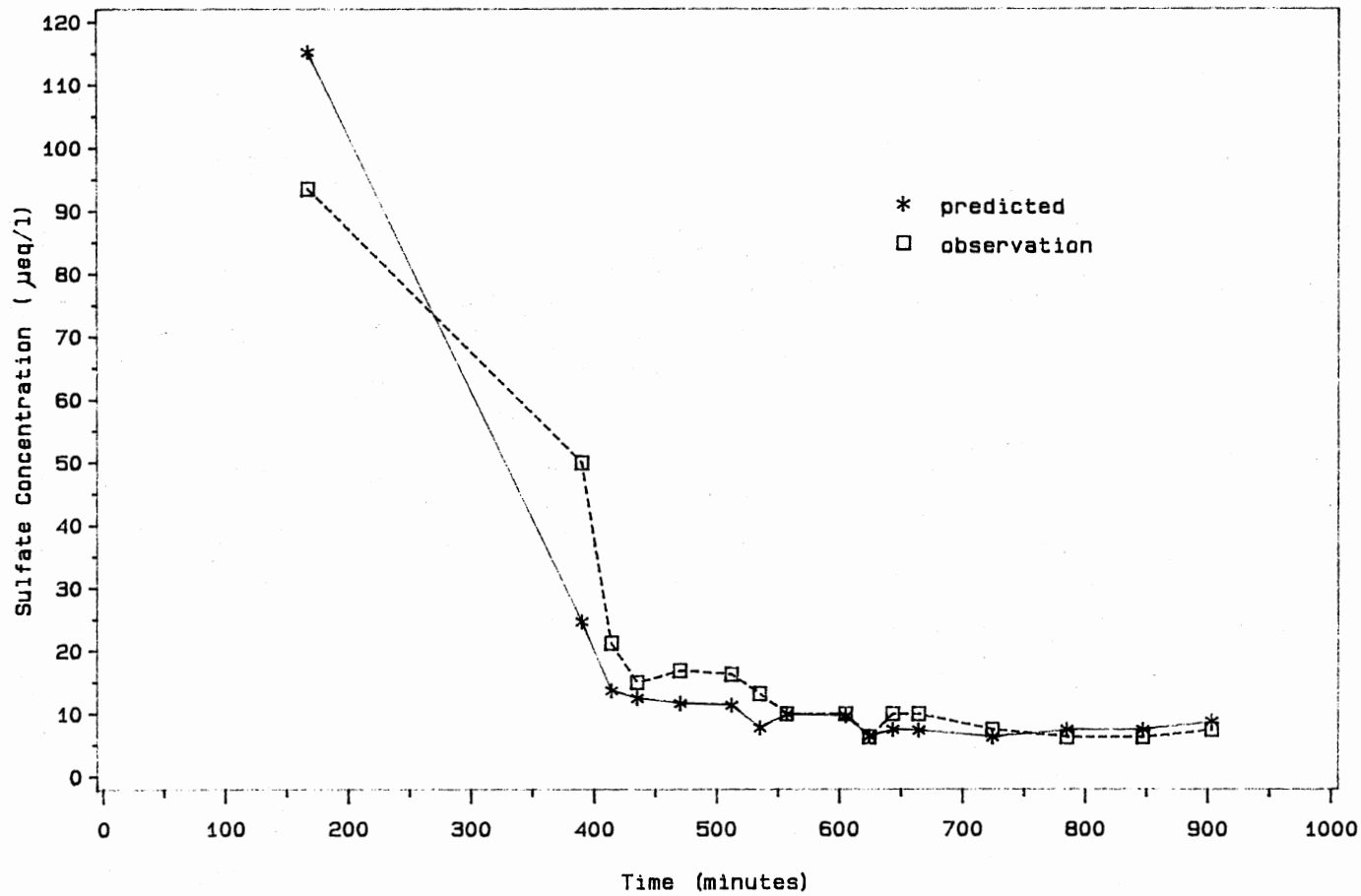


Figure 20. Concentration Distribution of Sulfate Ion in Event 2 with Dry Deposition (American Beech)

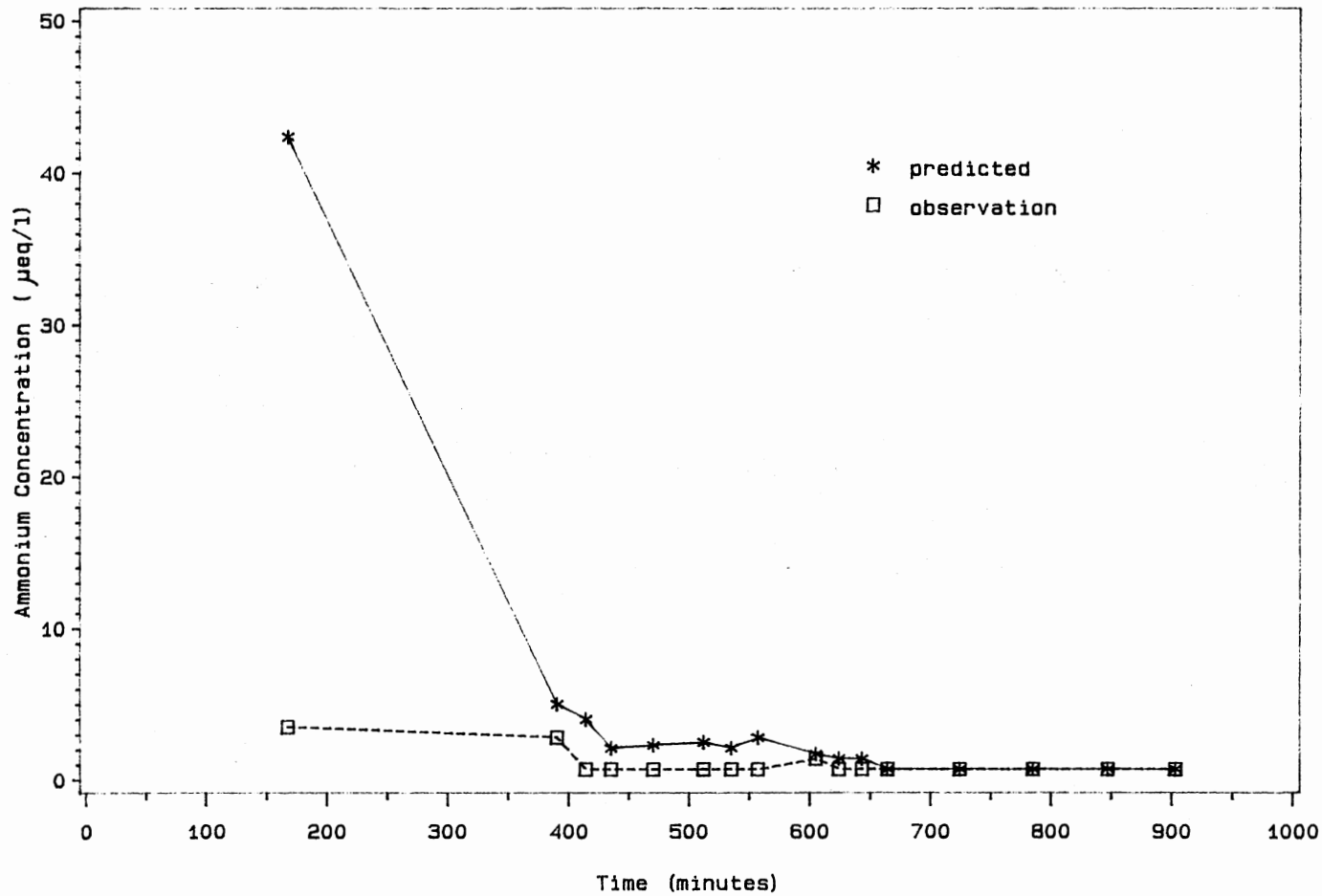


Figure 21. Concentration Distribution of Ammonium Ion in Event 2 with Dry Deposition (American Beech)

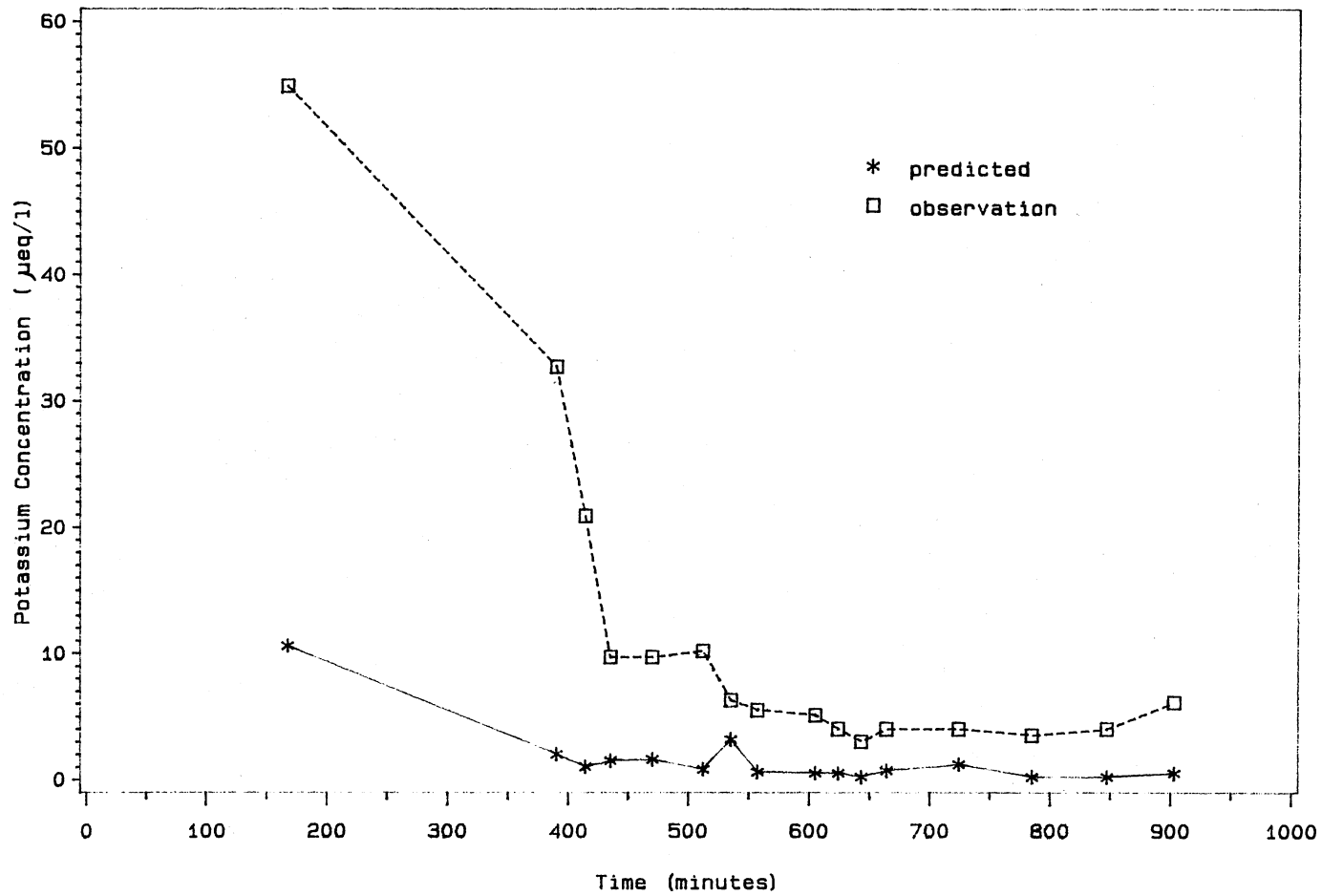


Figure 22. Concentration Distribution of Potassium Ion in Event 2 with Dry Deposition (American Beech)

TABLE VIII
LEACHING COEFFICIENTS USED IN THE MIXING MODEL
(American Beech)

Ion	<u>Leaching Coefficients</u> ($\mu\text{eq}/\text{min}$)
Hydrogen	-0.022
Sulfate	0.0015
Nitrate	0.0
Chloride	0.0
Ammonium	0.0
Calcium	0.003
Magnesium	0.0003
Sodium	0.001
Potassium	0.01

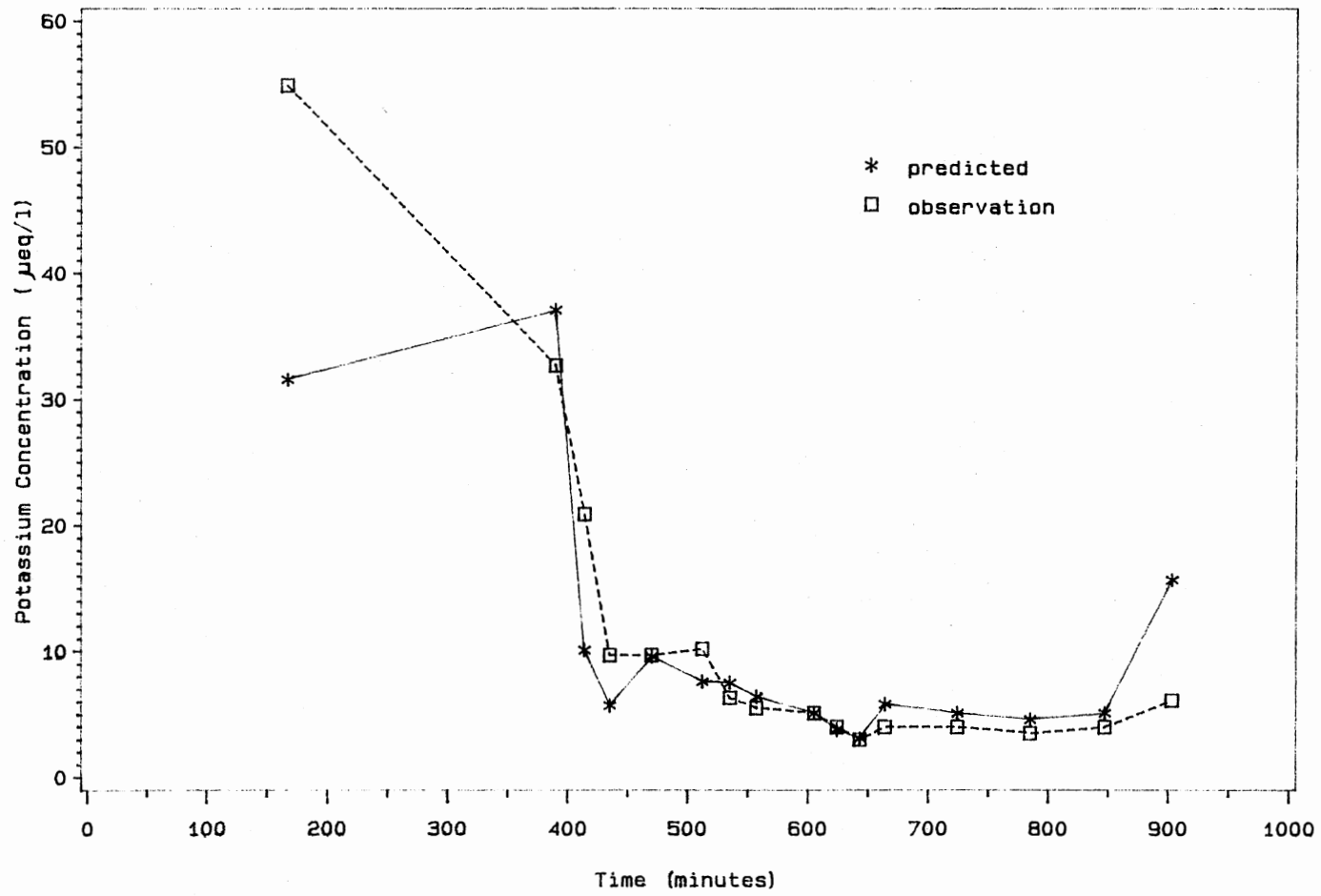


Figure 23. Concentration Distribution of Potassium Ion in Event 2 with Dry Deposition and Leaching (American Beech)

factor for potassium ion. Again, data for other species, with leaching parameters included, is presented in Table IX. Table X summarized the complete material balances which included the leaching parameters (in Table VIII) and dry deposition factors.

The model was then rerun on event 1 and 7 respectively, using the same leaching coefficients derived for Table VIII. Sulfate concentrations showed excellent agreement with the measured results for event 1, as shown in Figure 24. For potassium ion concentrations, shown in Figure 25, the accuracy of predictions are within 35 percent of observed values. Similar agreement was found for the other cations and anions except for H^+ , Ca^{+2} , and Mg^{+2} .

For event 7, the predictions of potassium concentrations showed a reasonable agreement with the measured results (Figure 26). Figure 27 shows that sulfate concentrations are generally underpredicted, which may be caused by the variability of the leaching parameter between events. In reality, the intensity and volume of rain has a significant effect on leaching efficiency. Rain which falls as a light drizzle will remove considerably more nutrients than will a greater quantity of water which falls in a short period of time. The results indicate a higher net effluent of SO_4^{-2} from the canopy, therefore, a higher positive leaching parameter is recommended.

TABLE IX
 THROUGHFALL CONCENTRATIONS VERSUS TIME IN EVENT 2
 WITH DRY DEPOSITION AND LEACHING COEFFICIENTS
 (American Beech)

concentrations ($\mu\text{eq/l}$)

Time (mins.)	H ⁺		NO ₃ ⁻		Cl ⁻	
	<u>Pred.</u>	<u>Meas.</u>	<u>Pred.</u>	<u>Meas.</u>	<u>Pred.</u>	<u>Meas.</u>
167	35.5	33.1	81.9	37.1	20.9	9.0
390	22.0	18.6	7.2	17.8	4.7	5.6
414	6.7	9.5	3.8	5.7	2.9	3.3
435	6.1	11.0	2.1	2.8	1.6	1.4
470	8.0	11.2	2.0	3.5	1.4	1.6
512	8.9	9.8	3.2	3.5	1.9	1.6
535	2.3	7.4	2.2	2.1	1.5	0.8
557	7.3	6.8	2.8	2.8	1.9	1.6
605	8.8	9.3	3.0	2.8	1.4	0.5
624	3.6	4.6	0.7	1.4	1.1	0.8
643	5.3	3.8	0.7	0.7	1.1	0.8
664	4.0	4.5	1.3	1.4	1.5	1.9
724	3.6	4.1	0.7	0.7	0.5	0.8
785	4.8	2.9	0.7	0.7	0.5	0.8
847	4.7	4.0	0.7	0.7	0.5	0.8
903	8.8	4.8	2.1	1.4	1.4	2.2

TABLE IX (Continued)

concentrations ($\mu\text{eq/l}$)

Time (mins)	Ca ⁺²		Mg ⁺²		Na ⁺	
	Pred.	Meas.	Pred.	Meas.	Pred.	Meas.
167	104.7	3.4	17.2	14.8	19.3	3.9
390	14.9	17.9	1.8	7.4	10.3	2.1
414	5.0	8.9	1.1	3.2	4.8	2.8
435	5.5	5.4	0.9	1.6	2.4	8.9
470	4.4	6.4	1.0	1.5	2.1	10.9
512	4.3	1.5	1.0	12.6*	2.6	10.2
535	2.7	3.4	1.3	1.5	2.2	2.3
557	3.5	0.4	1.0	1.4	2.7	125.0*
605	3.0	2.2	0.9	1.0	1.6	1.3
624	2.3	3.4	0.9	0.8	1.3	1.9
643	1.8	2.4	0.9	0.8	1.3	1.0
664	3.7	2.1	0.9	0.8	2.9	2.8
724	2.0	1.9	0.9	0.8	1.2	1.3
785	2.6	1.9	0.9	0.8	1.8	0.8
847	1.8	2.4	0.9	0.8	3.1	1.0
903	6.2	2.4	1.2	1.6	3.2	3.9

* : indicates the experimental data might be inaccurate

TABLE X
 FINAL MATERIAL BALANCE FOR EVENT 2
 WITH LEACHING AND DRY DEPOSITION
 (American Beech)

Water Balance (ml.)

Total Input Volume	2526.0
Total Thrufall Volume	
Predicted	1724.0
Measured	1568.0
Total Stemflow Volume	
Predicted	795.0
Volume Retained(Holdup)	7.0
Total In-Out-Holdup	0.0

Sulfate (μ eq)

Input Wet Mass	31.0
Total Dry Mass	10.0
Total Mass Leached	3.0
Total Thrufall Mass	30.0
Total Stemflow Mass	13.0
Total Mass Retained	0.0
Total In-Out-Holdup	0.0

Potassium (μ eq)

Input Wet Mass	2.0
Total Dry Mass	2.0
Total Mass Leached	18.0
Total Thrufall Mass	16.0
Total Stemflow Mass	5.0
Total Mass Retained	0.0
Total In-Out-Holdup	0.0

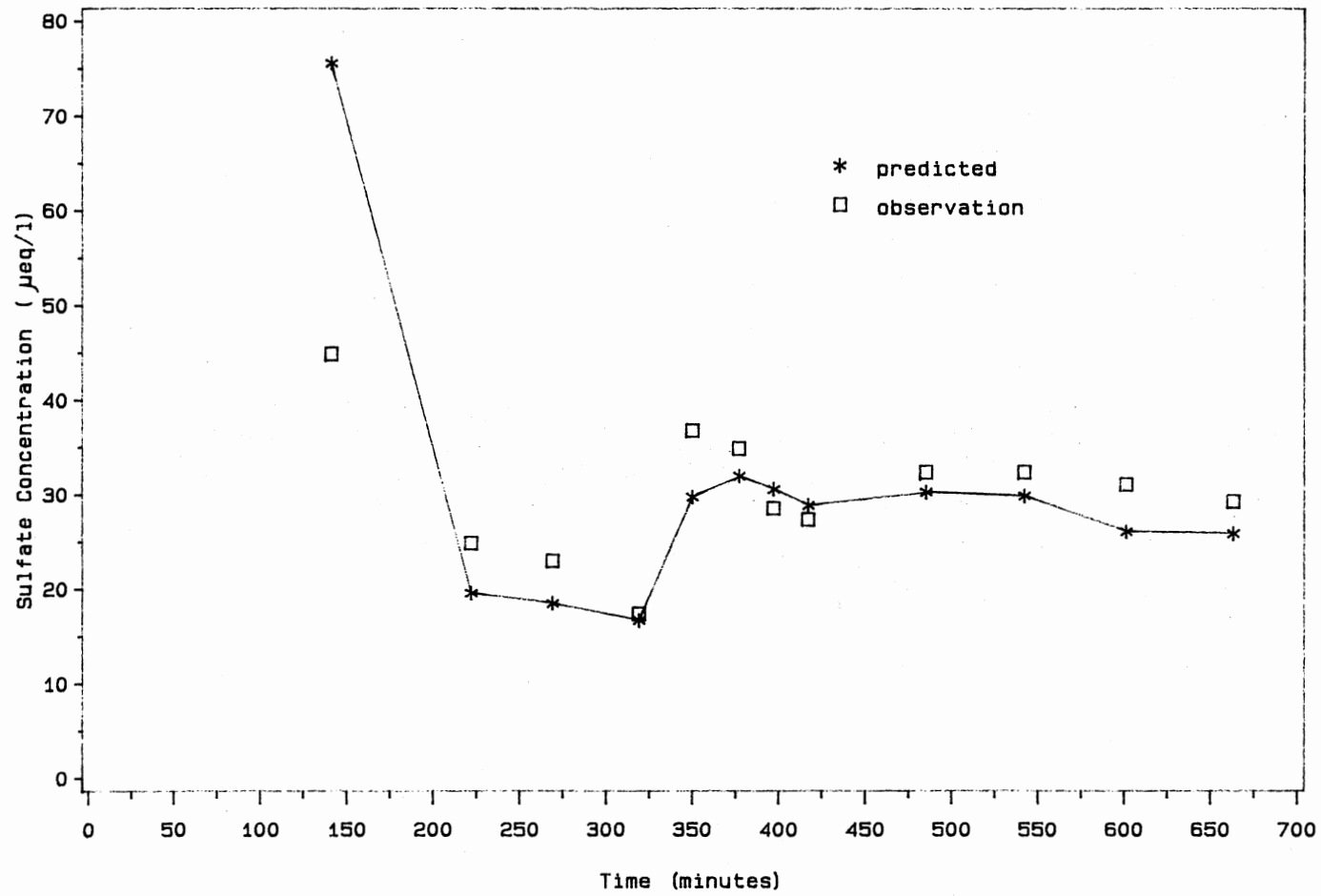


Figure 24. Throughfall Concentration of Sulfate Ion in Event 1 (American Beech)

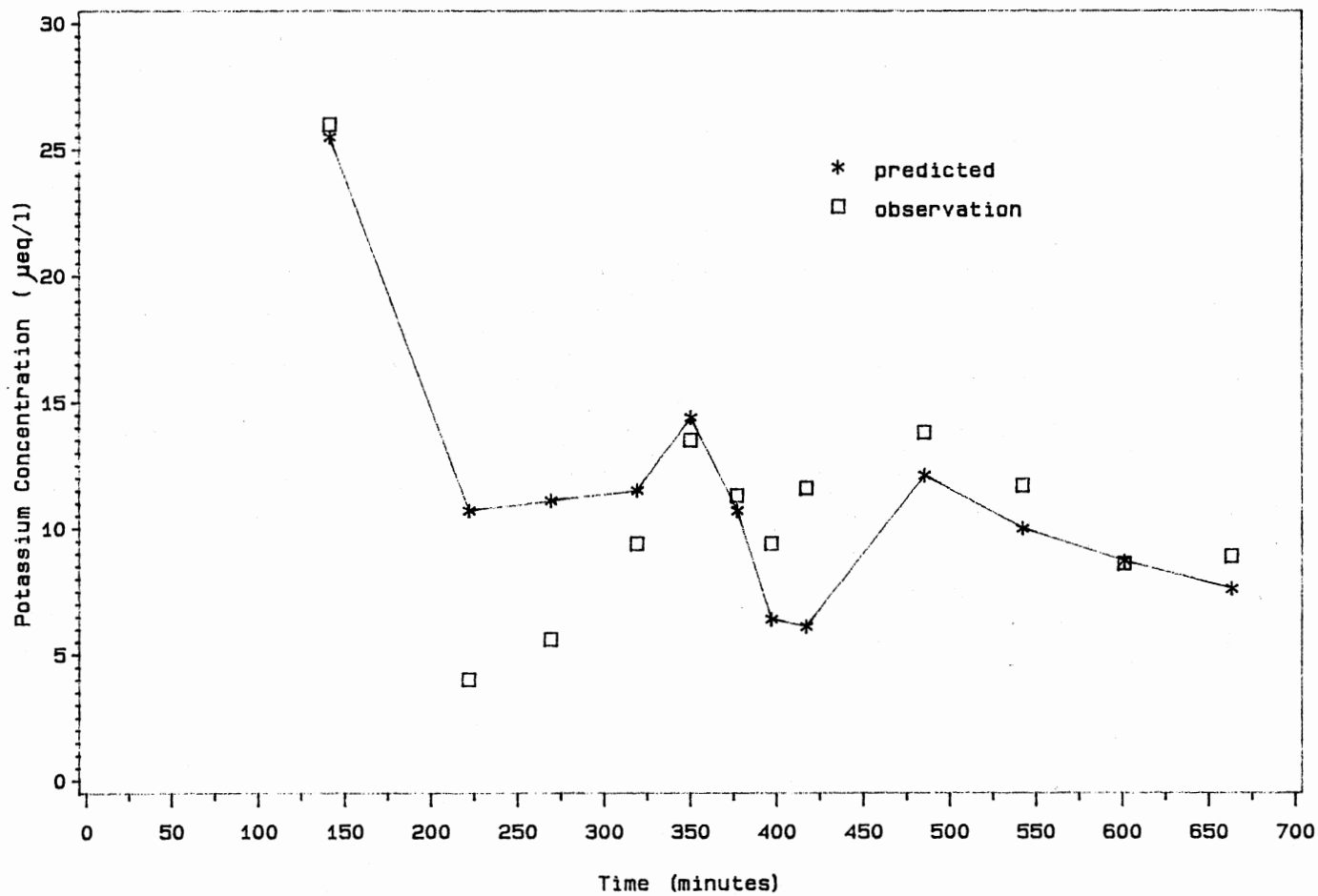


Figure 25. Throughfall Concentration of Potassium Ion in Event 1 (American Beech)

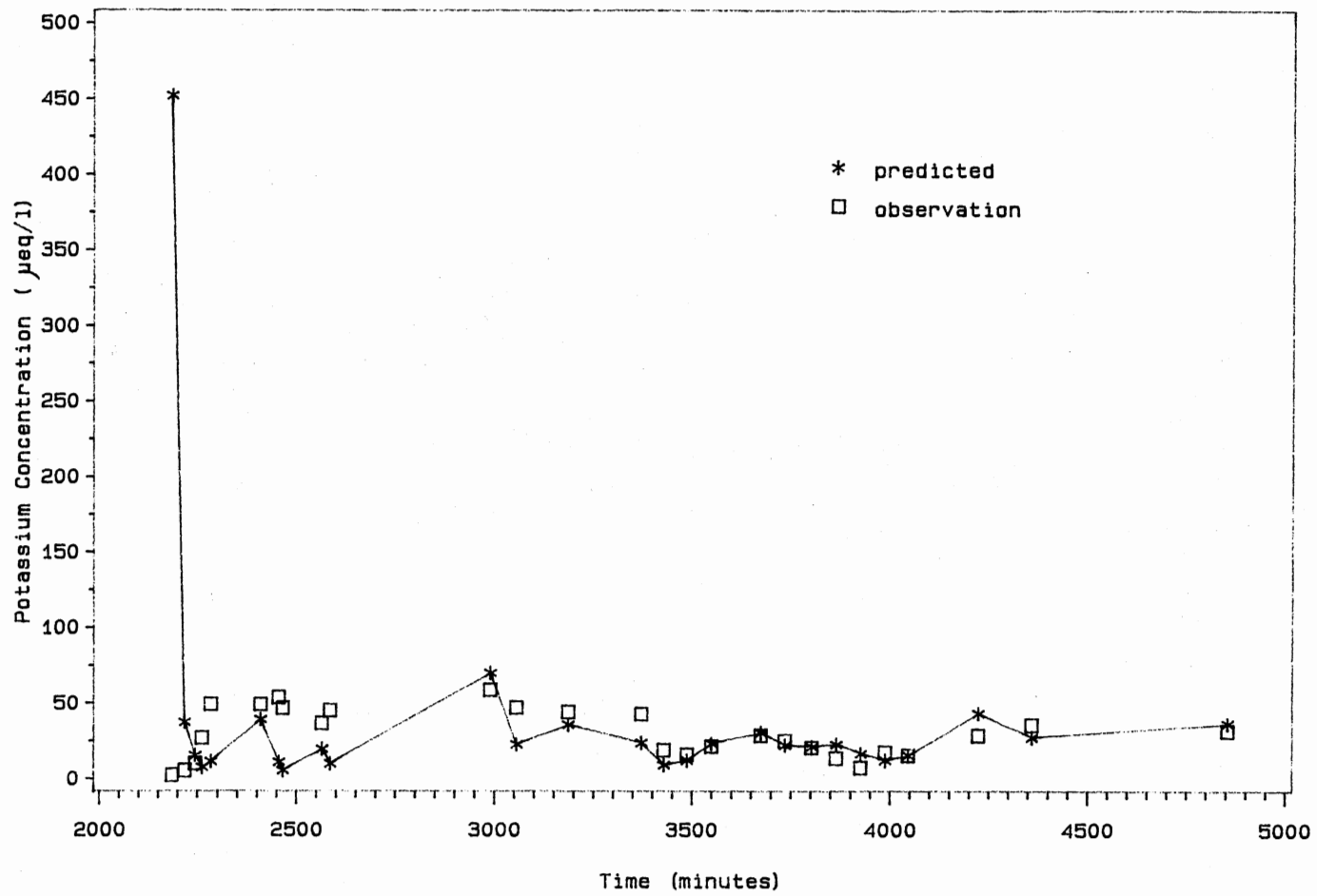


Figure 26. Throughfall Concentration of Potassium Ion in Event 7 (American Beech)

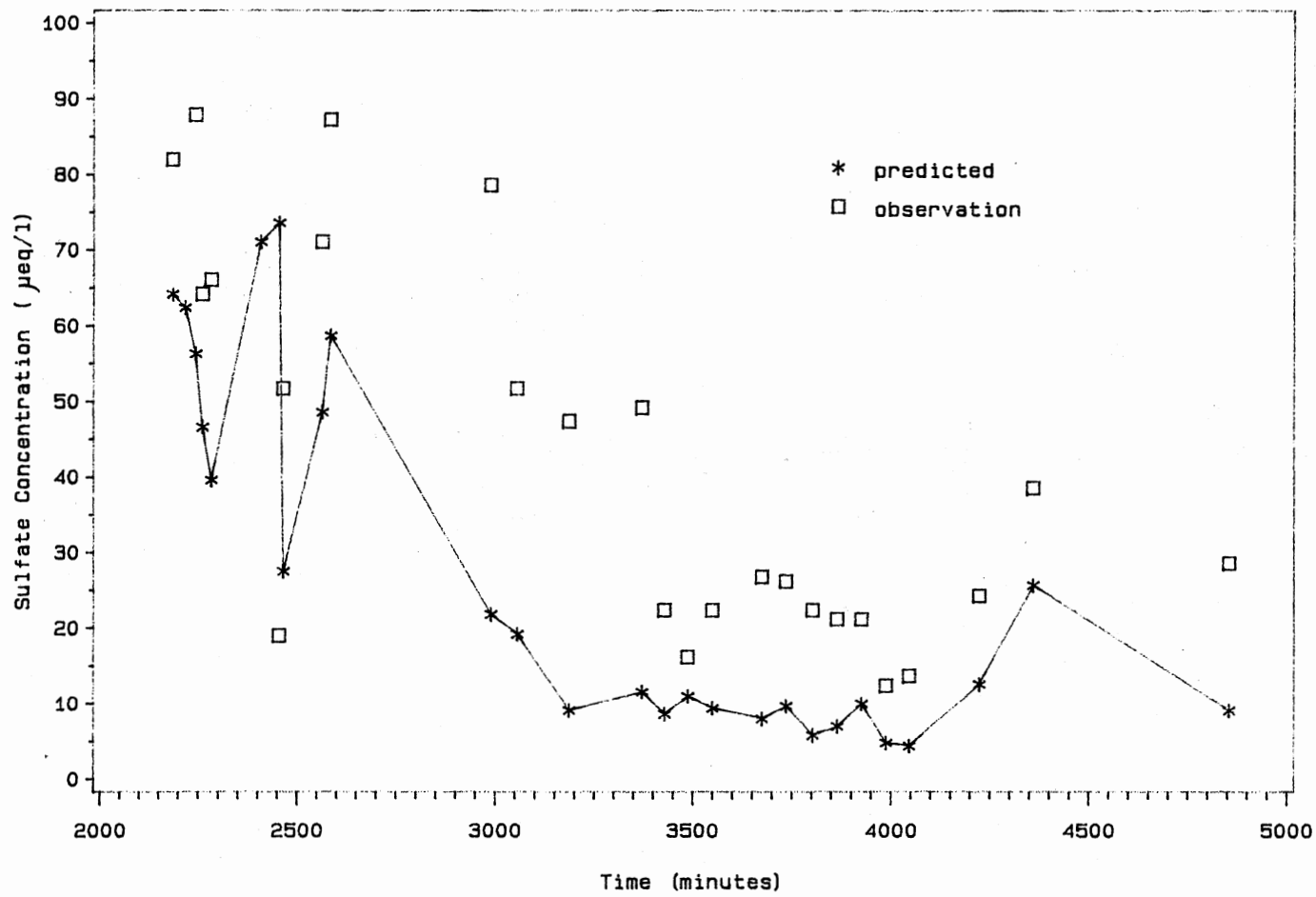


Figure 27. Throughfall Concentration of Sulfate Ion in Event 7 (American Beech)

Red Spruce

A check of simple material balance of Red Spruce for event 2, with no leaching and dry deposition, has been made (Table XI). The results, presented in Figure 28, showed an excellent agreement between predicted throughfall volume and the measured data. It is noted the predicted throughfall volume is zero at the first collection point because of large holdup volume requirement for Red Spruce.

The predicted throughfall concentrations of SO_4^{-2} is presented in Figure 29. A significant under-prediction of throughfall concentration has been observed. Further, a comparison of the experimental throughfall concentrations of sulfate ion of the two trees suggest a greater leaching ability of sulfate from Red Spruce than from American Beech. This may have occurred because of greater surface area of better retention capability of rainfall of the conifer.

Figure 30 showed the difference between the predicted throughfall concentration profile and the measured values of potassium ion. The fact that event wetfall did not account for the corresponding throughfall concentrations for potassium ion indicate inputs of throughfall other than wetfall. Moreover, the very high ranges of potassium ion in throughfall compared with those in wetfall apparently indicate important components of throughfall other than wetfall.

Table XII presented the throughfall concentration profile for H^+ , NO_3^- , Cl^- , Ca^{+2} , Mg^{+2} , and Na^+ .

TABLE XI
 MATERIAL BALANCE FOR EVENT 2
 WITHOUT LEACHING AND DRY DEPOSITION
 (Red Spruce)

<u>Water Balance</u> (ml.)	<u>Event2</u>
Total Input Volume	2526.0
Total Thrufall Volume	
Predicted	1563.0
Measured	1639.0
Total Stemflow Volume	
Predicted	621.0
Volume Retained(Holdup)	342.0
Total In-Out-Holdup	0.0
 <u>Sulfate.</u> (µeq)	
Input Wet Mass	31.0
Total Dry Mass	0.0
Total Mass Leached	0.0
Total Thrufall Mass	20.0
Total Stemflow Mass	8.0
Total Mass Retained	3.0
Total In-Out-Holdup	0.0
 <u>Potassium.</u> (µeq)	
Input Wet Mass	2.0
Total Dry Mass	0.0
Total Mass Leached	0.0
Total Thrufall Mass	2.0
Total Stemflow Mass	1.0
Total Mass Retained	0.0
Total In-Out-Retained	0.0

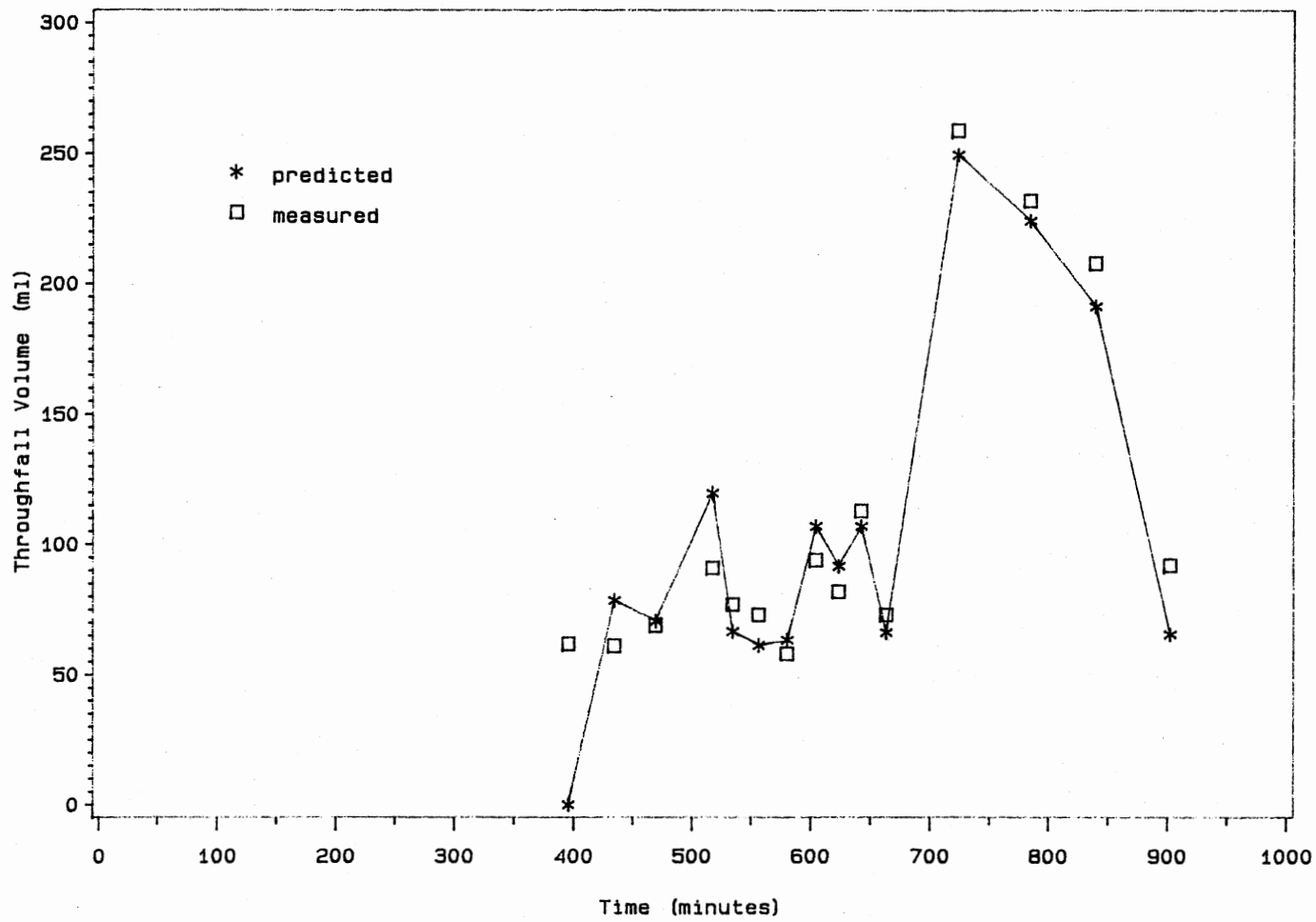


Figure 28. Predicted and Measured Throughfall Volume in Event 2 (Red Spruce)

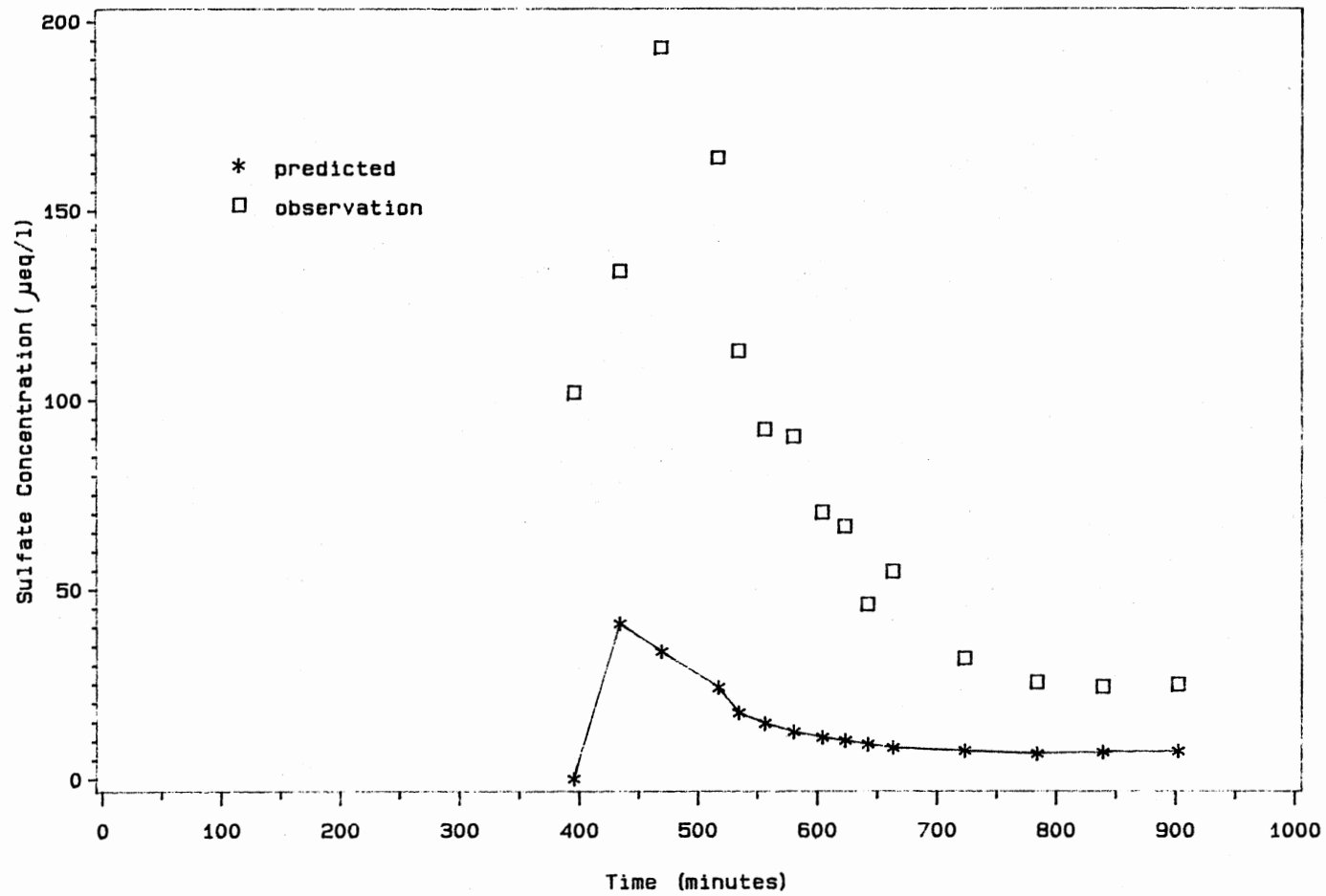


Figure 29. Throughfall Concentration of Sulfate Ion in Event 2 (Red Spruce)

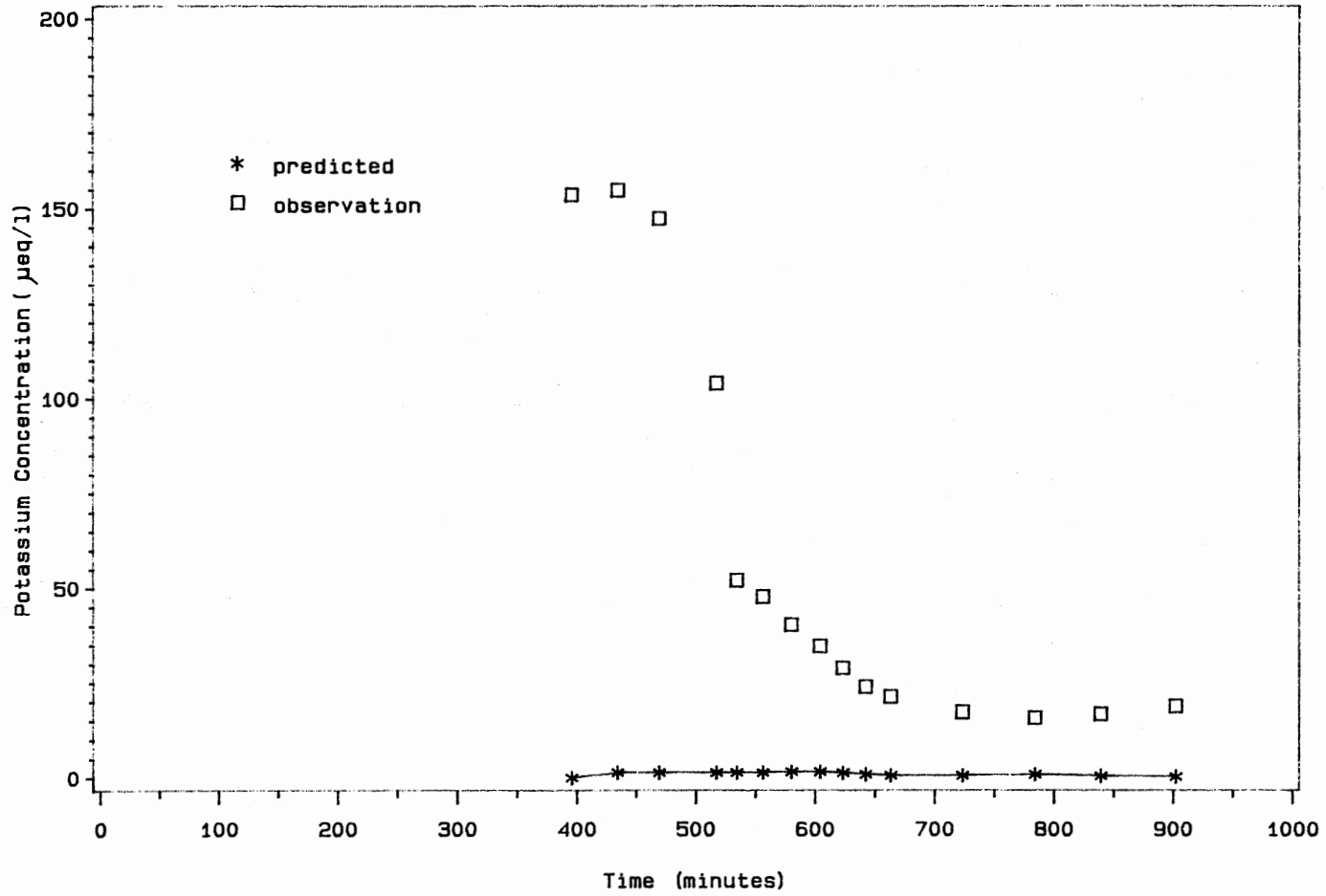


Figure 30. Throughfall Concentration of Potassium Ion in Event 2 (Red Spruce)

TABLE XII
 CONCENTRATION VERSUS TIME FOR EVENT2
 WITHOUT DRY DEPOSITION AND LEACHING
 (Red Spruce)

concentrations, $\mu\text{eq/l}$

Time (mins)	H ⁺		NO ₃ ⁻		Cl ⁻	
	Pred.	Meas.	Pred.	Meas.	Pred.	Meas.
395	0.0	61.7	0.0	22.8	0.0	12.9
434	28.9	69.2	23.5	9.9	3.5	15.2
469	23.4	91.2	17.6	4.9	3.4	21.1
517	15.9	83.2	10.5	4.2	2.9	18.3
534	11.0	63.1	6.0	2.8	2.3	15.7
556	9.0	56.2	4.5	2.8	2.0	20.3
580	7.3	51.3	3.6	2.1	1.9	14.1
604	6.3	39.8	3.1	2.1	1.8	12.6
623	6.6	34.7	3.0	1.4	1.7	15.5
642	6.4	27.5	2.6	1.4	1.5	8.7
663	5.6	25.1	2.0	1.4	1.3	10.1
723	4.5	20.0	1.2	0.7	1.1	7.3
784	3.4	18.6	0.8	0.7	0.7	7.6
839	3.8	17.0	0.7	1.4	0.5	7.8
902	4.0	16.2	0.7	1.4	0.5	8.1

TABLE XII (Continued)

concentrations, $\mu\text{eq/l}$

<u>Time</u> (mins)	<u>Ca+2</u>		<u>Mg+2</u>		<u>Na+</u>	
	<u>Pred.</u>	<u>Meas.</u>	<u>Pred.</u>	<u>Meas.</u>	<u>Pred.</u>	<u>Meas.</u>
395	0.0	N.A.	0.0	N.A.	0.0	N.A.
434	24.6	N.A.	1.1	6.9	4.2	18.2
469	18.0	N.A.	1.0	9.3	4.2	3.0
517	10.8	51.8	1.0	7.6	3.6	4.7
534	6.2	26.4	0.9	7.5	2.7	5.2
556	4.5	20.9	0.9	6.7	2.7	7.3
580	3.3	16.1	0.9	36.2*	2.1	6.2
604	2.5	12.4	0.9	4.2	2.0	5.4
623	2.1	12.9	0.9	4.1	1.7	3.6
642	1.8	10.9	0.8	2.8	1.4	2.6
663	1.6	9.9	0.8	3.2	1.2	3.6
723	1.4	6.4	0.8	1.6	1.3	13.2*
784	1.2	6.4	0.8	1.6	1.1	1.9
839	1.2	5.9	0.8	1.6	1.3	2.1
902	1.0	7.4	0.8	2.8	1.8	2.3

N.A. : experimental data is missing

* : indicates the experimental data might be inaccurate

Throughfall showed a gain in the quantities of most the elements, except NH_4^+ , over those in incident precipitation. It is probably that a large part of the throughfall enrichment in Cl^- , SO_4^{2-} , Ca^{+2} , Mg^{+2} , Na^+ , and K^+ is derived from the dry deposits and/or leached metabolites.

Dry deposition as well as the best fit of leaching coefficients for American Beech (listed in Table VIII) were introduced into the model. Plots of simulated and measured sulfates and potassium ions are presented in Figures 31 and 32. Concentrations profile for all other ions are given in Table XIII. As noted, the predicted concentrations of sulfate and potassium ions, although improved, were still lower than the measured values. This discrepancy suggests higher net effluent of SO_4^{2-} and K^+ from the Red Spruce tree.

In fact, throughfall loadings generally increased with increasing leaf surface area. This is probably due to greater dryfall collection and increased availability of leachable ions. Higher leaching parameters are therefore recommended so that the predicted concentrations are within the acceptable range.

Significant improvement of the predication of SO_4^{2-} and K^+ concentration profiles can be obtained by using the leaching coefficients listed in Table XIV (shown in Figures 33 and 34). As before, these leaching coefficients were obtained by trial and error. Results for other species, with leaching coefficients shown in Table XIV, are presented

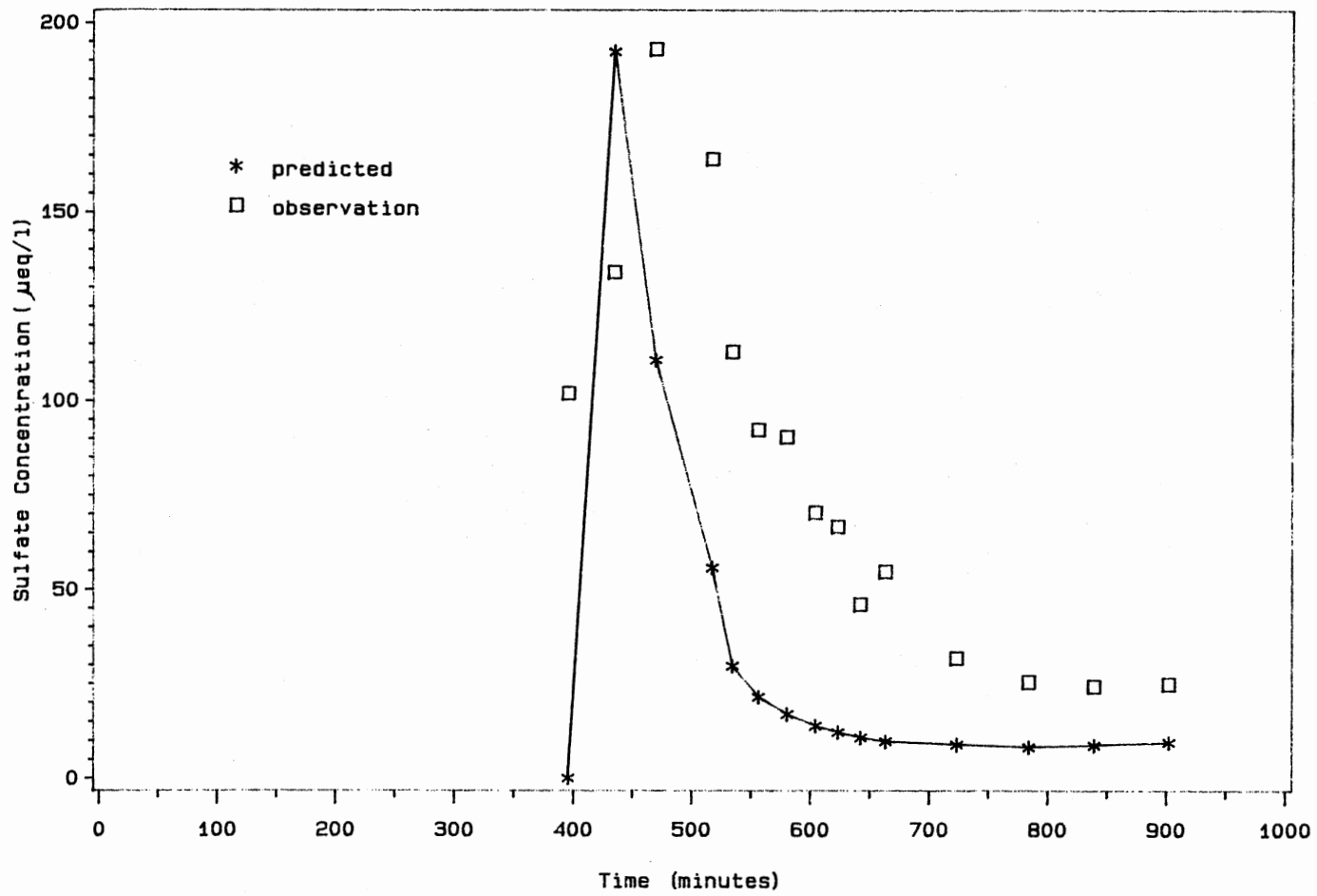


Figure 31. Throughfall Concentration of Sulfate Ion in Event 2 with Dry Deposition and Leaching (Red Spruce)

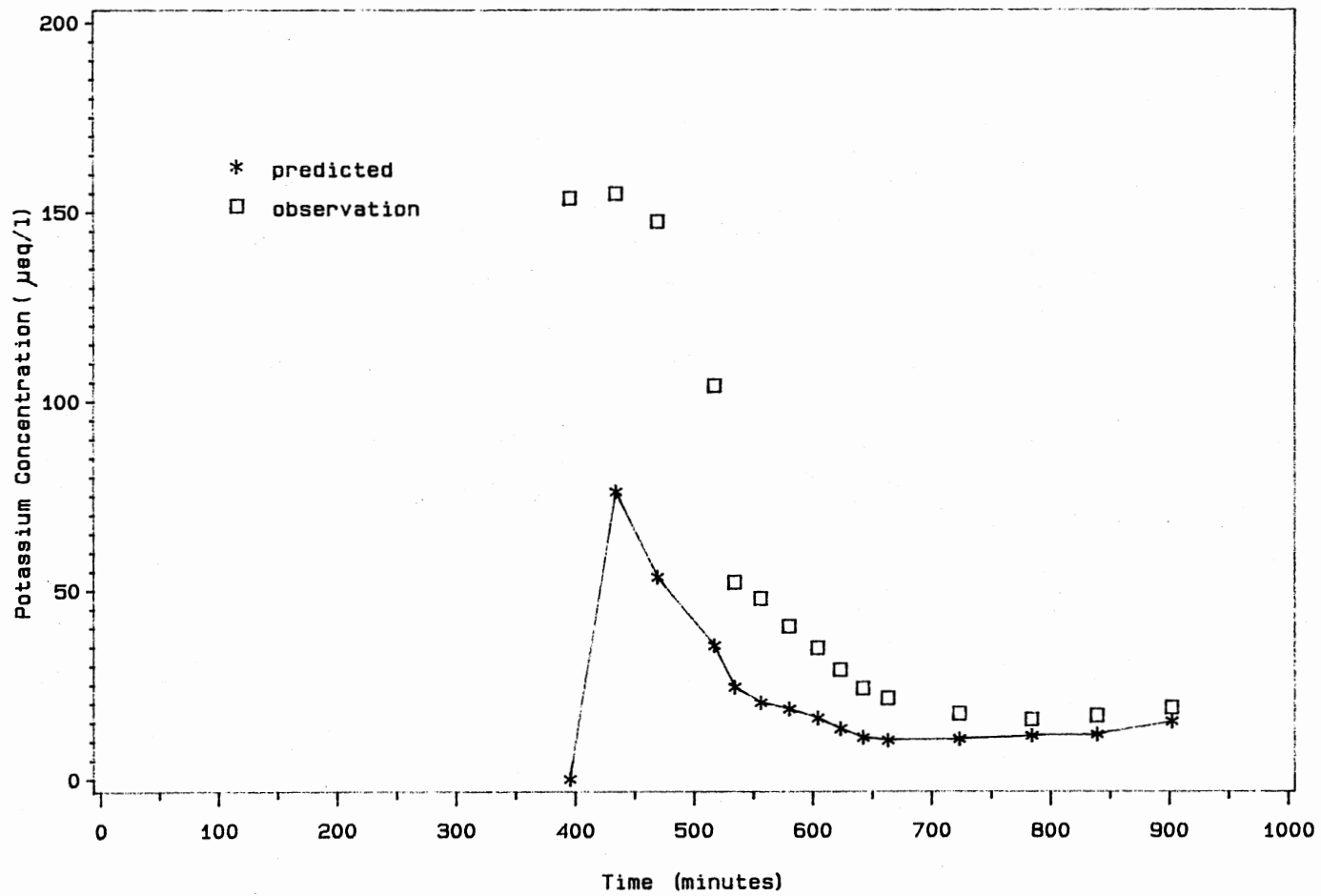


Figure 32. Throughfall Concentration of Potassium Ion in Event 2 with Dry Deposition and Leaching (Red Spruce)

TABLE XIII
 THROUGHFALL CONCENTRATIONS VERSUS TIME IN EVENT 2
 WITH DRY DEPOSITION AND LEACHING COEFFICIENTS
 (Red Spruce)

concentrations, $\mu\text{eq/l}$

<u>Time</u> (mins)	<u>H+</u>		<u>NO3-</u>		<u>Cl-</u>	
	<u>Pred.</u>	<u>Meas.</u>	<u>Pred.</u>	<u>Meas.</u>	<u>Pred.</u>	<u>Meas.</u>
395	0.0	61.7	0.0	22.8	0.0	12.9
434	21.2	69.2	132.9	9.9	43.2	15.2
469	19.6	91.2	71.7	4.9	23.0	21.1
517	14.5	83.2	31.2	4.2	10.4	18.3
534	10.5	63.1	12.9	2.8	4.8	15.7
556	8.7	56.2	7.7	2.8	3.2	20.3
580	7.2	51.3	5.1	2.1	2.5	14.1
604	6.3	39.8	3.7	2.1	2.5	14.1
623	6.6	34.7	3.2	1.4	1.7	15.5
642	6.4	27.5	2.6	1.4	1.5	8.7
664	5.6	25.1	2.0	1.4	1.3	10.1
723	4.5	20.0	1.2	0.7	1.1	7.3
784	3.4	18.6	0.8	0.7	0.7	7.6
839	3.8	17.0	0.7	1.4	0.5	7.8
902	4.0	16.2	0.7	1.4	0.5	8.1

TABLE XIII (Continued)

Time (mins)	concentrations, $\mu\text{eq/l}$					
	Ca ⁺²		Mg ⁺²		Na ⁺	
	<u>Pred.</u>	<u>Meas.</u>	<u>Pred.</u>	<u>Meas.</u>	<u>Pred.</u>	<u>Meas.</u>
395	0.0	N.A.	0.0	N.A.	0.0	N.A.
434	164.8	N.A.	35.0	6.9	36.1	18.2
469	87.4	N.A.	17.8	9.3	20.1	3.0
517	37.3	51.8	7.4	7.6	9.7	4.7
534	15.0	26.4	3.0	7.5	4.7	5.2
556	8.6	20.9	1.9	6.7	3.3	7.3
580	5.3	16.1	1.4	36.2*	2.6	6.2
604	3.2	12.4	1.1	4.2	2.1	5.4
623	2.3	12.9	0.9	4.1	2.1	5.4
642	1.8	10.9	0.9	2.8	1.4	2.6
663	1.6	9.9	0.8	3.2	1.2	3.6
723	1.2	6.4	0.8	1.6	1.3	13.2*
784	1.2	6.4	0.8	1.6	1.1	1.9
839	1.2	5.9	0.8	1.6	1.3	2.1
902	1.0	7.4	0.8	2.8	1.8	2.3

N.A. : indicates experimental data is missing

* : indicates experimental data might be inaccurate

TABLE XIV
LEACHING COEFFICIENTS USED IN THE MIXING MODEL
(Red Spruce)

Ion	Leaching Coefficeents ($\mu\text{eq}/\text{min}$)
Hydrogen	-0.50
Sulfate	0.03
Nitrate	-0.0005
Chloride	0.005
Ammonium	0.0
Calcium	0.005
Magnesium	0.001
Sodium	0.0005
Potassium	0.025

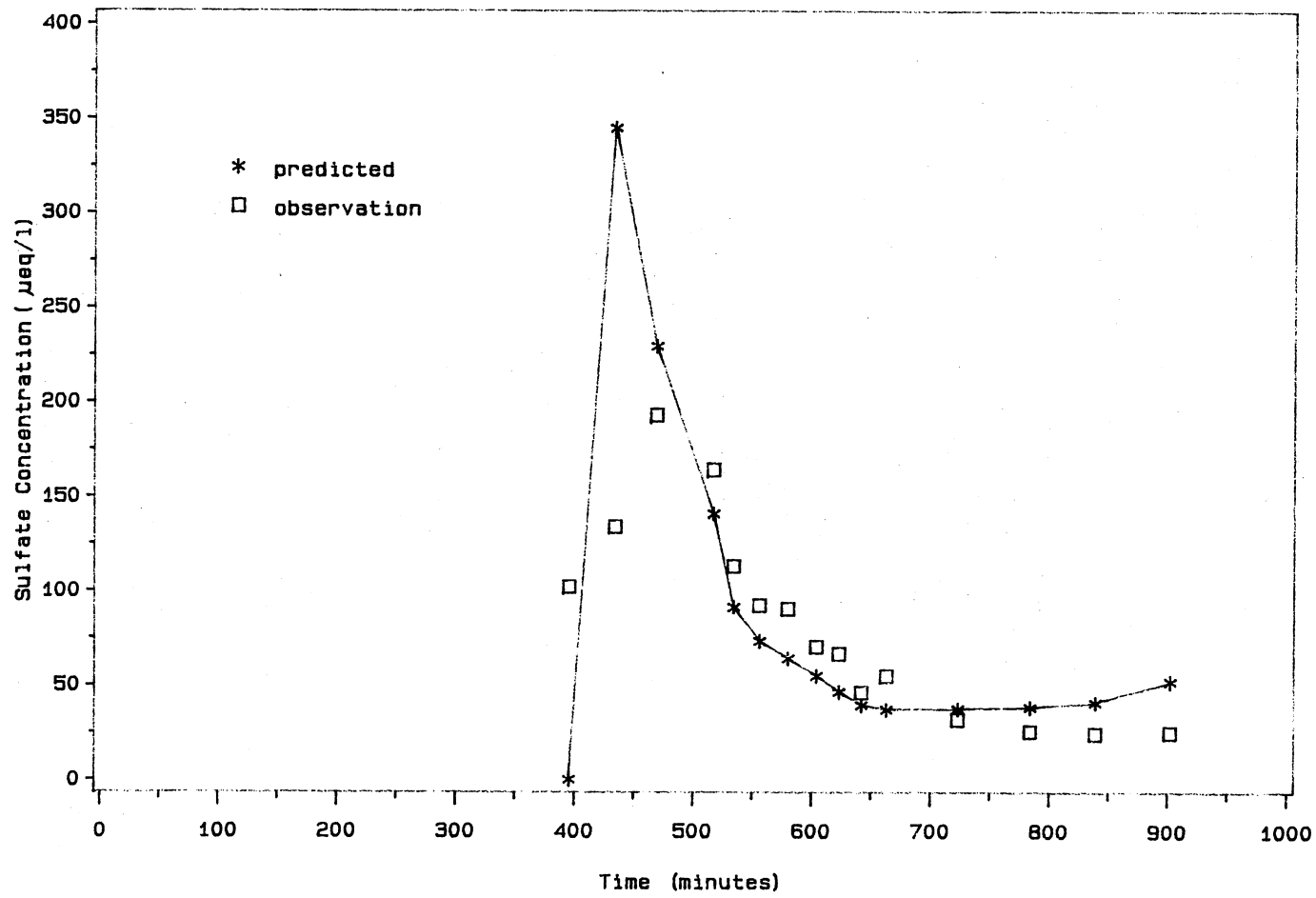


Figure 33. Throughfall Concentration of Sulfate Ion in Event 2 with Dry Deposition and Leaching (Red Spruce)

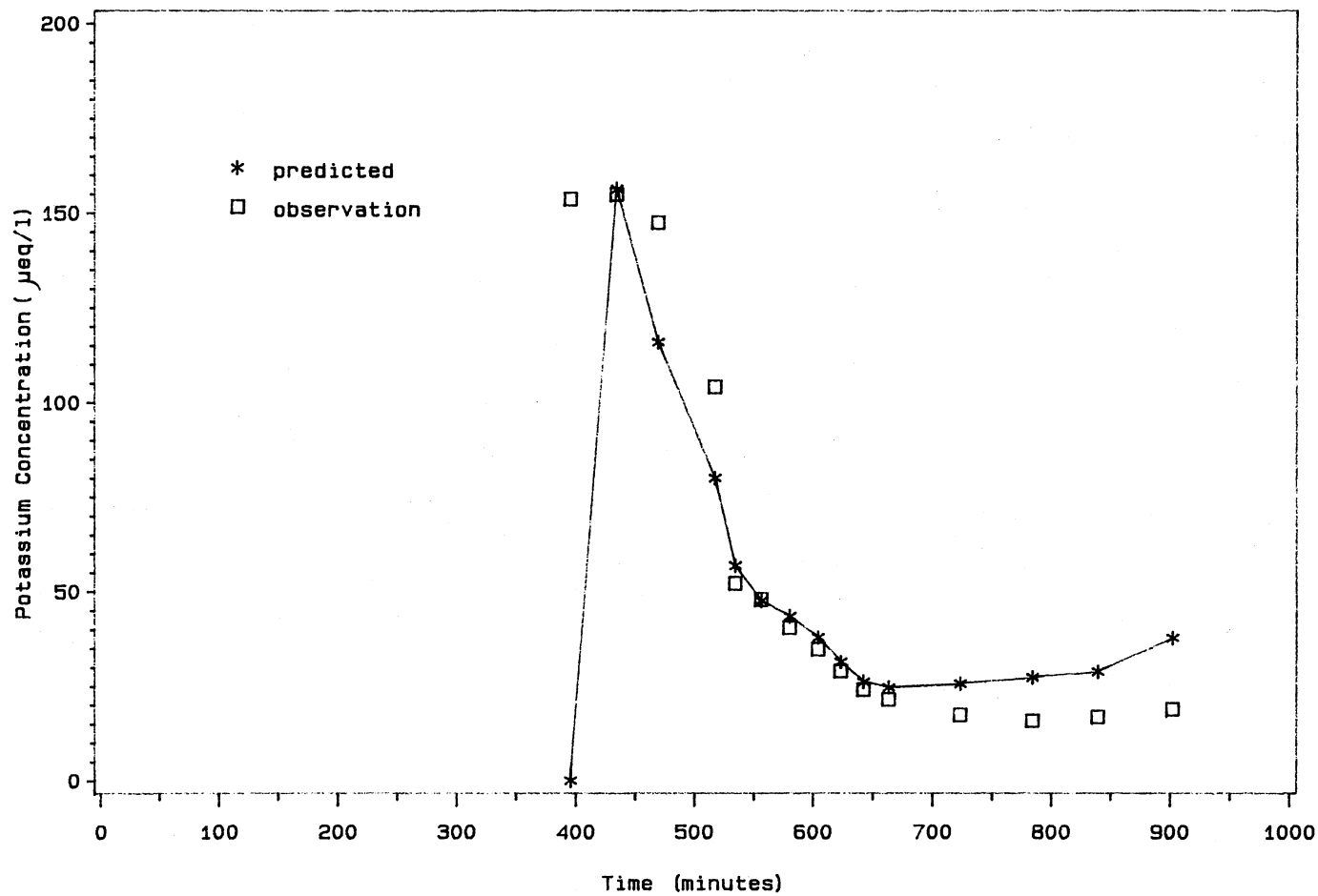


Figure 34. Throughfall Concentration of Potassium Ion in Event 2 with Dry Deposition and Leaching (Red Spruce)

in Table XV. The complete material balance in this case are summarized in Table XVI.

In this study, the forest cover may significantly alter the ionic content of incoming precipitation, therefore, the effect of tree canopies upon the atmospheric inputs to a watershed should not be underestimated.

The analysis of the throughfall chemistry revealed that hydrogen was apparently readily absorbed, or neutralized, by deciduous trees, and, perhaps to a lesser extent by coniferous trees. Sulfate, chloride, calcium, magnesium, sodium and especially potassium were apparently leached from both deciduous and coniferous trees. In fact, the relative magnitudes of the leachates varied with species quite often. Apparently then, the extent of leaching depends upon the plant species, the amount of precipitation, the intensity of rainfall and perhaps other geographically-related factors.

TABLE XV
 THROUGHFALL CONCENTRATIONS VERSUS TIME IN EVENT 2
 WITH DRY DEPOSITION AND LEACHING COEFFICIENTS
 (Red Spruce)

concentrations, $\mu\text{eq/l}$

Time	H ⁺		NO ₃ ⁻		Cl ⁻	
	Pred.	Meas.	Pred.	Meas.	Pred.	Meas.
395	0.0	61.7	0.0	22.8	0.0	12.9
434	206.6	69.2	130.2	9.9	69.9	15.2
469	163.5	91.2	69.6	4.9	43.8	21.1
517	117.7	83.2	29.7	4.2	25.3	18.3
534	85.4	63.1	11.8	2.8	15.6	15.7
556	71.1	56.2	6.8	2.8	12.3	20.3
580	64.6	51.3	4.3	2.1	10.8	14.1
604	56.3	39.8	2.9	2.1	9.2	14.1
623	48.3	34.7	2.6	1.4	7.8	15.5
642	41.2	27.5	2.1	1.4	6.5	8.7
663	38.8	25.1	1.5	1.4	6.1	10.1
723	39.0	20.0	0.7	0.7	6.1	7.3
784	39.9	18.6	0.3	0.7	6.0	7.6
839	42.9	17.0	0.2	1.4	6.2	7.8
902	55.6	16.2	0.0	1.4	8.0	8.1

TABLE XV (Continued)

concentrations, $\mu\text{eq/l}$

Time	Ca ⁺²		Mg ⁺²		Na ⁺	
	Pred.	Meas.	Pred.	Meas.	Pred.	Meas.
395	0.0	N.A.	0.0	N.A.	0.0	N.A.
434	191.5	N.A.	40.4	6.9	38.8	18.2
469	108.2	N.A.	22.0	9.3	22.2	3.0
517	52.3	51.8	10.4	7.6	11.2	4.7
534	25.8	26.4	5.2	7.5	5.8	5.2
556	17.7	20.9	3.7	6.7	4.2	7.3
580	13.6	16.1	3.0	36.2*	3.4	6.2
604	10.4	12.4	2.5	4.2	2.9	5.4
623	8.3	12.9	2.1	4.1	2.4	5.4
642	6.9	10.9	1.9	2.8	1.9	2.6
663	6.4	9.9	1.8	3.2	1.7	3.6
723	6.4	6.4	1.8	1.6	1.8	13.2*
784	6.4	6.4	1.9	1.6	1.6	1.9
839	6.8	5.9	1.9	1.6	1.8	2.1
902	8.4	7.4	2.3	2.8	2.5	2.3

N.A. : indicates experimental data is missing

* : indicates experimental data might be inaccurate

TABLE XVI
 FINAL MATERIAL BALANCE FOR EVENT 2
 WITH LEACHING AND DRY DEPOSITION
 (Red Spruce)

Water Balance (ml.)

Total Input Volume	2526.0
Total Thrufall Volume	
Predicted	1563.0
Measured	1639.0
Total Stemflow Volume	
Predicted	621.0
Volume Retained(Holdup)	342.0
Total In-Out-Holdup	0.0

Sulfate (μeq)

Input Wet Mass	31.0
Total Dry Mass	25.0
Total Mass Leached	111.0
Total Thrufall Mass	121.0
Total Stemflow Mass	30.0
Total Mass Retained	15.0
Total In-Out-Holdup	0.0

Potassium (μeq)

Input Wet Mass	2.0
Total Dry Mass	4.0
Total Mass Leached	93.0
Total Thrufall Mass	71.0
Total Stemflow Mass	16.0
Total Mass Retained	11.0
Total In-Out-Holdup	0.0

Performance of the Mixing Model

Modeling of a system is incomplete without testing the performance of the model. Testing of a model is performed by comparing the model results against the observed data for dependent variables. Model performance is judged on its ability to predict:

- . Temporal variation of throughfall volume and chemistry.
- . Accuracy of prediction of throughfall volume and chemistry.

Performance of a model prediction of temporal variation of a dependent variable may be judged by a correlation coefficient between predicted and observed values. This correlation coefficient is indication of a linear relationship between predicted and observed values. A correlation coefficient may be calculated as:

$$r = S_{xy} / (S_{xx} S_{yy})^{1/2} \quad (5.1)$$

$$S_{xx} = \sum_{i=1}^N (P_i - P_m)^2 \quad (5.2)$$

$$S_{yy} = \sum_{i=1}^N (O_i - O_m)^2 \quad (5.3)$$

$$S_{xy} = \sum_{i=1}^N (P_i - P_m) (O_i - O_m) \quad (5.4)$$

where P_i and O_i are predicted and observed values; P_m and O_m are mean predicted and mean observed values. A correlation coefficient may range from +1 to -1. A correlation

coefficient of +1 implies a direct and linear relationship between predicted and observed values, suggesting a good performance of the model to predict temporal variations of dependent variables. A correlation coefficient of -1 suggests a inverse linear relationship between predicted and observed values implying a poor performance of the model to predict temporal variations of dependent variables.

Accuracy of prediction of a dependent variable is characterized by a relative error (ϵ_1) expressed in equation (5.5).

$$\epsilon_1 = (P_1 - O_1) / O_1 \quad (5.5)$$

A positive value of a relative error suggests overprediction and a negative value of a relative error indicates underprediction of the variables by the model.

Correction coefficients between predicted and observed values and mean relative error (mean of relative errors of all collection points within an event) of throughfall concentration of ions and throughfall volume are summarized in Table XVII.

American Beech

Correlation coefficients between predicted and observed throughfall concentration of sulfate, nitrate, chloride, magnesium and potassium ions are 0.96, 0.93, 0.91, 0.92 and 0.90, respectively, suggesting a good prediction of temporal

TABLE XVII
 EVALUATION OF MIXING MODEL FOR THROUGHFALL VOLUME
 AND CONCENTRATION OF IONS
 (EVENT 2)

Variable	American Beech		Red Spruce	
	r	ϵ_m	r	ϵ_m
Volume	0.98	0.155	0.98	0.097
Sulfate	0.96	-0.037	0.75	0.171
Nitrate	0.93	-0.028	0.97	2.433
Chloride	0.91	0.197	0.54	0.167
Ammonium	0.74	1.751	0.40	3.931
Calcium	0.86 ¹	0.721 ¹	0.99 ²	-0.106 ²
Magnesium	0.92 ¹	-0.127 ¹	0.61 ³	0.332 ³
Sodium	-0.01 ¹	1.639 ¹	0.78 ³	0.471 ³
Potassium	0.90	0.10	0.97	0.218
Hydrogen	0.89	0.005	0.67	0.838

r : correlation coefficient for linear relationship
 between predicted and observed values

ϵ_m : mean of relative errors within an event

¹ : 15 of 16 collection points being considered

² : 12 of 15 collection points being considered

³ : 13 of 15 collection points being considered

variations of these variables. Correlation coefficients between predicted and observed throughfall concentration of ammonium, calcium and hydrogen ions vary from a low 0.74 (NH_4^+) to a high 0.89 (H^+), suggesting fair to good prediction of temporal variations of these variables. Correlation coefficient of sodium ion is -0.01 indicates a poor prediction of temporal variation of this variable.

Mean relative errors of prediction of throughfall concentration of sulfate, nitrate, and potassium ions are 4, 3 and 10 percent respectively; mean relative errors of prediction of throughfall concentration of other ions range between 13 (Mg^{+2}) and 175 (NH_4^+) percent.

Correlation coefficients and mean relative errors of predicted and observed throughfall volume are 0.98 and 15.5 percent respectively. The prediction accuracy can be improved if regression between wetfall volume and throughfall volume was performed on an event basis. In general, the model overpredicts throughfall concentration of metallic cations (except Mg^{+2}), chloride, ammonium ions and throughfall volume; underpredicts throughfall concentration of sulfate and nitrate ions.

Red Spruce

Correlation coefficients between predicted and observed throughfall concentrations of nitrate, calcium and potassium ions are 0.97, 0.99 and 0.97 respectively, indicating an excellent prediction of temporal variations of

these variables. Corresponding correlation coefficients of other ions vary from 0.40 (NH_4^+) to 0.78 (Na^+), indicates poor to fair prediction of temporal variation of these variables.

Mean relative errors of prediction throughfall concentrations of sulfate and potassium ions are 17.1 and 21.8 percent respectively; mean relative errors of other ions vary from 10.6 (Ca^{+2}) to 393 (NH_4^+). Although the prediction of temporal variation for nitrate ion is excellent, the gross overprediction of concentration at the first two collection points cause a large value of mean relative error. If the first two collections data are subtracted from the remaining data, the mean relative errors drops from 244 percent to 92.8 percent.

Correlation coefficients and mean relative error of predicted and observed throughfall volume are 0.98 and 9.7 percent, respectively. Generally, the model overpredict throughfall volume and all throughfall concentrations except calcium ion.

CHAPTER VI

DISSOLUTION OF DRY DEPOSITION

Rainwater that has passed over the surfaces of a tree shows a net gain in the concentration of many chemical elements. This gain is partly through wash-off of elements trapped from the atmosphere by impaction or adsorption (i.e. dissolution of dry deposition) and partly from elements derived from within the plant tissues (crown leaching). Thus, while crown leaching represents part of the cycle of elements internal to the ecosystem, the wash-off of elements derived from the atmosphere represents an input to the sites. Clearly it is important to be able to distinguish between internal redistribution and external input.

In previous chapters, a simple mixing process without chemical reaction has been used to predict the throughfall concentrations for nine major ions. Although results were within the accepted tolerance, the volume, and ultimately mass loading was overpredicted.

By evaluating the throughfall data, Johannes et al (1983) found that nitrate concentration, for example, decreased exponentially during the initial period of the event and was greatly enriched over wetfall in the early portion of the event. This enrichment and subsequent decay

conceptually supports dissolution and washoff of dry deposition. A model consisting of unsteady solid dissolution in a falling liquid film is proposed in hopes to improve the prediction of initial throughfall qualities. The problem formulation and the method of solution will be addressed in the following sections.

Formulation of the Problem

Consider the problem of mass transfer from a solid surface into the laminar boundary layer of an established flow past the surface. The solid layer contains a mixture of N independently diffusing solutes which may differ in both solubilities and diffusivities. At time $t \leq 0$, there is no dissolution along the surface. For time $t > 0$, it is assumed that a solid layer, having a thickness S_0 , begins to dissolve in the surrounding liquid (of large extent compared with the solid mass). At any instant after dissolution starts, the system consists of distinct liquid and solid portion containing dissolved and undissolved materials.

A schematic view of the situation to be studied is shown in Figure 35. As seen there the interface between the solid and liquid phase for a two-dimensional dissolution in which a solid wall, initially contained in the region $0 < x < S_0$ is dissolved. As dissolved solutes are removed by convection and diffusion, its thickness is decreased and the solid-liquid interface moves in the negative x -direction. The diffusion of the various species inside the solid layer

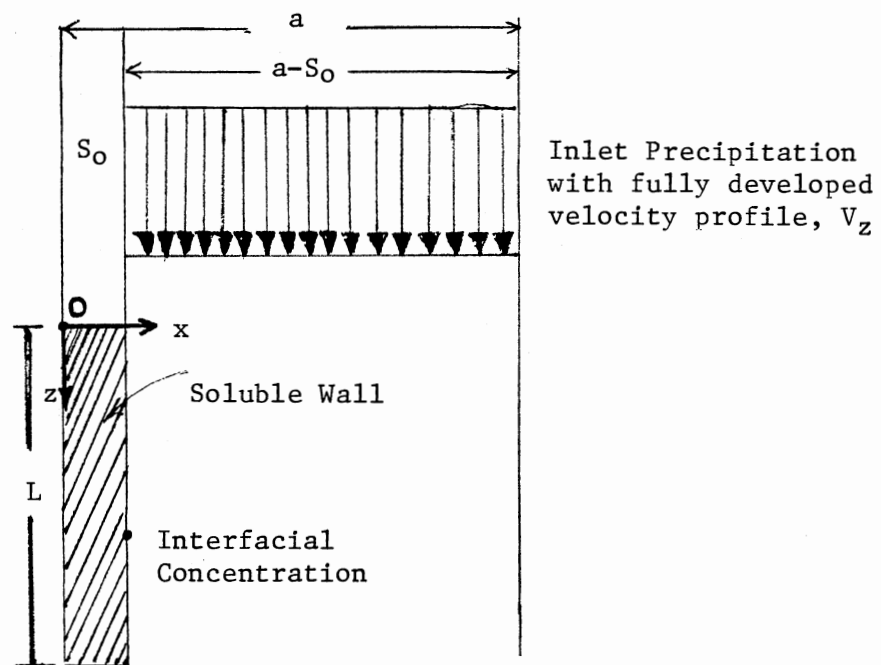


Figure 35. Solid Dissolution into a Falling Film, with Fully Developed Velocity Profile

and equilibration at the interface are assumed to occur rapidly compared to diffusion in the liquid. Thus, the mass fraction inside the solid layer are assumed to be uniform. Also, assuming the mass density of the solid phase (ρ_s) to be constant, only the concentration distribution of the dissolved solutes in the liquid phase needs to be considered.

In the mathematical analysis, additional assumptions are made: diffusivities are independent of concentration, and equilibrium is maintained at the solid-liquid interface; temperature and pressure are constants. Possible effects of viscosity or inertia of the liquid, surface tension and interfacial reaction kinetics are ignored; the volume and density of liquid may be assumed independent of dissolved solute concentrations. The last assumption will not hold in situations in which dissolution of large quantities of solid solute results in substantial change of the volumetric concentration in the surrounding fluid. In dissolving relative small quantities of highly soluble solids however, the driving force remains essentially constant.

Under these simplifying assumptions, the relevant convective-diffusion equation in the liquid reduces to

$$\frac{\delta C_1}{\delta t} = D_1 \frac{\delta C_1^*}{\delta x^2} - V_z \frac{\delta C_1}{\delta z} \quad (6.1)$$

where C_1 and D_1 denote the concentration and diffusivity of the solute i in the liquid, and V_z (cm/s) is the z -

direction volume flux of rainwater. It has been assumed that diffusive transport in the z-direction is negligible as compared to convective transfer.

The initial and boundary conditions are:

$$t = 0 \quad s(0) < x < a \quad C_1 = 0 \quad (6.2)$$

$$t > 0 \quad s(t) < x < a \quad C_1 = C_{11} \quad z=0 \quad (6.3)$$

$$t > 0 \quad 0 < z < L \quad \frac{\delta C_1}{\delta x} \Big|_{x=a} = 0 \quad x=a \quad (6.4)$$

In addition to serving as boundary conditions for the basic system, equation (6.3) specify the conditions for the inflow concentrations. Clearly, additional boundary information is needed. This information must define the concentration at the moving interface between the liquid and the solid phase.

The interface, designated as $s=s(t)$, creates the unique part of the problem considered here. Because of its movement, the position is not known a priori. This position must be computed as part of the overall solution. Such a mathematical problem is generally called a moving boundary problem or a Stefan problem. In the present case, for any given time $t=T$ and $T < t_c$, time required to dissolve the solid phase completely, one natural boundary condition is equilibrium from thermodynamics,

$$C_1(x=s(T), z, T) = H_1 * g_1(T) * \rho_s \quad (6.5)$$

where g_1 is the mass fraction of solute i in the solid

phase, and H_1 is the solubility of the solute under consideration. Equation (6.5) explicitly points out the time dependence of the thickness $s(T)$ and the mass fractions of the species inside the solid layer $g_1(T)$. Because the sum of the mass fractions of the species in the solid phase is always unity, therefore, a change in the driving force for the transport of any species will affect the driving forces for the rest of the species. This feature is unique to multicomponent problems since, when surface-tension effects are ignored, the interfacial concentration is a constant in the single-component case.

Another boundary condition for the interface is derived by writing a mass-balance equation for the interface. For the problem under consideration, the flux of solute i into the liquid is given by $D_1(\delta C_1/\delta x)_{x=s(T)}$, hence

$$\frac{d}{dt}(s \cdot \rho_s \cdot g_1) = D_1 \left(\frac{\delta C_1}{\delta x} \right)_{x=s(T)} \quad (6.6)$$

Performing the differentiation indicated yields

$$\rho_s \cdot g_1 \cdot \frac{ds}{dt} + s \cdot \rho_s \cdot \frac{dg_1}{dt} = D_1 \left(\frac{\delta C_1}{\delta x} \right)_{x=s(T)}$$

$$\frac{dg_1}{dt} = \frac{1}{s} \left(\frac{D_1}{\rho_s} \frac{\delta C_1}{\delta x} \right)_{x=s(T)} - \frac{g_1}{s} \frac{ds}{dt} \quad (6.7)$$

and the sum of all terms must satisfy

$$\frac{ds}{dt} = \left(\frac{\delta s}{\delta t} \right)_z = \frac{1}{\rho_s} \sum_{i=1}^N D_i \left(\frac{\delta C_i}{\delta x} \right)_{x=s(t)} \quad (6.8)$$

where ds/dt is the rate of travel of the interface, so-called dissolution front in this case, and ρ_s is the mass density of the solid phase. As stated, Equation (6.7) applies to each species and actually represents (N-1) independent equations. Since $\sum_{i=1}^N g_i = 1$, only (N-1) of the mole fractions are truly independent. To integrate Equations (6.7) and (6.8), initial conditions are necessary and are given as

$$\begin{aligned} g_i(0) &= g_{i0} \\ s(0) &= S_0 \end{aligned} \quad (6.9)$$

In order to identify the true parameters in the problem, the following dimensionless variables are defined,

$$T = \frac{D_1 t}{a^2} \quad (6.10a)$$

$$f_i = \frac{D_i}{D_1} \quad (6.10b)$$

$$X = \frac{x}{a} \quad (6.10c)$$

$$R = \frac{s(t,z)}{a} \quad (6.10d)$$

$$Z = \frac{D_1 * z}{a^2 * V_z} \quad (6.10e)$$

$$\bar{C}_1 = \frac{C_1 - C_{11}}{C_1(t, z, s(t, z)) - C_{11}} \quad (6.10f)$$

$$B_1 = \frac{C_{11}}{\rho_s} \quad (6.10g)$$

and

$$N_1(T) = H_1 * g_1(T) - B_1 \quad (6.10h)$$

In these definitions, species 1 was chosen as the reference species in scaling time and the various diffusivities. Using these variables, Equations (6.1) to (6.8) may be transformed to the following set:

$$\frac{\delta \bar{C}_1}{\delta T} + \frac{\bar{C}_1}{N_1(T)} \frac{dN_1(T)}{dT} = f_1 \frac{\delta^2 \bar{C}_1}{\delta X^2} - \frac{\delta \bar{C}_1}{\delta Z} \quad (6.11)$$

$$\frac{dg_1}{dT} = \frac{1}{R} \left(f_1 * N_1(T) * \frac{\delta \bar{C}_1}{\delta X} \Big|_{x=R} - g_1 * \frac{\delta R}{\delta T} \Big|_z \right) \quad (6.12)$$

$$\frac{\delta R}{\delta T} \Big|_z = \sum_{i=1}^N f_i * N_i(T) \frac{\delta \bar{C}_1}{\delta X} \Big|_{x=R} \quad (6.13)$$

The interfacial concentration $C_i(x=s(T), z, t)$ is now given by

$$\bar{C}_1(R, Z, T) = 1 \quad (6.14)$$

and the boundary conditions now are

$$\begin{aligned} T > 0, \quad Z = 0, \quad \bar{C}_1 &= 0 \\ T > 0, \quad X = 1, \quad \frac{\delta \bar{C}_1}{\delta X} \Big|_{x=1} &= 0 \end{aligned} \quad (6.15)$$

with initial conditions

$$\begin{aligned}
 T > 0, \quad \bar{C}_1 &= - \frac{C_{11}}{C_1(t,z,s(t))-C_{11}} \\
 &= - \frac{C_{11}}{1.0 - C_{11}} \qquad (6.16)
 \end{aligned}$$

Note that, by defining a dimensionless concentration using equation (6.10f), the time dependence of the interfacial concentrations is eliminated and exchanged for a new term $\bar{C}_1/N_1*(dN_1/dT)$ which appears in the governing equation (6.11). Constant boundary conditions are convenient for a finite difference formulation.

The problem is to determine the thickness of solid phase and the concentration distribution in the liquid phase, so as to satisfy the mass balance equation (6.11), as well as the boundary conditions (6.14) to (6.15). However, at some particular instant of time after the dissolution has started, the position of the interface has been changed. Thus, the required domain of interest varies with time. When $t = t_c$, the interface meets the z-axis and the dissolution process is complete.

Method of Solution

Because of the complexity of the unsteady two-dimensional case, most of the available solution techniques are numerical rather than analytical in nature. The major

difficulty inherent in the finite-difference solution of 2-dimensional phase change problems is that concentration has a jump discontinuity across the phase-change front due to equilibrium. Moreover, the location of the moving interface is not known a priori and introduces a non-linearity into the problem. It is apparent that an immobilization of the phase boundary by an appropriate coordinate transformation would greatly reduce the difficulties associated with the solution of the problems (Duda et al., 1975; Willis and Rubin, 1987).

The basic philosophy of this approach is to simplify the numerical analysis by transforming the moving boundary to a fixed boundary of simple geometry at the expense of complicating the governing partial differential equations. Since finite difference technique can readily handle complex partial differential equations but are difficult to adapt to a moving boundary, the transformation technique casts the problem into a form which utilizes the strength of the finite-difference techniques while at the same time minimizes their shortcomings.

The specific transformation utilized in this study is:

$$y = 1 - \frac{1-X}{1-R} \quad (6.17)$$

The problem is transformed to a coordinate system where the moving interface is defined by $y=0$. Utilization of this coordinate transformation in equations (6.11)-(6.16) gives the following set of equations which completely describe the

problem:

$$\frac{\overline{\delta C_i}}{\delta T} + \frac{\overline{C_i}}{N_1(T)} \frac{dN_1}{dT} = f_1 \frac{1}{(1-R)^2} \frac{\delta^2 \overline{C_i}}{\delta y^2} - \frac{\overline{\delta C_i}}{\delta Z} + \frac{(1-y)}{(1-R)} \left(\frac{\delta R}{\delta T} + \frac{\delta R}{\delta Z} \right) \frac{\overline{\delta C_i}}{\delta y} \quad (6.18)$$

$$\frac{dg_1}{dT} = \frac{1}{R} \left(f_1 * N_1(T) \frac{1}{1-R} \frac{\delta \overline{C_i}}{\delta y} \Big|_{y=0} - g_1 \frac{\delta R}{\delta T} \right) \quad (6.19)$$

and

$$\frac{\delta R}{\delta T} \Big|_Z = \sum_{i=1}^N f_i * N_1(T) * \frac{1}{1-R} \frac{\delta \overline{C_i}}{\delta y} \Big|_{y=0} \quad (6.20)$$

Appendix D shows the derivation of these equations in detail.

Solution Procedures

In solving the preceding equations by the finite-difference method, central differences in spatial derivatives, and backward differences for time derivatives were used, so that implicit forms of all the difference equations were obtained. Therefore, equation (6.18) can be written in finite difference form as:

$$\frac{\overline{C_{i(k,j)}^{m+1}} - \overline{C_{i(k,j)}^m}}{\Delta T} + \frac{\overline{C_{i(k,j)}^m}}{H_1 * g_1^{m-B_1}} \frac{H_1 * (g_1^{m+1} - g_1^m)}{\Delta T} = \frac{1-y}{1-R_j^m} \left(\frac{R_j^{m+1} - R_j^m}{\Delta T} + \frac{R_{j+1}^m - R_{j-1}^m}{2\Delta Z} \right) * \left(\frac{\overline{C_{i(k+1,j)}^{m+1}} - \overline{C_{i(k-1,j)}^{m+1}}}{2\Delta y} \right)$$

$$\begin{aligned}
& + f_1 \frac{1}{(1-R_j^m)^2} * \left(\frac{C_{1(k+1,j)}^{m+1} - 2C_{1(k,j)}^{m+1} + C_{1(k-1,j)}^{m+1}}{\Delta y^2} \right) \\
& - \frac{C_{1(k,j+1)}^{m+1} - C_{1(k,j-1)}^{m+1}}{2\Delta Z}
\end{aligned} \tag{6.21}$$

where $\Delta y, \Delta Z$ are space increment in y and Z direction, respectively. ΔT is time increments and k, j , denote space position and m denotes time level.

Once rearranging the above difference equation to a form such that

$$\begin{aligned}
& A_1 C_{1(k-1,j)}^{m+1} + A_2 C_{1(k,j)}^{m+1} + A_3 C_{1(k+1,j)}^{m+1} + A_4 C_{1(k,j+1)}^{m+1} \\
& + A_5 C_{1(k,j-1)}^{m+1} = B C_{1(k,j)}^m
\end{aligned} \tag{6.22}$$

where

$$\begin{aligned}
A_1 &= \frac{1-y_k}{1-R_j^m} \left(\frac{R_j^{m+1} - R_j^m}{\Delta T} + \frac{R_{j+1}^m - R_{j-1}^m}{2\Delta Z} \right) \frac{\Delta T}{2\Delta y} - \frac{f_1}{(1-R_j^m)^2} \frac{\Delta T}{\Delta y^2} \\
A_2 &= 1 + \frac{2f_1}{(1-R_j^m)^2} \frac{\Delta T}{\Delta y^2} \\
A_3 &= - \frac{1-y_k}{1-R_j^m} \left(\frac{R_j^{m+1} - R_j^m}{\Delta T} + \frac{R_{j+1}^m - R_{j-1}^m}{2\Delta Z} \right) \frac{\Delta T}{2\Delta y} + \frac{f_1}{(1-R_j^m)^2} * \frac{\Delta T}{\Delta y^2}
\end{aligned}$$

$$A_4 = \frac{\Delta T}{2 \Delta Z}$$

$$A_5 = - \frac{\Delta T}{2 \Delta Z}$$

and

$$B = 1 - \frac{H_1 * (g_1^{m+1} - g_1^m)}{H_1 * g_1^m - B_1}$$

Equation (6.22) can now be written in matrix form, excluding the boundary points, and the technique used to solve the system of difference equation is based on the Gaussian elimination method.

The derivative $\overline{\delta C_1} / \delta y$ ($y=0$) at the interface appearing in equations (6.20) and (6.21) was approximated with a forward difference formulation. Thus,

$$\frac{\overline{\delta C_1}}{\delta y \quad y=0} = \frac{\overline{C_{i(k+1,j)}}^{m+1} - \overline{C_{i(k,j)}}^{m+1}}{\Delta y}$$

where $k=0$. Applying the boundary condition (6.14), $\overline{C_i(0,j)}=1.0$, the equation can be simplified as

$$\frac{\overline{\delta C_1}}{\delta y \quad y=0} = \frac{\overline{C_{i(1,j)}}^{m+1} - 1.0}{\Delta y} \quad (6.23)$$

Since equation (6.21) explicitly includes both g_1^{m+1} and R_1^{m+1} , it is necessary to employ an iterative scheme to

solve the difference equation (6.21).

First, assuming g_1^{m+1} equal to g_1^m and R_j^{m+1} has the same value as R_j^m , then equation (6.21) can be simplified as

$$\frac{C_{1(k,j)}^{m+1} - C_{1(k,j)}^m}{\Delta T} = f_1 * \frac{1}{(1-R_j^m)^2} * \left\{ \frac{C_{1(k+1,j)}^{m+1} - 2 C_{1(k,j)}^{m+1} + C_{1(k-1,j)}^{m+1}}{\Delta y^2} \right\} - \frac{C_{1(k,j+1)}^{m+1} - C_{1(k,j-1)}^{m+1}}{2\Delta Z} \quad (6.24)$$

Once the location of the interface and the concentration array were set according to the initial conditions, the sequence of computations for each time step is as follows:

- (a) solve for a new concentration distribution in the liquid phase with the current boundary position and mass fraction in the solid phase using the implicit difference form of equation (6.24). New values of concentration are calculated along each line in the y-direction by utilization of a Gaussian elimination to solve a block tridiagonal matrix system (subroutine LSARG in IMSL).
- (b) from the resulting concentration fields $\bar{C}_1(\Delta T, y, Z)$, the concentration gradients $\delta \bar{C}_1 / \delta y$ at $y=0$ were evaluated and used in equations (6.19) and (6.20) to obtain an

approximation for the right hand sides. These ordinary differential equations were integrated treating the slopes of dg_1/dT and $\delta R/\delta T$ as constant over the time intervals. The resulting value of R and g_1 at time ΔT was then used in a second iteration to integrate equation (6.21) for the first time step.

(c) procedure (b) was repeated until the value of $\delta R/\delta T$ which is sensitive to the estimate of the concentration gradient at the interface agreed to within 0.1% between successive iteration.

(d) At this point, the iteration for first time step were terminated and the concentration fields, as well as R and g_1 , were known accurately enough at time ΔT .

The procedure was repeated for successive time steps.

Program Description

A computer program is written in FORTRAN and run on an IBM-3081K computer. The program consists of a main program, and five subroutines. The main program reads input data, prints results, and calls five subroutines - COEFF, RHSIDE, LSARG, MOVING, and COMNEW to compute the concentration profiles.

The first subroutine COEFF computes the left-hand-side of tridiagonal elements and subroutine RHSIDE calculates the right-hand-side vectors, based on the centered-in-space, backward-in-time approximations. Then subroutine LSARG was called from IMSL to solve the block tridiagonal system of

equations. The computed values are then used in subroutines MOVING and COMNEW to calculate the new boundary position and mass fraction. The resulting new values of R and g_1 were then used in a second iteration to calculate the new concentration profiles. The procedure is repeated until the value of $\delta R/\delta T$ agreed to within 0.1% between successive iteration. The computer program together with documentation are listed in Appendix E.

CHAPTER VII

RESULTS AND DISCUSSIONS OF DISSOLUTION MODEL

Model Verification

One of the tasks which must be carried out in obtaining a numerical solution to any problem is to verify that the computer program and the final solution are correct. Verification often is carried out by comparing the model with an available analytical model and/or a numerical model. Lacking the general analytical solutions for a two-dimensional dissolution process, the accuracy of the model developed here was verified by comparing the numerical solution with the boundary position and the mass fraction calculated by Cable and Frade (1986) for a two-component system.

Figures 36 and 37 show the predicted change in terms of the position of the phase boundary and the mass fraction of component 1, with several different combinations of solubility and diffusivity for the second component while maintaining $H_1f_1 = H_2f_2 = 0.1$ and an initial mass fraction $g_1 = g_2 = 0.5$, respectively. Note that the numerical model agrees well with the results obtained by Cable and Frade (Figure 38) for $H_1f_1 = H_2f_2 = 1.0$ and $g_1 = g_2 = 0.5$ qualitatively. This qualitative agreement found between the

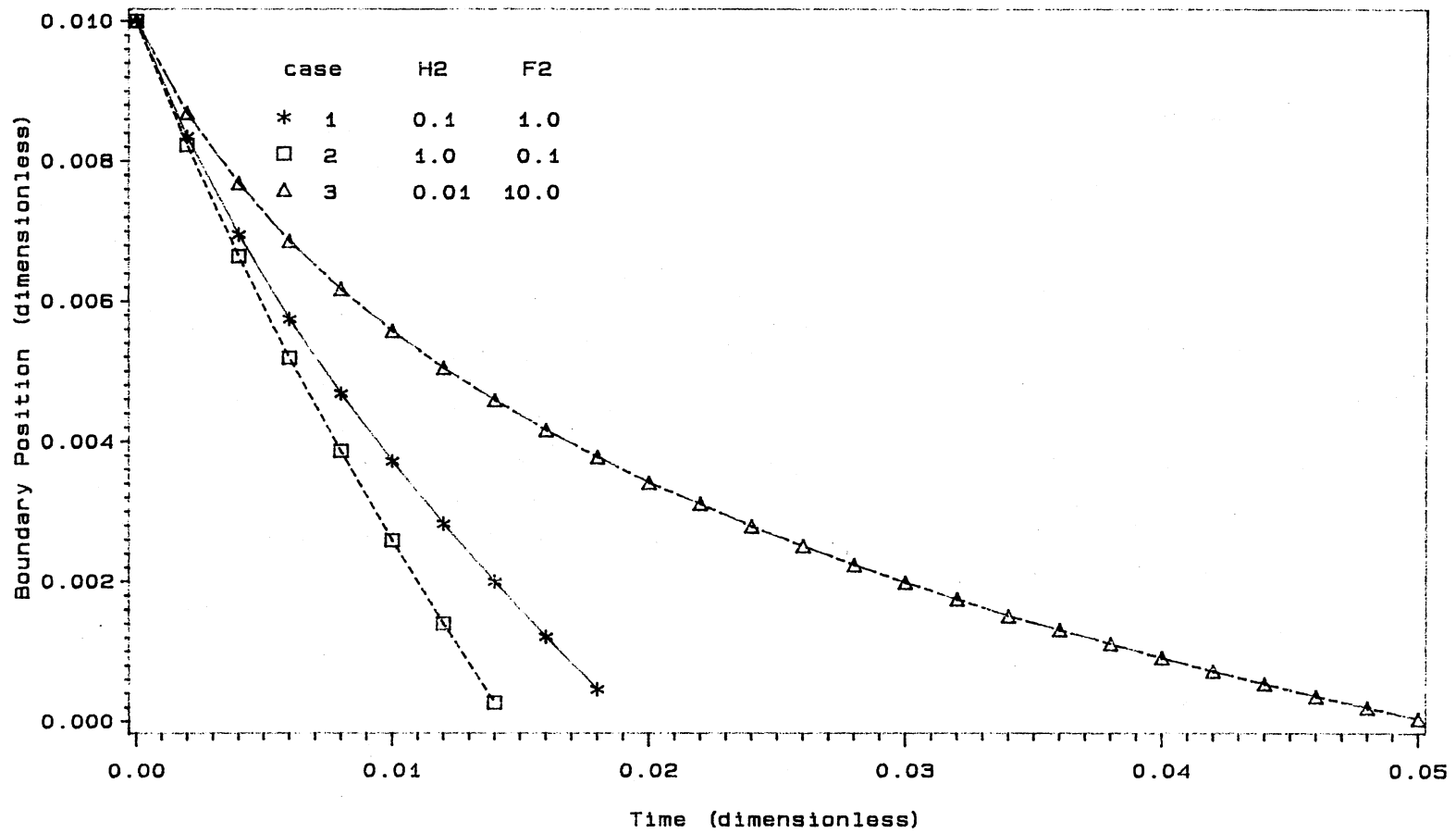


Figure 36. Boundary Position in 2-Component Dissolution Process for Different Combinations of Solubilities and Diffusivity Parameters

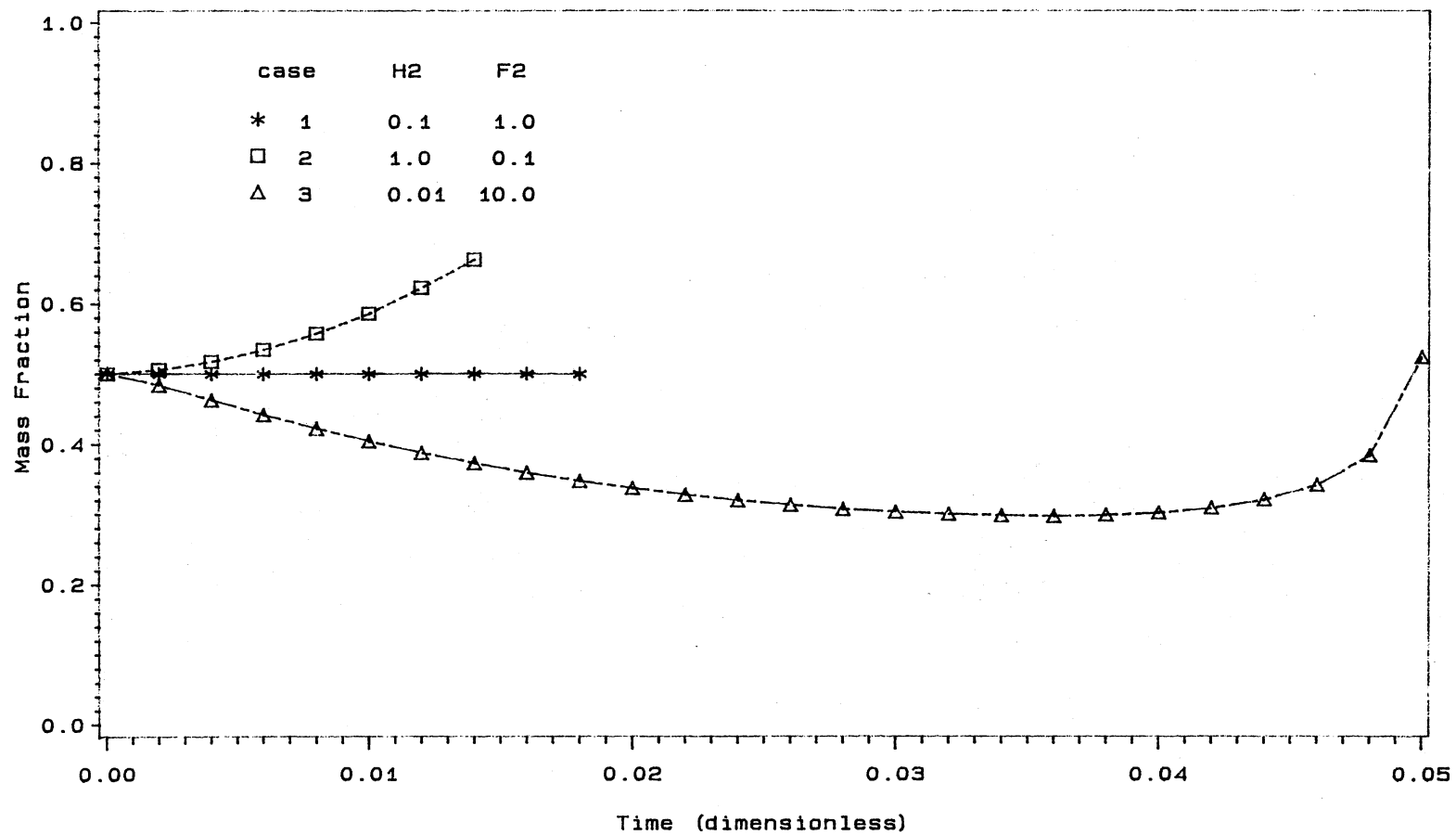


Figure 37. Mass Fraction in 2-Component Dissolution Process for Different Combinations of Solubilities and Diffusivity Parameters

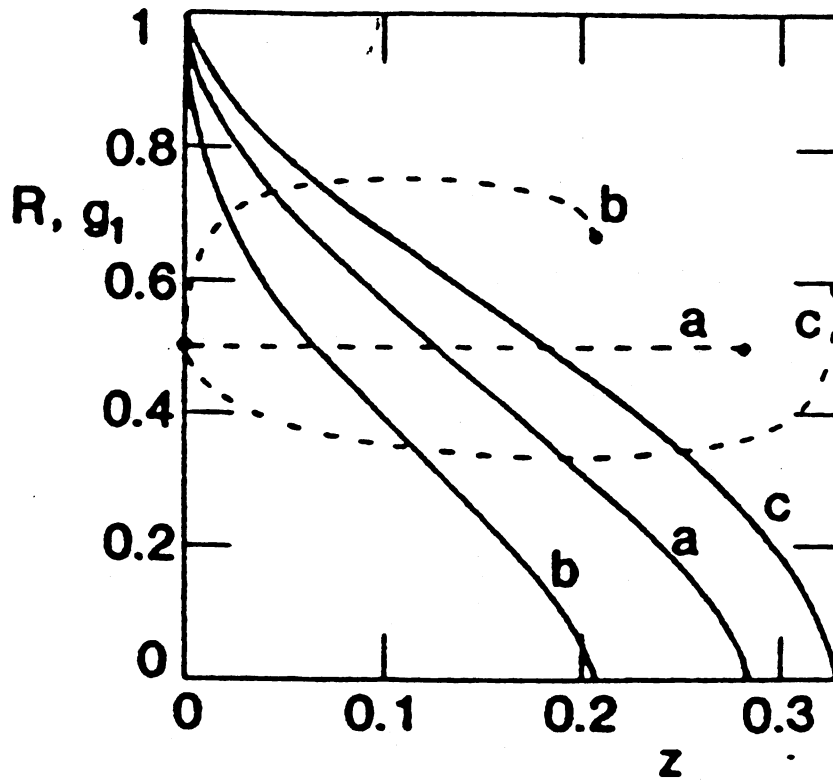


Figure. 38 Dissolution of 2 Components for Differing Solubilities but Constant Permeabilities

- (a) $H_2 = f_2 = 1.0$
 (b) $H_2 = 10, f_2 = 0.1$
 (c) $H_2 = 0.1, f_2 = 10$

R : radius —
 g_1 : mass fraction ----

(from Cable and Frade, 1986)

present method and Cable and Frade is taken to be sufficient evidence that the proposed model gives valid results.

Results and Discussions

As an illustration, examples with up to four components were solved in order to demonstrate the applicability of the immobilization transformation and the associate finite-difference method developed in chapter VI.

For the present calculations, 10 spatial increments were used in the y-direction and in the Z-axial direction, respectively. Systems with particular ions were modelled in the present study. In these, component 1 is SO_4^{2-} , component 2 is NO_3^- , component 3 is Cl^- and component 4 is taken to be NH_4^+ . Results for four different cases are presented in Figures 39-49, and the values of the parameters used in these cases are listed in Table XVIII. The initial liquid concentrations are on the order of about 10^{-6} for each species. The initial thickness of the solid phase is taken to be 0.01(dimensionless) for the present study.

One Component System

Figure 39 shows the boundary position of single component dissolution as a function of time computed from finite difference approximation with time increment equal to 0.001 and 0.002, respectively. The difference has been noticed at time somewhat equal to 0.006.

Since no specific stability criteria was established

TABLE XVIII
 PARAMETERS USED IN THE DISSOLUTION MODEL
 (from Handbook of Chemistry and Physics)

	species			
	SO ₄ ⁻²	NO ₃ ⁻	Cl ⁻	NH ₄ ⁺
Diffusivity (10 ⁻⁵ cm ² /sec)	1.97	2.98	2.20	2.0
Diffusivity Parameter, f ₁	1.00	1.513	1.115	1.015
Solubility Parameter, H ₁ (grams/g water)	0.095	0.0527	0.3655	0.6928
Inlet Wet Concentration, C ₁ (I), ueq/l	23.7	24.9	8.7	14.9
Inlet Wet Concentration, C ₁ (I), * 10 ⁻⁸ g/cm ³	1.14	1.54	0.31	0.27

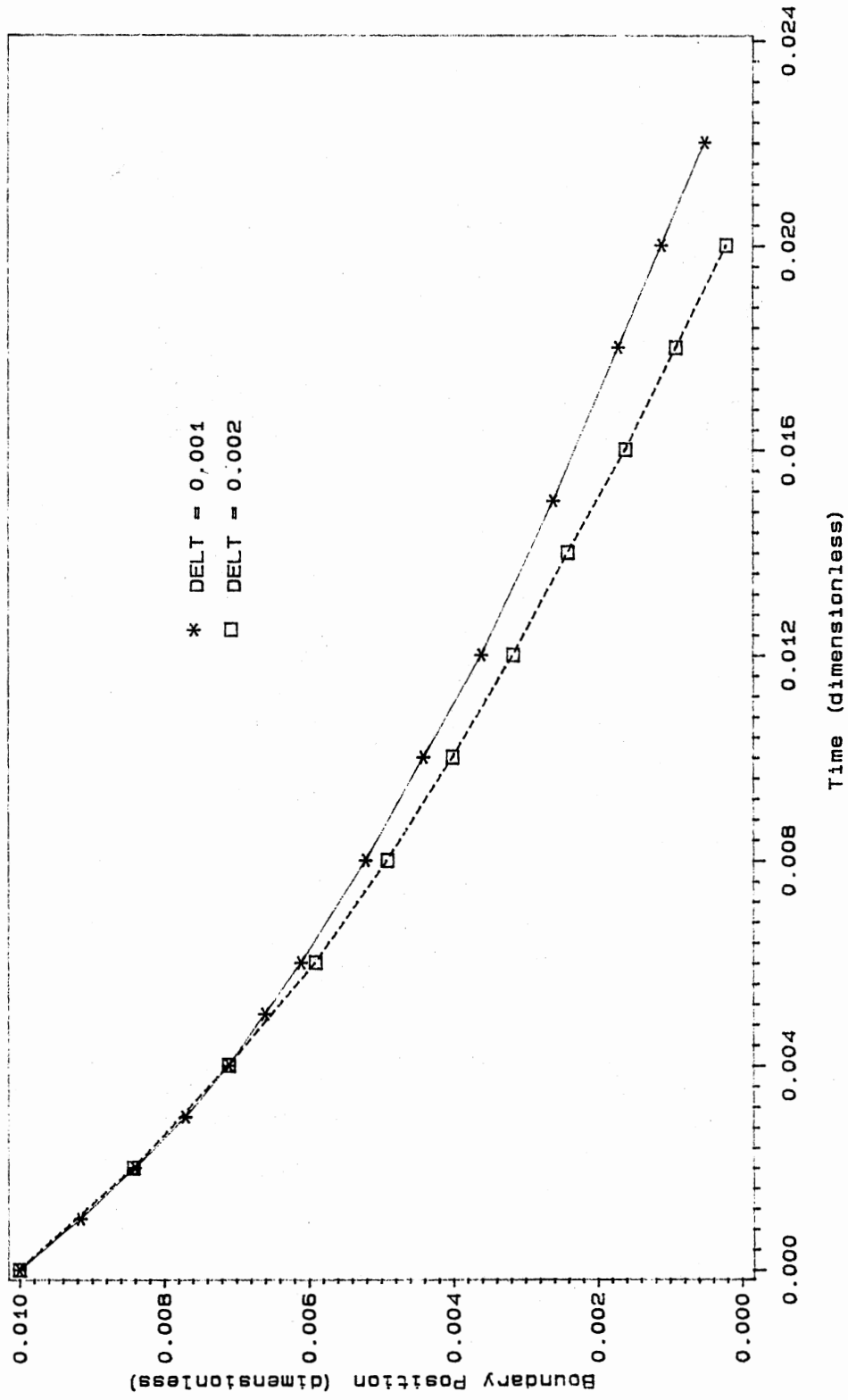


Figure 39. Boundary Position for Single Component Dissolution

for the implicit difference equations, the general rules are to look into the relationships among the parameters, the simulation distance and time, the number of space and time steps, and to consider the requirements of the accuracy and computational cost.

For the one component system with the same parameters, the average CPU time of solving a 10×10 space steps is about 0.0045 hours for $\Delta T = 0.001$ which is about twice as required for $\Delta T = 0.002$ (0.00254 CPU hour). In order to save the computational cost for multicomponents cases, a value of ΔT corresponding to 0.002 was used throughout the study.

Figure 39 indicated that the interfacial concentration is much larger than the concentration in liquid, therefore, the solute dissolve until the concentration in the liquid next to the interface approached the interfacial concentration. This causes a decrease in solid thickness.

Analysis of concentration profiles help to understand the development of concentration boundary layer. Figure 40 shows the effluent concentration profile for single component dissolution process at distance of $0.1y$, $0.2y$, $0.3y$, $0.5y$, $0.8y$ and $1.0y$. Results for distances greater than $0.5y$ become indistinguishable from each other. This may be explained as follows: if the diffusion coefficient is small, the depth of penetration of solute molecules into the neighboring liquid is small. The thickness of this diffusion boundary layer is small compared with the dispersion in the Z-direction.

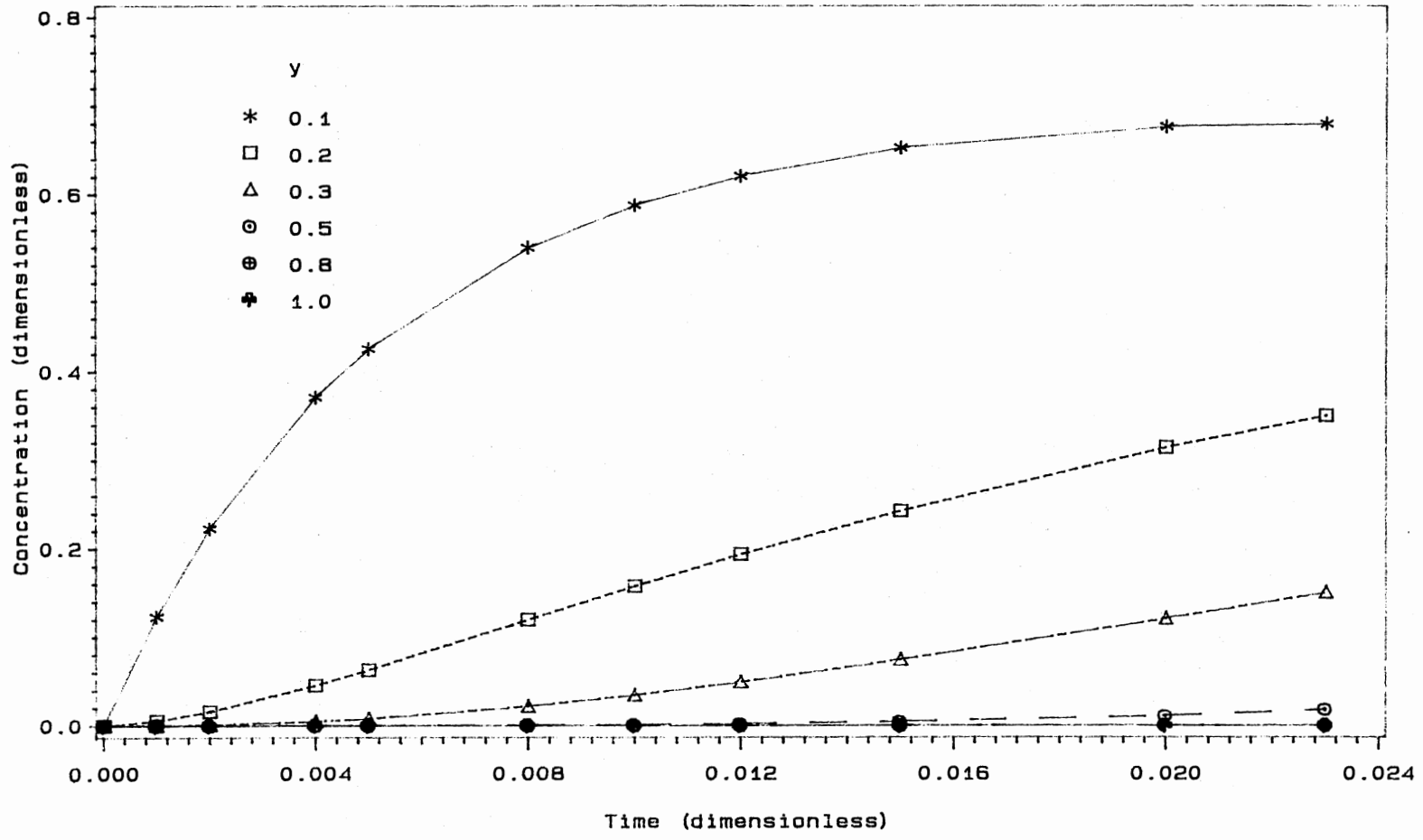


Figure 40. Effluent Concentration Profile at Different Location of y for Single Component Dissolution

Two Components System

As an illustration, the case will be considered where one of the two solutes has larger solubility than the other. The predicted mass fraction of two components dissolution as a function of time is shown in Figure 41 for the parameters also listed in Table XVIII. It can readily be seen that the mass fraction is dependent on both relative solubility and diffusivity of the solute concerned. It is also worthwhile to note that the result suggests that the changes in mass fraction are more sensitive to differences in the parameters than the change in thickness. Obviously solubility and diffusivity affect the behavior in different ways.

Figure 42 presents the results of the concentration profiles for the same parameters. Evaluating the concentration profiles in Figure 42 has shown that the dissolution causes the concentration profiles to approach its interfacial concentration with an increase in time. The two concentration profiles occupy different distances because Cl^- has higher solubility than SO_4^{2-} . Since Cl^- has four times higher solubility than the SO_4^{2-} , it is reasonable to expect that Cl^- dissolves more rapidly in the liquid than the SO_4^{2-} . The faster dissolution of Cl^- therefore causes a brief increase in the mass fraction of SO_4^{2-} in solid phase.

The peak of the curve in Figure 42 represents the maximum concentration of Cl^- in the liquid. In this case, when time equals to 0.008, the concentration of Cl^-

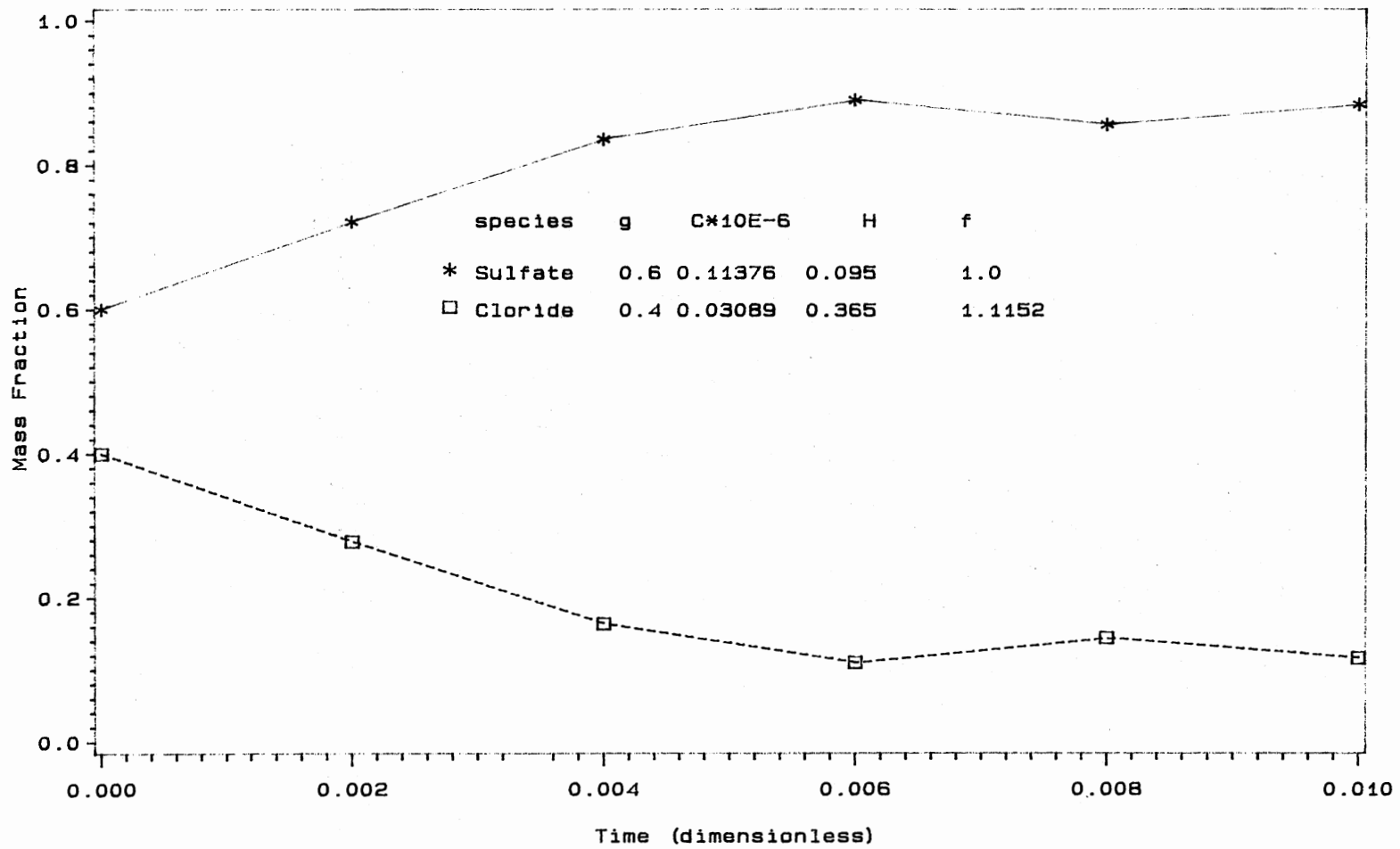


Figure 41. Mass Fraction for Two Components Dissolution

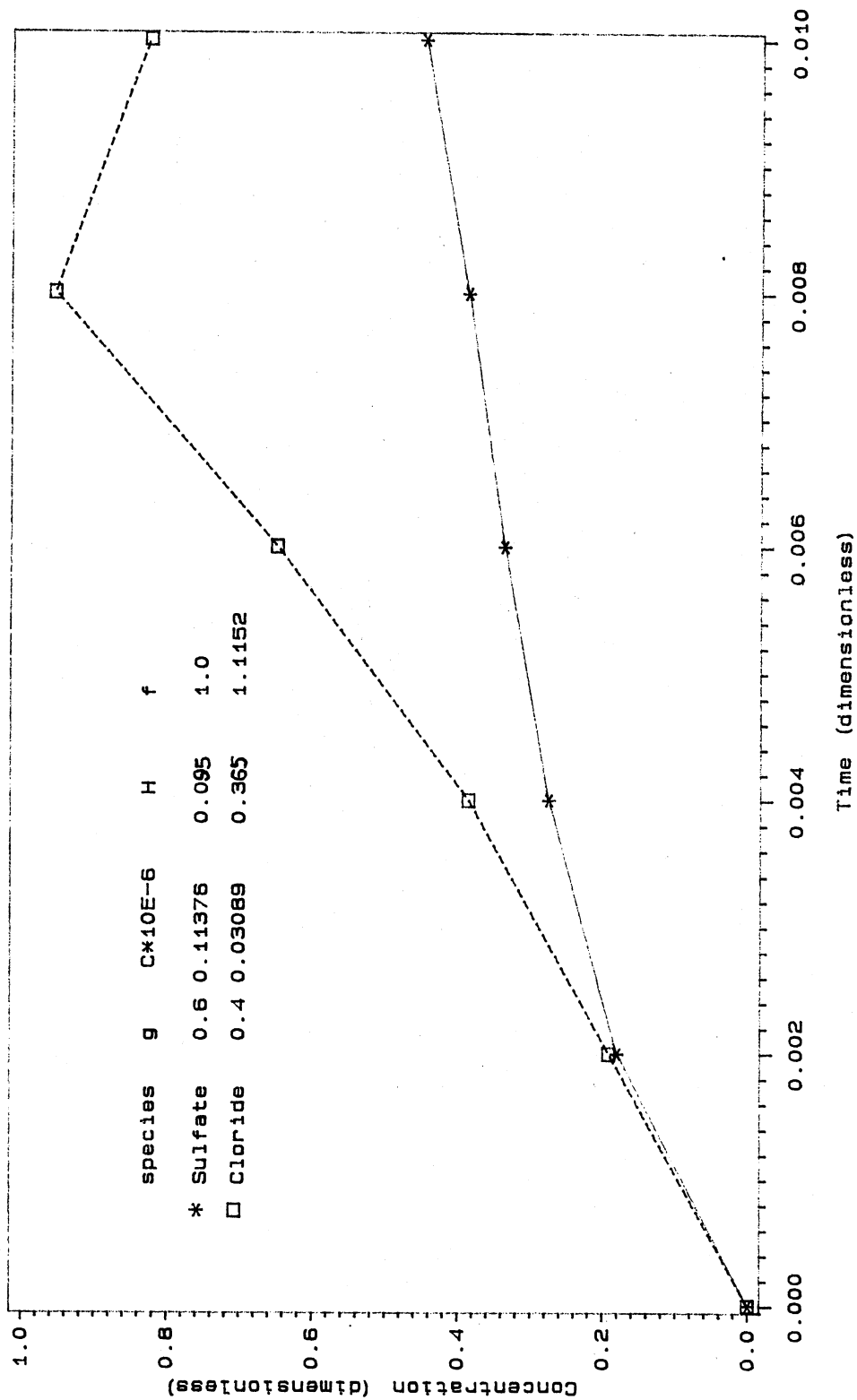


Figure 42. Effluent Concentration Profile for Two Components Dissolution

approaches its interfacial value, thus the driving force for dissolution of Cl^- is smaller than that of SO_4^{2-} . As a consequence, the predicted concentration for Cl^- is decreased after 0.008.

Three Components System

To illustrate the versatility of the computer program, we extend our implicit scheme to the case of dissolution with three components. No major changes are needed in the program. The only difference lies in the dimension of the variables and the input data. Finite-difference results for three-component system are presented in Figures 43 and 44 in terms of mass fraction and the concentration profile, respectively.

Since species 3 (Cl^-) has a relatively high solubility, it dissolves rapidly in the liquid until the concentrations next to the interface approaches its interfacial concentration. Species 1 (SO_4^{2-}) has lower solubility and a lower diffusivity than species 3; the faster dissolution of species 3 nevertheless causes the increase in the mass fraction of species 1 in the solid region before it approaches its interfacial concentration. Meanwhile, species 2 (NO_3^-) behaves much like species 1 but the changes occur more slowly as it has the lowest solubility of any component.

Figure 45 plots the position of the boundary against time for the three different cases. As was expected, the

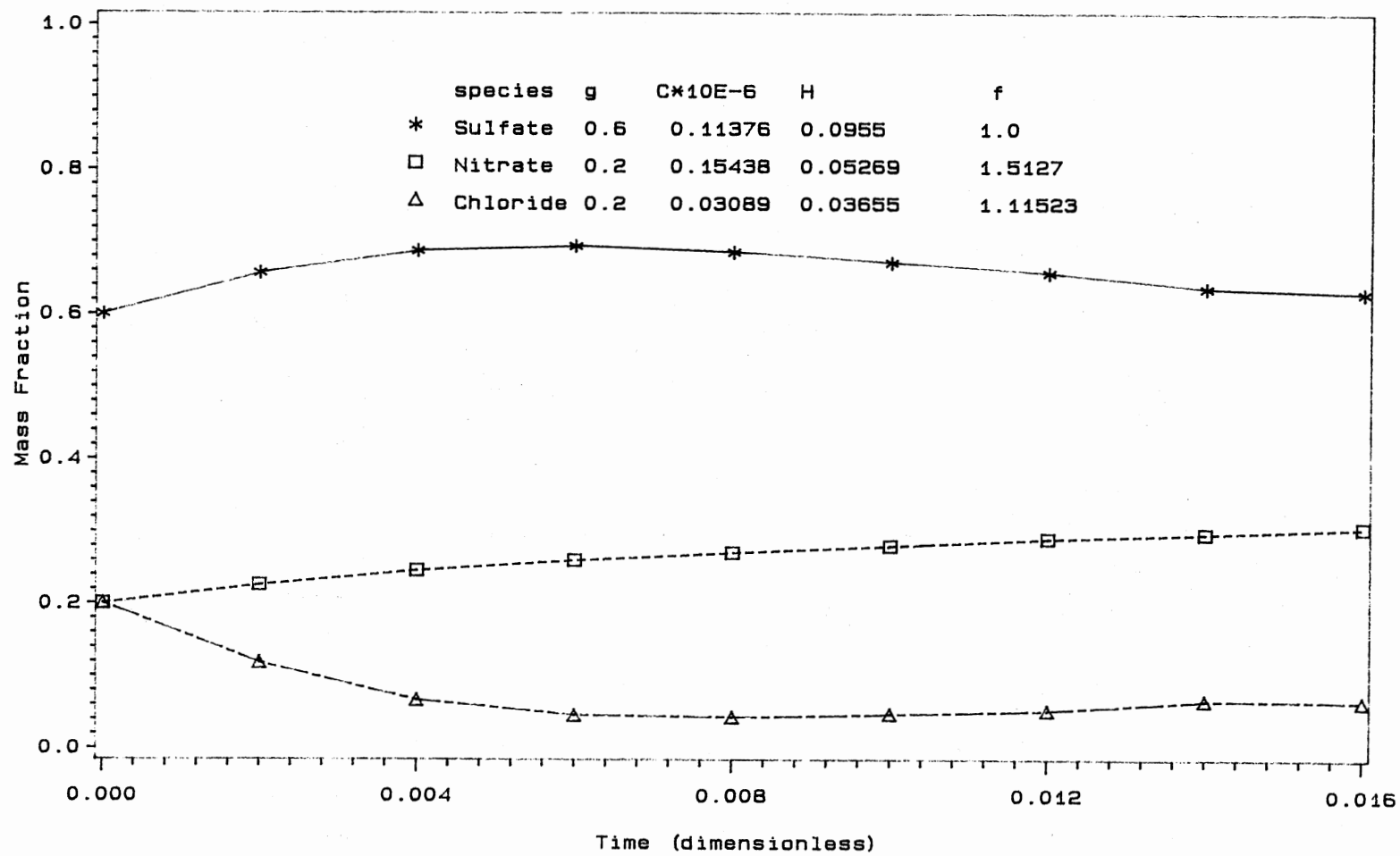


Figure 43. Mass Fraction for 3 Components Dissolution

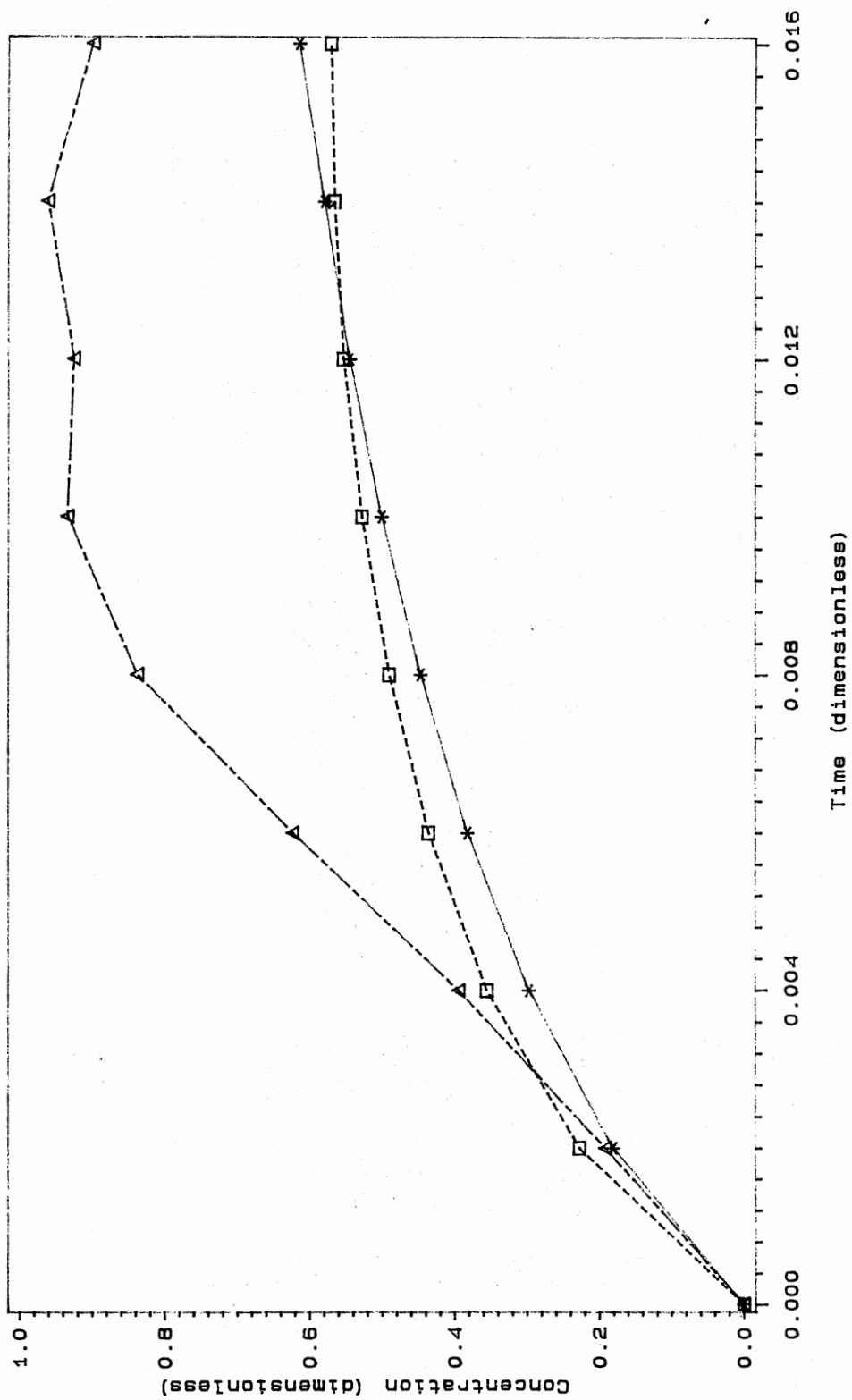


Figure 44. Concentration Distribution for 3 Components Dissolution

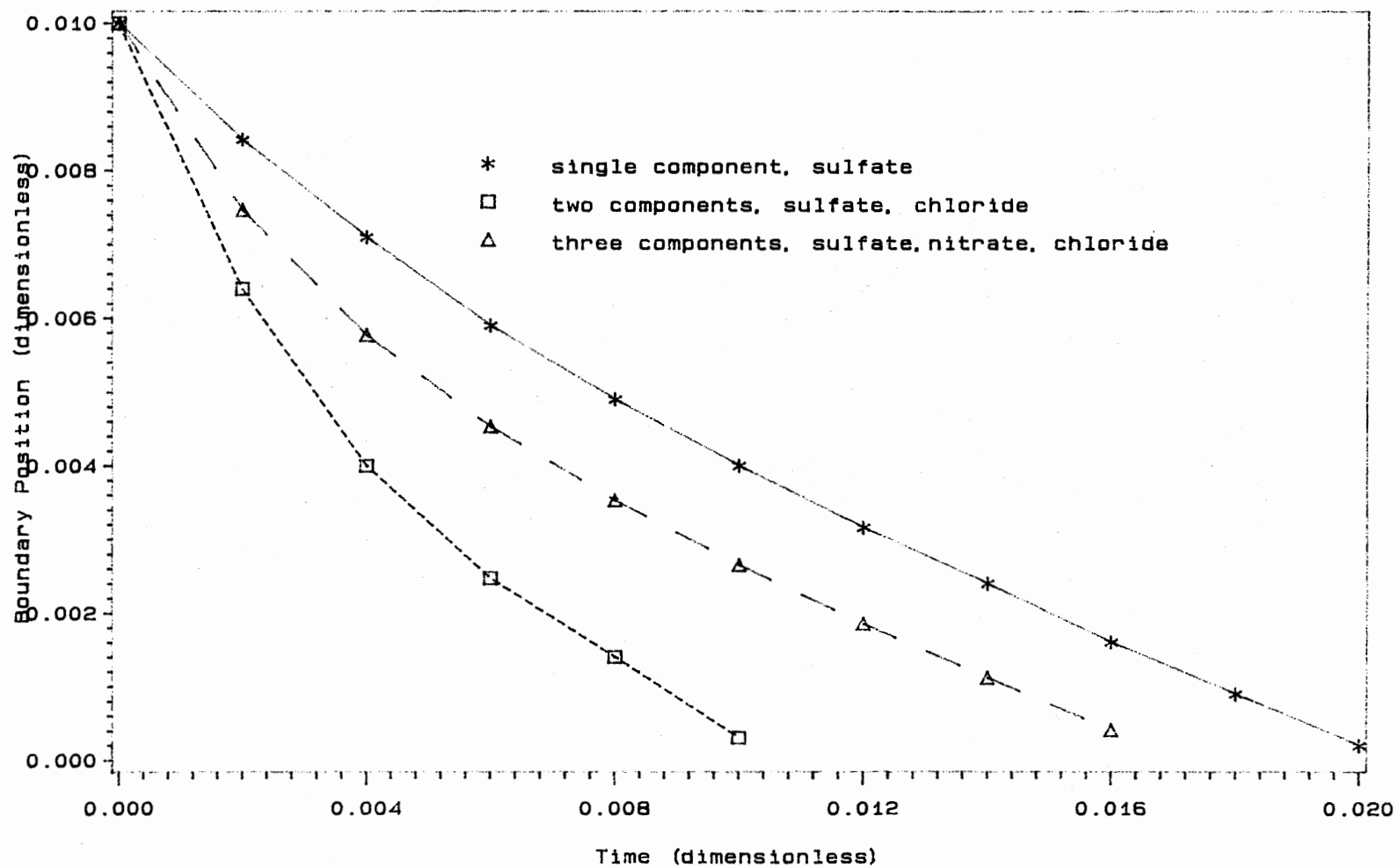


Figure 45. Boundary Position Versus Time for One, Two and Three Components Cases

movement of the boundary increased with the solubility of the solute. Note that solubility has a greater effect on the movement of boundary than does diffusivity. This is because an increase in solubility causes an increase in the gradient of the profile of the species, i.e. in $\delta C_i / \delta y$ $y=0$.

Four Components System

Two runs were made to study the effect of initial mass fraction on the rate of dissolution of the solids. The results are presented in Figure 46. Since a rapid decrease in thickness requires rapid dissolution of the components with highest solubilities, again the model is shown to be consistent and the trends are expected.

Figure 47 shows the transient mass fraction of a four-component system having a particular initial mass fraction as listed in the figure. As species 4 (NH_4^+) has highest solubility, it therefore dissolves rapidly in the liquid, species 3 (Cl^-) also has high solubility but a higher diffusivity than species 4. This solute likewise dissolves but does somewhat slowly than species 4; the faster dissolution of species 3 and 4 causes an increase in the mass fraction of species 1 (SO_4^{2-}) and 2 (NO_3^-). The changes of mass fraction of species 1 and 2 are, however, at first largely governed by the faster transport of species 3 and 4.

Figure 48 shows an example of this for same components as in Figure 47 but the original mass fraction now contain 30% for each of components 1, 2, and 3 and 10% of component

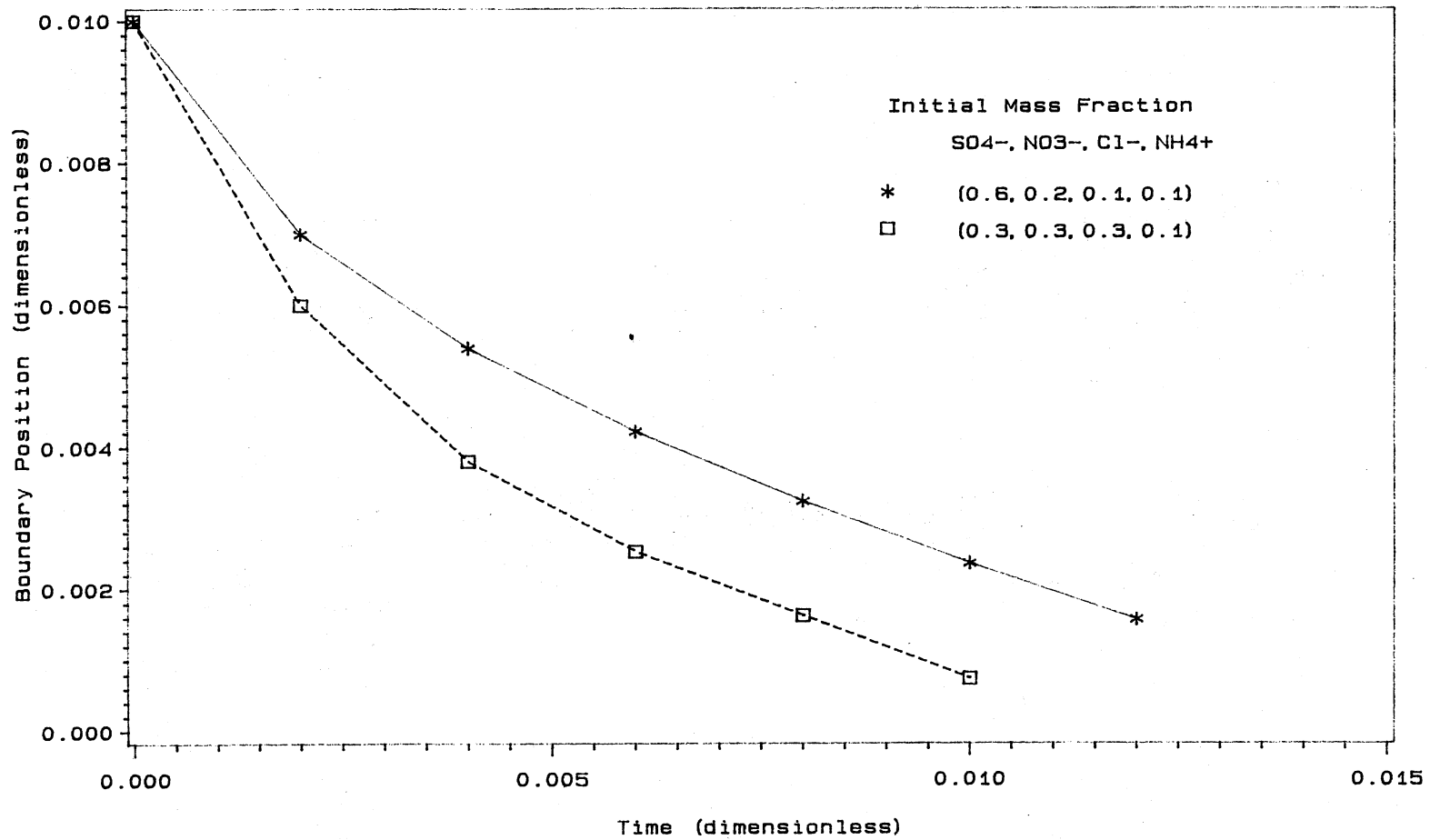


Figure 46 Boundary Position Versus Time for Four Components with Different Initial Mass Fraction

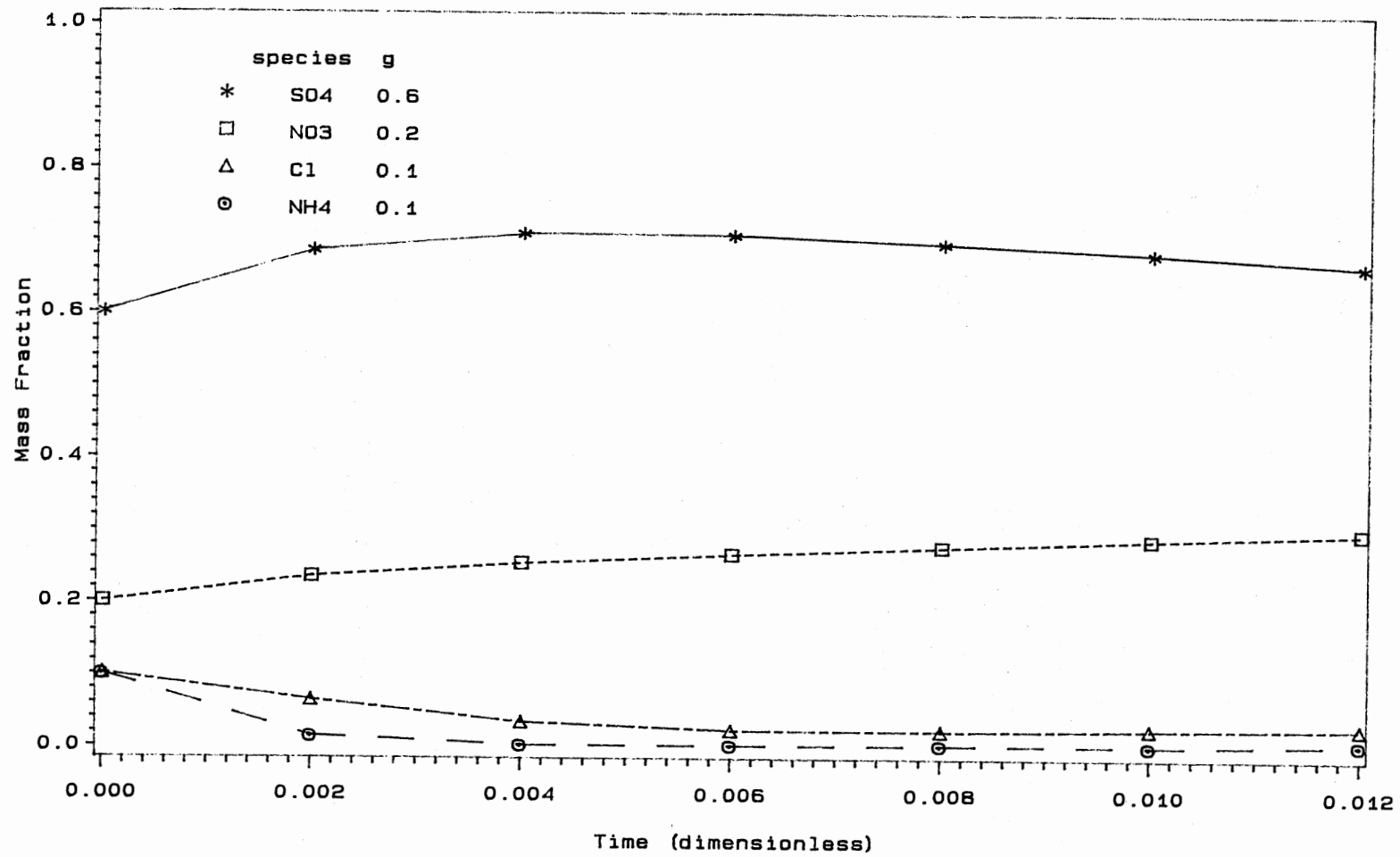


Figure 47. Variation of Mass Fraction Versus Time for Four Components Dissolution

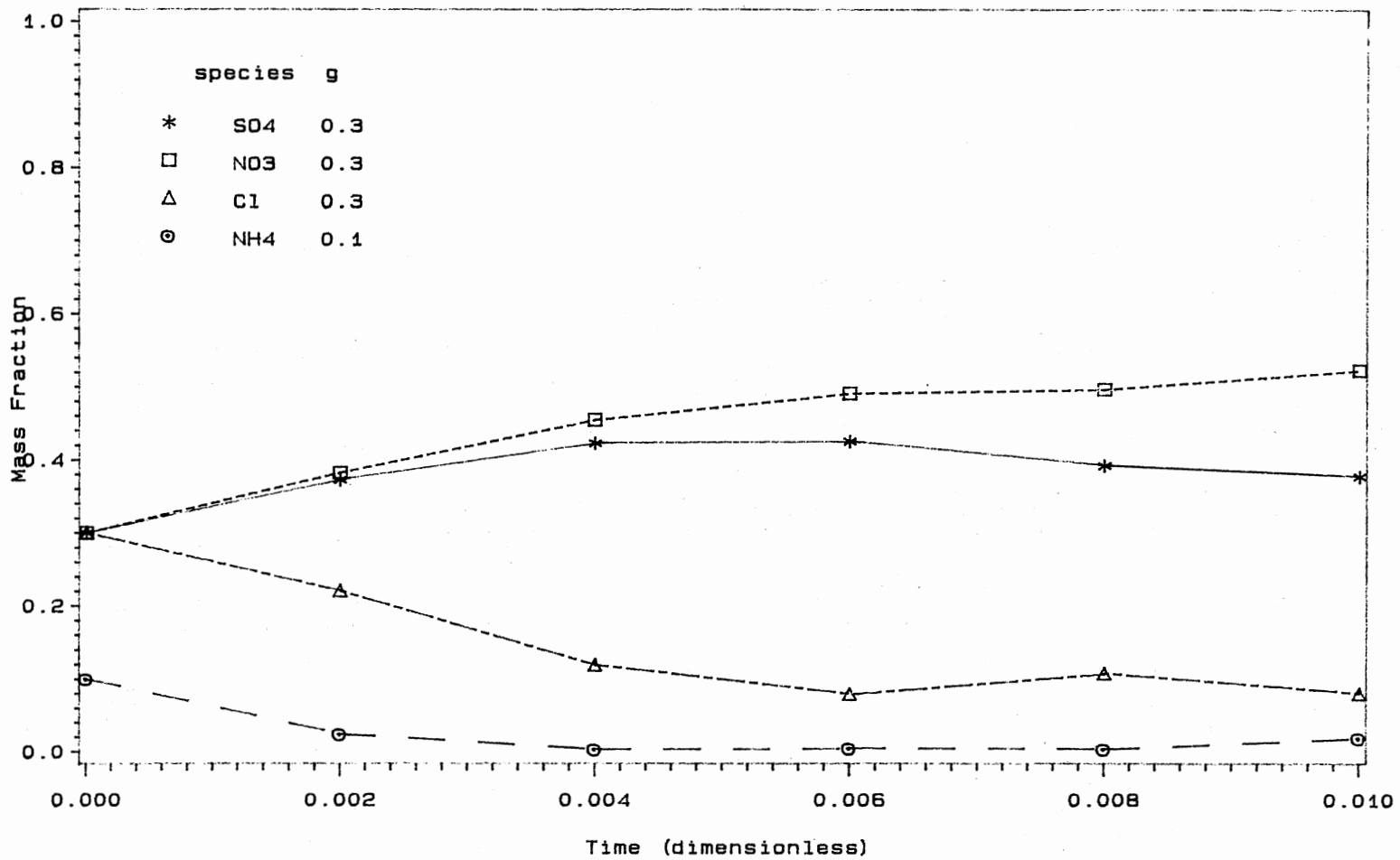


Figure 48. Variation of Mass Fraction Versus Time for Four Components Dissolution

4. The same qualitative trends have been observed.

Figure 49 shows the predicted effluent concentrations for four components next to the interface. The initial mass fractions for each component are listed in the figure. Because of our restriction that the thickness of solid phase is no more than 0.01 initially, the dissolution of the solid has a significant effect on the concentration profile for a relatively short time period if the solubility of the species is high. Since Cl^- and NH_4^+ have the highest solubilities, the concentrations increase dramatically compared with those of SO_4^{2-} and NO_3^- .

After NH_4^+ reaches its interfacial concentration value, it begins to drop. This is expected for the concentration gradient approaches to zero, the driving force to dissolve NH_4^+ in the solid layer becomes smallest. However, it remains unresolved why the concentration of NH_4^+ is greater than 1.0 at time greater than 0.008. The explanation is possible due to the unrealistic parameters used in the simulation model.

Time transient effects generally persist throughout the whole course of dissolution and, as a result, there are no generally valid approximations for boundary position-time curves, time to dissolve completely, or concentration distribution. Although, the mathematical formulation derived in Chapter VI allow the predictions of dissolution behaviors, the results will not be useful if measures of the transport parameters and coefficients are not adequate. The

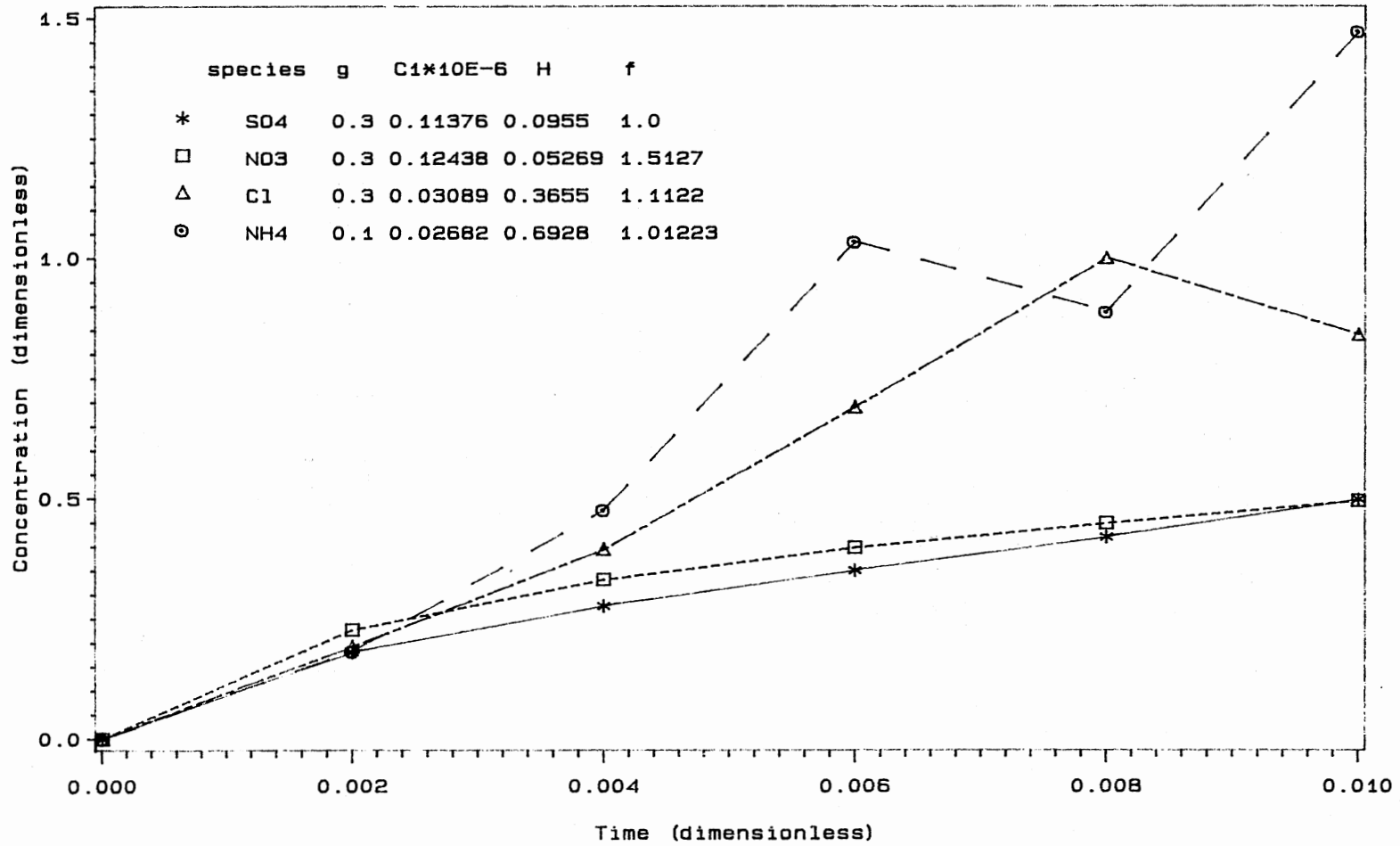


Figure 49. Effluent Concentration Profile for Four Components Dissolution

major obstacle in applying the model in a useful manner for the solutions of field problems is often not the computational difficulty but, rather, deficiency in measuring the appropriate transport parameters and coefficients for the model input.

CHAPTER VIII

SUMMARY AND RECOMMENDATIONS

Acidic deposition is comprised of two components: wet and dry. Dry deposition includes all processes by which airborne contaminants are removed from the atmosphere at the surface of the earth, excluding those processes directly aided by precipitation. Dry deposition contributes substantially to the total acidic deposition burden. Thus, efforts to investigate its behavior will provide insight on the role that it assumes in the larger problem of acidic deposition.

The purpose of this study is to improve our understanding of the impact of dry deposition on throughfall chemistry. In the first part of this study, a mixing model has been developed based on canopy properties, precipitation quantity and quality. The model simulates the biogeochemical processes which alter the chemistry of the rainwater when it travels through the forest canopy.

Briefly, the model follows the movement of water through various components of the canopy. Simultaneously, it calculates the water volume and the concentrations of the chemical species in the water by simulating various biogeochemical processes occurring in each component. The conceptualization of the model has been described in chapter

IV in detail.

The model has been calibrated with data collected at Woods Lake in the Adirondack Mountains of New York. The model has accurately simulated throughfall volume and the concentration of nitrate and potassium ions for both American Beech and Red Spruce. Prediction of throughfall concentrations of sulfate, chloride and magnesium ions are better for American Beech than those of Red Spruce. Moreover, the overprediction of ammonium ion for American Beech and Red Spruce suggests that NH_4^+ may be absorbed by its leaves.

Inaccuracies in prediction by the model of certain ions for the first two collection points may be due to the variability in rainfall intensity and/or under- or overprediction of the dryfall loadings. Overall, the results of model simulation suggests that sulfate, potassium, calcium, sodium and magnesium are leaching controlled.

The second part of the present work was undertaken to investigate the possibility of deriving a mathematical equation involving the multicomponents dissolution process and extend the range for numerical methods. A unsteady state, partial differential equation characterized by a moving boundary was obtained. A method based on coordinate transformation which transforms the time-varying domain into an invariant one is derived, for solving a two-dimensional moving boundary problem. Two components systems have been

tested and the numerical results obtained by the present method are found to be in good agreement with those of Cable and Frade (1986). The method is further extended to three and four-component systems, and results are presented in chapter VII.

Based on the results obtained from these two different approaches, the following conclusions are presented:

1. Modeling of dissolution of dry deposited mass is an essential step in determining the impact of dry deposition on throughfall chemistry for the initial period of an event. It is believed that the dissolution model, proposed in this study is capable of simulating the movement of dry deposited substances through a solid-layer media into the liquid phase and can be carried right up to the end of the dissolution process.

2. A mixing model can be referred to as an integral model because input data is required over some period of time. Dissolution model, referred to as the differential model, has significant effect on the throughfall chemistry during the first two collections of the event. Although, the dissolution is useful when dealing with small times, data input in this model have to be more precise than those for the mixing model.

3. The combination of dissolution and mixing models can improve the understanding of the role of dry deposition on acidic deposition. The accuracy of a predicted concentration distribution depends primarily on the accuracy

of the transport parameters and coefficients used in the simulation models.

4. Though no stability criterion was established for the implicit difference equations, it is found that the time steps utilized in dissolution model should not be greater than 0.002 (dimensionless) for an initial thickness of 0.01 (dimensionless).

Although the model developed in this study gives promising results, the following recommendations for further study are made:

1. Leaching is probably the major source for many elements in throughfall, such as potassium and other metallic cations. In spite of its known rapidity and magnitude in laboratory trials, however, the importance of leaching is unresolved for other elements in field situations. Therefore, intensive experimental procedures in laboratory and field over a longer period time should be conducted to study leaching of ions from canopy surfaces and absorption of ions by the canopy surfaces.

As discussed previously, leaching parameters are not constant throughout the event. In this respect, time-dependent studies of leaching parameters are necessary. Furthermore, gaining an understanding of the effect of hydrogen ion concentration in rainwater on leaching rate is highly encouraged.

2. Vegetation is an important sink for airborne materials because of the reactivity of its large surface

area. Leaves indiscriminately sorb many gaseous substances that may be biologically toxic (HF, H₂S) or life supporting (CO₂). Pollutants assimilated by plants enter biological cycles which in turn change the chemical characteristics of the pollutants, thereby altering subsequent availability to plant system. Rates and types of biochemical transformations are not known for pollutants absorbed directly from the atmosphere. Therefore, integrated studies of biogeochemical cycling of atmospheric substances by vegetation, including transfer to other plant components, soil exudation, and re-emission to the atmosphere, need to be performed.

3. Both stemflow and throughfall from the same tree should be analyzed in order to close water and material balance, and characterize more accurately the effect of the canopy on the incident precipitation.

4. The regression procedure between wetfall volume and throughfall volume should be employed on an event basis due to the variability of rainfall intensity. In addition, an adjustment of throughfall volume with respect to wetfall collection should be done to account for the difference in collection area between throughfall and wetfall collectors. In this study, the correction factor is 1.13.

5. Mass residue in the tree after an event was not taken into account in the mixing model. The effect of residue would be to increase the initial dry deposition. A thorough study in this respect is suggested to improve the

predictability of mixing model.

6. Little information is available with respect to the dissolution kinetics. In order to develop adequate predictive model, additional studies in mechanisms of the dissolution process are needed.

7. The simplicity of the dissolution model imposes obvious limitations on its applications, for example, insoluble or poor soluble gases/particles. It is believed that insoluble gases/particles will most likely behave differently than soluble ones. Among the properties of dry deposited materials that are known or postulated to affect their interactions with the canopy surfaces are (i) size, density and shape, (ii) chemical composition, especially solubility in water and (iii) electric charge. A better understanding of the chemical species of pollutants and the various chemical forms is needed to accurately predict the throughfall chemistry during the initial period of rainfall event.

8. A variable time step is recommended for the dissolution model in the solution procedure, so that a smaller time step could be utilized at the early period of the event when the concentration gradients are large.

BIBLIOGRAPHY

- Bache, D.H. "Sulphur dioxide uptake and the leaching of sulfates from a Pine forest." J. Appl. Ecology, 14 (1977), pp.881-895
- Baldocchi, D.D., Hicks, B.B. and Camara, P. "A canopy stomatal resistance model for gaseous deposition to vegetated surfaces." Atmos. Environ., 20 (1986), pp.1-11
- Cable, M. and Frade, J.R. "Diffusion Controlled Growth and Dissolution of Spheres of Finite Initial Size." Materials Sci. Forum, 7 (1986), pp. 187-194
- Chen, C.W., Hudson, R.J.M., Gherinis, S.A., Dean, J.D. and Goldstein, R.A. "Acid rain model : canopy module." J. Environ. Eng., 109 (1983), pp.583-603
- Clesceri, N.L. and Vasudevan, C. "Acid precipitation, throughfall chemistry and canopy processes." Proc. Int. Conf. Eco. Impact Acid Precip. SNSF Project, Norway, (1980), pp.258-259
- Clough, W.S. "The deposition of particles on moss and grass surfaces." Atmos. Environ., 9 (1975), pp.1113-1119
- Cole, D.M., Gessel, S.P. and Rice, S.F. "Distribution and cycling of nitrogen, phosphorus, potassium and calcium in a second-growth Douglas Fir ecosystem." Symposium on Primary Productivity and Nutrient Cycling in Natural Ecosystems, University of Maine Press, Orono, Maine, (1967), pp.197-232
- CRC Handbook of Chemistry and Physics, 69th Edition, 1988-1989, CRC Press, Boca Raton, Florida
- Cronan, C.S., and Reiners, W.H. "Canopy processing of acid precipitation by coniferous and hardwood forests in New England." Oecologia, 57 (1983), pp.216-223
- Dackson, K. "Prediction of time-varying throughfall quality and quantity using a simple mixing model." MS Thesis, Rensselaer Polytechnic Institute, New York, 1983
- Dasch, J.M. "A comparison of surrogate surfaces for dry deposition collection." Precipitation, Scavenging, Dry

- Deposition, and Resuspension vol. 2, Ed. Pruppacher, H.R., Semonin, R.G. and Slinn, W.G.N., Elsevier Press, New York, (1983), pp.883-902
- Dasch, J.M. "Measurement of dry deposition to vegetative surfaces." Water, Air and Soil Pollut., 30 (1986), pp.205-210
- Davidson, C.I., Lindberg, S.E., Schmidt, J.A., Cartwright, L.G. and Landis, L.R. "Dry deposition of sulfate onto surrogate surfaces." Geophys. Res., 90 (1985), pp.2123-2130
- Desjardins, R.L. and Lemon, E.R. "Limitations of an eddy-correlation technique for determination of the carbon dioxide and sensible heat fluxes." Boundary-Layer Meteorol., 5 (1974), pp.475-488
- Desjardins, R.L. "Energy budget by an eddy correlation method." J. Appl. Meteorol., 16 (1977), pp.248-250
- Dolske, D.A. and Gatz, D.F. "A field intercomparison of sulfate dry deposition monitoring and measurement methods: preliminary results." Proceedings, American Chemistry Society, Acid Rain Symposium, Las Vegas, Nevada, (1982)
- Drablos, D. and Tollan, A., (eds), Proceedings of the International Conference on Ecological Impact of Acid Precipitation, Oslo: SNSF Project, Norwegian Council for Scientific and Industrial Research, Sandefjord, Norway, March 11-14, (1980)
- Droppo, J.G. "Dry deposition processes on vegetation canopies." Atmospheric-Surface Exchange of Particulate and Gaseous Pollutants, Ed. Engelmann, R.J. and Sehmel, G.A. National Tech. Info. Serv., (1976), pp. 104-110
- Droppo, J.G. "Experimental techniques for dry deposition measurements." Atmospheric Sulfur Deposition, Ed. Shriner, D.S., Richmond, C.R. and Lindberg, S.E. Ann Arbor Sci., Ann Arbor, Michigan, (1979), pp.209-221
- Droppo, J.G. and Doran, J.C. "Experimental constraints in micrometeorological gaseous pollutant fluxes." Precipitation, Scavenging, Dry Deposition, and Resuspension vol. 2, Ed. Pruppacher, H.R., Semonin, R.G. and Slinn, W.G.N., Elsevier Press, New York, (1983), pp.807-816
- Duda, J.L., Malone, M.F. and Notter, R.H. "Analysis of Two-Dimensional Diffusion-Controlled Moving Boundary Problems." Int. J. Heat Mass Transfer, 18 (1975), pp. 901-910

- Eastman, J.A. and Stedman, D.H. "A fast response sensor for ozone eddy-correlation measurements." Atmos. Environ. 11 (1977), pp.1209-1212
- Eaton, J.S., Likens, G.E. and Bormann, F.H. "Throughfall and stemflow chemistry in a northern hardwood forest." J. Ecology, 61 (1973), pp.495-508
- Eaton, J.S., Likens, G.E. and Bormann, F.H. "The input of gaseous and particulate sulfur to a forest ecosystem." Tellus, 30 (1978), pp.546-551
- Feely, H.W., Bowen, D.C., Nagourney, S.J. and Torquat, C.C. "Rates of dry deposition determined using wet/dry collectors." J. Geophys. Res., 90 (1985), pp.2161-2165
- Fowler D. "Dry deposition of SO₂ on agricultural crops." Atmos. Environ., 12 (1978), pp.366-373
- Fowler, D. and Unsworth, M.H. "Turbulent transfer of sulphur dioxide to a wheat crop." Quart. J. Roy. Meteorol. Soc., 105 (1979), pp.767-784
- Fowler, D. "Removal of sulfur and nitrogen compounds from the atmosphere in rain and by dry deposition." Proceedings of the International Conference on Ecological Impact of Acid Precipitation, Sandefjord, Norway, SNSF project, (1980), pp.22-32
- Galloway, J.N., Whelpdale, D.M. and Wolff, G.T. "An atmospheric sulfur budget for eastern North America." Atmos. Environ., 14 (1980), pp.409-417
- Garland, J.A. "Field measurements of the dry deposition of small particles to grass." Deposition of Atmospheric Pollutants. Ed. Georgii, H.-W. and Pankrath, J. D. Reidel Pub., (1982), pp.9-16
- Gholz, H.L., Fitz, F.K. and Waring, R.H. "Leaf area differences associated with Old-Growth Forest Communities in the weastern Oregon cascades." Canadian J. Forest Research, 6 (1976), pp.49-57
- Gorham, E. Atmosphere-Biosphere Interactions: Toward a Better Understanding of the Ecological Consequences of Fossil Fuel Combustion. National Academy Press, Washington, D.C., (1981), pp.9-21
- Hicks, B.B., Wesely, M.L. and Durham, J.L. "Critique of methods to measure dry deposition: workshop summary." Report EPA-600/9-80-050 (NTIS Publication PB81-126443), 83pp., Springfield, Va, (1980)

- Hicks B.B. and Wesely, M.L. "Turbulent transfer processes to a surface and interaction with vegetation." Atmospheric Sulfur Deposition. Ed. Shriner, D.S., Richmond, C.R., and Lindberg, S.E. Ann Arbor, Mich., Ann Arbor Sci. Pub., 568 pp. (1980), pp.199-207
- Hicks, B.B., Wesely, M.L. Coulter, R.L., Hart R.L., Durham, J.L., Speer, R.E. and Stedman, D.H. "An experimental study of sulfur deposition to grassland." Precipitation Scavenging, Dry Deposition and Resuspension. vol. 2, Ed. Pruppacher, H.R., Semonin, R.G. and Slinn, W.G.N. Elsevier, New York, (1982), pp.933-942
- Hicks, B.B. and McMillen, R.T. "A simulation of the eddy accumulation method for measuring pollutant fluxes." J. Climate and Appl. Meteorol., 23 (1984), p.637
- Hicks, B.B. "Dry deposition processes." The Acidic Deposition Phenomenon and its Effects: EPA Critical Assessment Review Papers. vol. 1, Atmos. Sci. chapter 7, (1984)
- Hicks, B.B., Hosker, R.P. Jr., and Womack, J.D. "A prototype meteorological and chemical system for determining dry deposition." ATDL 85/32, (1985)
- Hicks, B.B. "Measuring dry deposition: A re-Assessment of the state of the art." Water, Air, and Soil Pollution, 30 (1986), pp.75-90
- Hicks, B.B., Hosker, R.P. Jr. and Womack, J.D. "Comparison of wet and dry deposition derived from the first year of trial dry deposition monitoring." Symposium on Acid Rain, I. Sources and Atmospheric Process. American Chemistry Society, New York, (1986), pp.486-490
- Hoffman, W.A. Jr., Lindberg, S.E. and Turner, R.R. "Precipitation acidity: the role of the forest canopy in acid exchange." J. Environ. Qual., 9 (1980), pp.95-100
- Hutchinson, T.C. and Havas, M. (eds), Effects of Acid Precipitation on Terrestrial Ecosystem. 654pp., Plenum Press, New York, (1980)
- Ierardi, M.E. "The Interrelationship of Wet, Total and Dry Deposition." MS Thesis, Rensselaer Polytechnic Institute, New York, 1981
- IMSL, MATH/LIBRARY FORTRAN Subroutines for Mathematical Application, (1987)
- Iwatsubo, G. and Tautsumi, T. "On the amount of plant nutrients supplied to the ground by rainwater in adjacent open plot and forest." Kyoto University For.

- Bull., 39 (1967), pp.110-120
- Johannes, A.H., Altwicker, E.R. and Clesceri, N.L.
"Characterization of acidic precipitation in the
Adirondack region." EPRI EA-1826, RP 1155-1, May (1981)
- Johannes, A.H. et al., "Results from the integrated lake
watershed acidification study - unpublished data,"
(1983)
- Johannes, A.H., Altwicker, E.R., Clesceri, N.L., Chen, C.W.,
and Gherini, S.A. "ILWAS Report Series: Integrated
Lake-Watershed Acidification Study Vol. 4 : Basin Input
Analyses, Draft Final Report," submitted to Electric
Power Research Institute, (1984)
- Johannes, A.H., Chen, Y.L., Dackson, K. and Suleski, T.
"Modeling of throughfall chemistry and indirect
measurement of dry deposition." Water, Air and Soil
Pollut., 30 (1986), pp.211-216
- Johnson, D.W., Turner, J. and Kelly, J.M. "The effects of
acid rain on forest nutrient status." Water Resour.
Res., 18 (1982), pp.449-461
- Kittredge, J. Forest Influences. 394 pp, McGraw-Hill, New
York, (1948)
- Lakhnai, K.H. and Miller, H.G. "Assessing the contribution
of crown leaching to the element content of rainwater
beneath trees." Effects of Acid Precipitation on
Terrestrial Ecosystems. Ed. Hutchinson, T.C. and
Havas, M., Plenum Publishing, New York, (1980), pp.151-
172
- Lenschow, D.H., Pearson, R. Jr. and Stankov, B.B.
"Measurements of ozone vertical flux to ocean and
forest." J. Geophys. Res., 87 (1982), pp.8833-8837
- Likens, G.E. and Bormann, F.H. "Acid rain: a serious
regional environmental problems." Sci., 184 (1974),
pp.1176-1179
- Likens, G.E., Bormann, F.H., Pierce, R.S., Eaton J.S. and
Johnson, N.M. "Bio-geochemistry of a Forested Ecosystem",
Springer-Verlag, New York, (1977)
- Lindberg, S.E., Harriss, R.C., Turner, R.R., Shriner, D.S.
and Huff, D.D. "Mechanisms and rates of atmospheric
deposition of selected trace elements and sulfate to a
deciduous forest watershed." Oak Ridge National Lab.
Environmental Sciences Division, Publ. No. 1299,
ORNL/TM- 6674, (1979)

- Lindberg, S.E. and Lovett, G.M. "Application of surrogate surface and leaf extraction method to estimation of dry deposition to plant canopies." Precipitation Scavenging, Dry Deposition and Resuspension. vol. 2, (1983), pp.837-848
- Lindberg, S.E. and Lovett, G.M. "Field measurement of particle dry deposition rates to foliage and inert surfaces in a forest canopy." Environ. Sci. and Technol., 19 (1985), p.238
- Lindberg, S.E., Lovett, G.M., Richter, D.D. and Johnson, D.W. "Atmospheric deposition and canopy interactions of major ions in a forest" Sci., 231 (1986), pp.141-145
- Linthurst, R.A. Direct and Indirect Effects of Acidic Deposition on Vegetation. Butterworth Pub., Boston, (1984)
- Little, P. "A study of heavy metal contamination of leaf surfaces." Environ. Pollut., 5 (1973), pp.159-172
- Little, P. "Deposition of 2.75, 5.0 and 8.5 μ m particles to plants and surfaces." Environ. Pollut., 12 (1977), pp.293-305
- Lovett, G.M. and Lindberg, S.E. "Dry deposition and canopy exchange in a mixed oak forest as determined by analysis of throughfall." J. Appl. Ecol., 21 (1984), pp.1013-1028
- Mahendrapa, M.K. "Chemical composition of stemflow from some eastern Canadian tree species." Can. J. For. Res., 4 (1974), pp.1-7
- Mayer, R. and Ulrich, B. "Conclusion on the filtering action of forests from ecosystems analysis." Ecol. Plant., 9 (1974), pp.157-168
- Mayer, R., and Ulrich, B. "Input of atmospheric sulphur by dry and wet deposition to two central European forest ecosystems." Atmos. Environ., 12 (1978), pp.375-377
- Mayer, R. and Ulrich, B. "Input to soil, especially the influence of vegetation in intercepting and modifying input - a review." Effects of Acid Precipitation on Terrestrial Ecosystem. Ed. Hutchinson, T.C., and Havas, M. NATO Conference Series, Plenum Press, New York, (1980)
- McMillen, R.T., Matt, D.R., Hicks, B.B. and Womack, J.D. "Dry deposition measurements of sulfur dioxide to a Spruce- Fir forest in the Black Forest: A data report." NOAA Technical Memo. ERL ARL-152, 66pp., (1987)

- Miller, H.G., Cooper, J.M. and Miller, J.D. "Effect of nitrogen supply on nutrients in litterfall and crown leaching in a stand of Corsican Pine.", J. Appl. Ecology, 13 (1976), pp.233-248
- Miller, H.G. and Miller, J.D. "Collection and retention of atmospheric pollutants by vegetation." Proceedings of the International Conference on Ecological Impact of Acid Precipitation. Sandefjord, Norway, SNSF Project, (1980), pp.33-40
- Mina, V.N. "Influence of stemflow on soil." Soviet Soil Sci., 1967(1967), pp.1321-1329
- National Research Council of Canada, Acidification in the Canadian Aquatic Environment: Scientific Criteria for Assessing the Effects of Acid Deposition on Aquatic Ecosystems. NRCC No. 18475, Ottawa, National Research Council of Canada, (1981)
- Organization for Economic Cooperation and Development, "The OECD Programme on Long-Range Transport of Air Pollutants", OECD: Paris, (1977)
- Overrein, L.H., Seip, N.M. and Tollan, A. "Acid precipitation - Effects on Forest and Fish." Final Report of the SNSF Project 1972-1980. Oslo: Norwegian Council for Scientific and Industrial Research, (1980)
- Parker, G.G. Quality, variability and sources of summertime throughfall in two Virginia Piedmont forests. Thesis, University of Virginia, Charlottesville, Virginia, (1982)
- Parker, G.G. "Throughfall and stemflow in the forest nutrient cycle." Advances in Ecological Research. vol. 13, Ed. MacFadyen, A. and Ford, E.D. Academic Press, New York, (1983), pp.57-133
- Raybould, C.C., Unsworth, M.H. and Gregory, P.J. "Sources of sulfur in rain collected below a wheat canopy." Nature, 267 (1977), pp.146-147
- Reiners, W.A. and Olson, R.K. "Effects of canopy components on throughfall chemistry: An experimental analysis." Oecologia, 63 (1984), pp.320-330
- Richter, A. and Granat, L. "Pine forest canopy throughfall measurements." Report AL-43, Department of Meteorology, University of Stockholm, Sweden, (1978)
- Ritchit, B.W. and Togby, A.H. "The angle of mixedness model of micromixing general environment." Chem. Eng. Sci. 29

- (1974), pp. 533-536
- Sehmel, G.A. "Particle and gas dry deposition: a review." Atmos. Environ., 14 (1980), pp.983-1012
- Sickles, J.E., Bach, W.D. and Spiller, L.L. "Comparison of several techniques for determining dry deposition flux." Precipitation, Scavenging, Dry Deposition, and Resuspension. vol 2, Ed. Pruppacher, P.R., Semonin, R.G. and Slinn, W.G.N. Elsevier Press, New York, (1983), pp.979-989
- Sollins, P. and Drewry, G. "Electrical conductivity and flow rate of water through the forest canopy." A Tropical Rain Forest. Ed. Odum, H.T., and Pigeon, R.F., USAEC, Washington, D.C., (1970), pp.H137-H153
- Tamm, C.O. "Removal of plant nutrients from tree crowns by rain." Physiol. Plant., 4 (1951), pp.184-188
- Technicon Corporation: Automated Method for Low Level Sulfate Determinations." Technicon Industrial Method NO. 226-72, Technicon Corp., New York
- Tukey, H.B. Jr. "The leaching of substances from plants." Annul. Rev. Pl. Phys., 21 (1970), pp.305-329
- Unsworth, M.H. "The exchange of carbon dioxide and air pollutants between vegetation and the atmosphere." Plants and Their Atmospheric Environment. Ed. Grace, J., Ford, E.D. and Jarvis, P.G., Blackwells, London, (1980), pp.111-138
- Vasudevan, C. "Computer Simulation of Throughfall: A Deterministic Model to Simulate Transport of Acid Deposition to a Forested Watershed." Ph.D. Dissertation, Rensselaer Polytechnic Institute, New York, (1982)
- Wesley, M.L., Hicks, B.B., Dannevik, W.P., Frisella, S. and Husar, R.B. "An eddy correlation measurement of particulate deposition from the atmosphere." Atmos. Environ., 11 (1977a), pp.561-563
- Wesely, M.L., Cook, D.R., Hart, R.L., Hicks, B.B., Durham, J.L., Speer, R.E., Stedman, D.H. and Tropp, R.J. "Eddy-correlation measurements of the dry deposition of particulate sulfur and submicron particles." Precipitation, Scavenging, Dry Deposition, and Resuspension. vol. 2, (1983), pp.943-952
- White, E.J. and Turner, F. "A method of estimating income of nutrients in catch of airborne particles by a woodland canopy." J. Appl. Ecology, 7 (1970), pp.441-

461

- Whittaker, R.H., Likens, G.E., Bormann, F.H., Eaton, J.S. and Siccama, T.G. "The Hubbard Brook Ecosystem Study: Forest Biomass and Production; Ecological Monographs, 44 (1974), pp. 233-254
- Willis, C. and Rubin, J. "Transport of Reacting Solutes Subject to a Moving Dissolution Boundary: Numerical Methods and Solutions." Water Resour. Res., 23 (1987), pp.1561-1574
- Yawney, H.W. and Leaf, A.L. "Nutrient release from Red Pine crowns under artificial rain." Agron. Abstr., (1971), p.121
- Zinke, P.J. "Forest interception studies in the United States." Forest Hydrology. Ed. Sopper, W.E., and Lull, H.W., New York, (1966), pp.137-161

APPENDIX A

Experimental Data

Explanation of symbols used in table:

<u>Heading</u>	<u>Meaning</u>
T	Type:W = Wetfall F = Throughfall (American Beech) R = Throughfall (Red Spruce)
Time	time from event start (minutes)
Vol.	volume (ml.)
pH	pH value measured in Laboratory
SO ₄	sulfate concentration (μeq./l)
NO ₃	nitrate concentration (μeq./l)
Cl	chloride concentration (μeq./l)
NH ₄	ammonium concentration (μeq./l)
Ca	calcium concentration (μeq./l)
Mg	magnesium concentration (μeq./l)
Na	sodium concentration (μeq./l)
K	potassium concentration (μeq./l)
ACR	anion/cation ratio

Event 1

Time	Vol.	SO4	NO3	Cl	NH4	Ca	Mg	Na	K	pH	T
130	88.	23.7	24.9	8.7	14.9	19.6	3.6	5.4	5.1	4.34	W
140	128.	19.9	9.9	5.6	5.9	5.9	1.1	2.1	2.3	4.66	W
166	56.	16.2	7.8	9.3	3.5	9.9	1.1	6.0	1.9	4.74	W
188	61.	21.2	8.5	5.6	5.7	6.9	1.1	2.6	1.2	4.70	W
220	65.	15.5	9.2	4.7	2.8	6.9	1.3	2.3	1.0	4.70	W
244	68.	13.1	6.4	7.8	4.2	7.4	1.2	2.3	1.0	4.75	W
295	68.	20.5	11.4	4.2	6.4	6.4	1.3	2.3	1.2	4.66	W
326	67.	34.9	19.2	3.1	9.9	6.9	1.3	1.9	1.2	4.46	W
355	72.	29.9	17.1	7.8	8.5	6.4	0.9	2.1	1.5	4.50	W
384	81.	31.1	21.4	8.4	9.9	7.4	1.3	2.3	1.2	4.43	W
405	119.	29.3	19.9	5.6	9.9	5.4	0.8	2.1	1.5	4.45	W
422	69.	26.8	19.2	5.6	9.2	4.9	0.8	3.9	1.5	4.50	W
454	56.	24.9	21.4	3.3	7.8	6.9	1.0	6.0	0.2	4.49	W
497	73.	34.3	22.1	2.2	9.2	4.4	0.8	2.6	1.2	4.39	W
550	158.	27.4	14.9	6.4	6.4	4.9	0.8	1.9	1.7	4.48	W
609	164	24.3	12.8	2.5	4.2	2.4	0.8	1.3	0.7	4.52	W
670	196.	24.9	9.9	0.5	4.2	1.4	0.8	0.8	0.5	4.57	W
141	93.	44.9	24.2	7.6	11.4	18.9	7.0	3.6	26.0	4.77	F
182	63.	24.9	12.8	2.8	3.5	11.9	3.2	13.0	4.0	4.82	F
222	64.	23.0	11.4	2.5	1.4	15.9	1.6	61.7	5.6	4.81	F
269	62.	17.4	9.2	2.2	4.2	8.9	2.2	2.3	9.4	5.01	F
319	60.	36.8	19.2	2.5	7.8	12.4	10.6	46.9	13.5	4.70	F
350	56.	32.4	18.5	3.9	6.4	13.9	8.0	21.7	11.3	4.78	F
377	61.	34.9	20.7	3.3	7.1	15.4	5.5	7.1	11.3	4.68	F
397	67.	28.6	19.9	3.3	7.8	10.4	3.1	2.6	9.4	4.65	F
417	50.	27.4	19.2	3.1	6.4	25.4	8.6	31.3	11.6	5.30	F
485	70.	32.4	23.5	3.6	7.1	12.4	5.7	10.8	13.8	4.63	F
542	122.	32.4	14.9	2.2	4.2	7.9	3.2	1.7	11.7	4.61	F
601	102.	31.1	12.8	2.8	3.5	8.9	2.8	2.3	8.6	4.63	F
663	118.	29.3	12.8	3.1	2.1	11.4	4.1	8.9	8.9	4.70	F
202	78.	28.6	34.2	1.4	7.1	77.3	21.3	11.5	54.9	4.10	R
222	62.	61.1	42.8	5.3	4.9	79.8	29.9	19.1	24.0	3.97	R
243	76.	289.	47.8	191.	7.1	104.	27.3	22.6	46.8	3.92	R
270	72.	299.	42.8	64.8	5.7	79.8	25.3	10.3	46.0	3.91	R
294	86.	165.	29.2	37.5	7.1	62.8	16.8	9.3	60.1	4.05	R
318	85.	135.	17.8	32.7	4.9	50.3	12.8	7.8	51.1	4.09	R
353	63.	126.	16.4	32.4	5.7	47.9	12.8	8.6	49.3	4.14	R
387	90.	107.	14.9	24.8	4.9	37.4	9.0	9.5	42.9	4.17	R
418	94.	87.3	13.5	22.2	5.7	28.4	6.9	8.2	41.4	4.24	R
445	100.	76.1	13.5	19.1	9.2	23.9	5.7	7.6	32.7	4.33	R
466	160.	60.5	12.8	10.7	3.5	13.9	3.7	5.8	26.0	4.36	R
483	108.	49.9	12.1	12.6	2.8	14.4	4.1	3.9	23.0	4.42	R
511	85.	51.7	12.1	8.7	3.5	14.4	3.7	4.3	25.0	4.43	R
556	84.	60.5	12.8	11.0	2.1	15.9	5.3	5.2	28.6	4.39	R
611	222.	54.2	10.7	7.8	2.8	12.4	3.7	3.6	24.5	4.41	R
670	246.	48.0	8.5	7.0	2.1	9.9	4.9	6.5	24.5	4.43	R

Event 2

Time	Vol	SO ₄	NO ₃	Cl	NH ₄	Ca	Mg	Na	K	pH	T
165	174.	49.9	32.1	2.8	9.2	34.9	1.2	2.6	1.0	4.23	W
290	77.	24.9	5.7	6.4	5.7	2.9	0.8	10.2	3.0	4.68	W
394	65.	21.2	6.4	2.5	3.5	4.4	1.2	2.6	0.7	4.68	W
412	64.	12.4	3.5	3.1	4.2	1.9	0.8	4.3	1.0	5.00	W
433	114.	12.4	2.1	1.6	2.1	4.4	0.8	1.9	1.5	4.85	W
460	68.	11.2	1.4	1.4	2.1	1.9	0.8	1.3	2.0	4.93	W
489	100.	12.4	3.5	1.4	2.8	2.4	0.8	1.3	0.7	4.81	W
513	73.	9.9	2.8	2.5	2.1	2.4	0.8	2.6	1.0	4.94	W
533	109.	7.4	2.1	1.4	2.1	1.4	1.2	1.7	3.5	5.06	W
555	84.	9.9	2.8	1.9	2.8	1.9	0.8	2.1	0.5	5.06	W
579	84.	12.4	4.9	1.9	2.1	2.4	0.8	1.7	0.5	4.93	W
603	146.	8.1	2.1	1.1	1.4	1.4	0.8	0.8	0.5	5.06	W
622	124.	6.2	0.7	1.1	1.4	1.4	0.8	1.0	0.5	5.22	W
641	150.	7.4	0.7	1.1	1.4	0.9	0.8	1.0	0.2	5.30	W
662	89.	7.4	1.4	1.6	0.7	2.4	0.8	2.6	0.7	5.28	W
722	342.	6.2	0.7	0.5	0.7	0.9	0.8	0.8	1.2	5.18	W
782	302.	7.4	0.7	0.5	0.7	1.4	0.8	1.3	0.2	5.21	W
838	270.	7.4	0.7	0.5	0.7	0.4	0.8	2.6	0.2	5.24	W
901	91.	8.7	2.1	1.4	0.7	1.9	0.8	1.7	0.5	5.12	W
167	87.	93.5	37.1	9.0	3.5	3.4	14.8	3.9	54.9	4.48	F
390	61.	49.9	17.8	5.6	2.8	17.9	7.4	2.1	32.7	4.73	F
414	61.	21.2	5.7	3.3	0.7	8.9	3.2	2.8	20.9	5.02	F
435	70.	14.9	2.8	1.4	0.7	5.4	1.6	8.9	9.7	4.96	F
470	60.	16.8	3.5	1.6	0.7	6.4	1.5	10.9	9.7	4.95	F
512	83.	16.2	3.5	1.6	0.7	5.9	1.5	12.6	10.2	5.01	F
535	76.	13.1	2.1	0.8	0.7	3.4	1.5	2.3	6.3	5.13	F
557	52.	9.9	2.8	1.6	0.7	0.4	1.4	125.0	5.5	5.17	F
605	130.	9.9	2.8	0.5	1.4	2.2	1.0	1.3	5.1	5.03	F
624	75.	6.2	1.4	0.8	0.7	3.4	0.8	1.9	4.0	5.34	F
643	97.	9.9	0.7	0.8	0.7	2.4	0.8	1.0	3.0	5.42	F
664	53.	9.9	1.4	1.9	0.7	2.1	0.8	2.8	4.0	5.19	F
724	222.	7.4	0.7	0.8	0.7	1.9	0.8	1.3	4.0	5.39	F
785	199.	6.2	0.7	0.8	0.7	1.9	0.8	0.8	3.5	5.54	F
847	182.	6.2	0.7	0.8	0.7	2.4	0.8	1.0	4.0	5.40	F
903	60.	7.4	1.4	2.2	0.7	2.4	1.6	3.9	6.1	5.32	F
395	57.	102.0	22.8	12.9	2.1	N.A.	N.A.	N.A.	153.7	4.21	R
434	61.	134.0	9.9	15.2	2.1	N.A.	6.9	18.2	154.2	4.16	R
469	69.	193.0	4.9	21.1	4.9	N.A.	9.3	3.0	147.5	4.04	R
517	91.	164.0	4.2	18.3	4.2	51.8	7.6	4.7	104.0	4.08	R
534	77.	113.0	2.8	15.7	1.4	26.4	7.5	5.2	52.1	4.20	R
556	73.	92.3	2.8	20.3	2.1	20.9	6.7	7.3	47.8	4.25	R
580	58.	90.4	2.1	14.1	1.4	16.1	36.2	6.2	40.4	4.29	R
604	94.	70.4	2.1	12.6	2.1	12.4	4.2	5.4	34.7	4.40	R
623	82.	66.7	1.4	15.5	2.8	12.9	4.1	3.6	28.9	4.46	R
642	113.	46.1	1.4	8.7	2.1	10.9	2.8	2.6	24.0	4.56	R
663	73.	54.8	1.4	10.1	2.1	9.9	3.2	3.6	21.4	4.60	R
723	259.	31.8	0.7	7.3	2.1	6.4	1.6	13.2	17.3	4.70	R
784	232.	25.5	0.7	7.6	1.4	6.4	1.6	1.9	15.8	4.73	R
839	208.	24.3	1.4	7.8	1.4	5.9	1.6	2.1	16.8	4.77	R
902	92.	24.9	1.4	8.1	0.7	7.4	2.8	2.3	18.9	4.79	R

Event 7

Time	vol.	SO ₄	NO ₃	Cl	NH ₄	Ca	Mg	Na	K	pH	T
2183	108.	119.0	84.2	6.4	44.2	18.4	5.0	4.3	4.0	3.91	W
2212	68.	66.1	34.9	8.7	25.7	6.4	2.6	2.6	5.3	4.28	W
2242	79.	58.6	21.4	6.4	24.2	4.4	1.6	2.6	7.1	4.33	W
2259	83.	47.4	12.1	2.5	12.8	2.4	0.8	0.4	2.3	4.26	W
2286	65.	41.1	11.4	2.8	11.4	2.4	0.8	0.6	2.2	4.37	W
2408	62.	89.8	25.7	3.3	23.5	5.4	1.1	0.6	2.2	4.16	W
2454	133.	76.7	27.1	1.9	19.9	4.9	1.2	0.6	2.2	4.19	W
2461	68.	26.2	5.7	1.4	7.1	1.9	0.8	0.8	2.2	4.64	W
2476	61.	25.5	7.8	1.4	7.1	2.4	0.8	1.4	2.0	4.54	W
2565	75.	73.6	42.1	3.1	35.	6.4	1.8	1.4	2.0	4.15	W
2583	75.	58.6	27.8	2.8	34.	3.9	0.9	1.4	2.5	4.35	W
2988	130.	34.9	15.7	3.3	9.2	5.4	1.8	1.7	4.6	4.60	W
3054	89.	22.4	10.7	2.2	5.7	4.9	1.8	1.9	3.3	4.88	W
3184	86.	15.5	8.5	1.6	4.2	3.9	0.9	2.1	3.3	5.15	W
3369	198.	16.2	2.8	1.4	2.8	3.4	0.8	4.1	3.0	5.17	W
3426	197.	9.9	0.7	0.5	0.7	1.4	0.8	1.5	2.3	5.27	W
3485	137.	13.1	0.7	1.6	0.7	1.4	0.8	3.0	2.5	5.29	W
3547	67.	13.7	2.1	3.3	0.7	3.4	0.8	2.6	3.5	5.14	W
3673	104.	13.7	2.1	2.2	0.7	3.4	0.8	2.1	3.8	5.22	W
3733	74.	13.7	3.5	2.2	0.7	3.4	0.8	2.8	3.5	5.05	W
3800	85.	9.3	2.8	1.6	1.4	2.4	0.8	3.0	3.5	5.06	W
3862	72.	11.2	2.1	2.8	1.4	2.4	0.8	3.9	3.8	5.03	W
3923	99.	13.1	1.4	2.2	2.1	2.4	0.8	1.7	2.5	4.97	W
3985	136.	6.8	0.7	1.4	1.4	1.4	0.8	1.3	1.7	5.14	W
4043	93.	7.4	0.7	1.4	1.4	1.4	0.8	1.5	1.5	5.24	W
4221	106.	21.2	3.5	7.0	0.7	5.4	1.4	7.3	7.6	4.90	W
4357	133.	31.1	9.9	2.5	7.1	3.9	1.1	4.1	4.0	4.58	W
4852	320.	16.2	5.7	1.4	9.2	1.4	0.8	1.5	2.5	4.90	W
2184	89.	82.0	14.0	15.2	44.2	60.3	35.2	20.8	2.0	4.06	F
2217	53.	109.0	56.4	7.8	20.7	29.4	16.9	12.6	5.1	4.33	F
2244	61.	87.9	30.6	4.7	16.4	18.4	12.1	12.6	9.7	4.41	F
2261	81.	64.2	15.7	4.2	10.7	11.4	6.9	3.6	26.8	4.53	F
2283	56.	66.1	13.5	5.3	9.9	11.9	6.2	4.2	49.0	4.53	F
2409	52.	138.0	28.5	7.0	15.7	29.4	16.9	4.2	49.0	4.32	F
2455	86.	19.0	34.2	5.6	16.4	25.4	15.5	4.7	53.7	4.32	F
2465	57.	51.7	9.2	3.6	6.4	11.4	6.1	46.0	46.6	4.64	F
2564	61.	71.1	28.5	6.2	14.9	20.4	11.9	4.6	36.5	4.51	F
2585	57.	87.3	37.8	6.4	29.9	22.4	12.6	4.6	45.0	4.51	F
2989	86.	78.6	18.5	18.3	1.4	26.9	16.7	4.5	58.8	4.66	F
3055	59.	51.7	11.4	14.9	3.5	16.9	10.3	2.9	47.0	4.92	F
3186	53.	47.4	9.9	16.9	5.7	17.9	11.1	2.9	44.1	5.09	F
3371	141.	49.2	5.7	20.0	3.5	14.4	10.6	1.9	42.9	5.23	F
3428	137.	22.4	2.1	5.3	0.7	4.9	2.9	1.9	18.9	5.35	F
3487	90.	16.2	2.1	5.0	0.7	3.9	2.1	5.8	15.8	5.21	F
3549	52.	22.4	2.8	5.0	0.7	5.9	3.9	5.6	21.3	5.31	F
3674	68.	26.8	3.5	5.9	0.7	7.4	5.4	5.6	28.6	5.22	F
3735	53.	26.2	4.9	5.3	0.7	6.4	4.6	5.6	24.9	5.28	F
3802	57.	22.4	5.7	5.9	0.7	6.4	4.6	5.6	20.4	5.25	F
3864	56.	21.2	4.9	12.1	2.8	5.4	3.7	5.6	13.4	5.78	F
3925	63.	21.2	3.5	5.0	0.7	5.4	3.2	5.4	7.1	5.26	F

3987	92.	12.4	2.8	5.0	0.7	3.9	1.8	4.1	17.3	5.38	F
4045	62.	13.7	1.4	4.2	0.7	3.9	1.9	5.8	15.3	5.38	F
4223	61.	24.3	2.8	6.7	1.4	6.9	4.7	3.4	28.6	5.38	F
4359	86.	38.6	11.4	5.0	0.7	9.9	7.0	1.7	35.5	5.04	F
4854	199.	28.6	7.1	6.4	2.8	6.4	4.6	0.8	31.7	5.12	F

N.A. : indicates the experimental data is unavailable

Event	Type	Time	ACR	Event	Type	Time	ACR
1	W	130	0.629	1	W	140	0.927
1	W	166	0.886	1	W	188	0.943
1	W	220	0.858	1	W	244	0.806
1	W	295	0.914	1	W	326	1.024
1	W	355	1.074	1	W	384	1.028
1	W	405	0.993	1	W	422	0.994
1	W	454	0.914	1	W	497	0.994
1	W	550	0.998	1	W	609	1.000
1	W	670	1.020	1	W	729	0.816
1	F	141	0.914	1	F	182	0.798
1	F	222	0.363	1	F	269	1.052
1	F	319	0.526	1	F	350	0.935
1	F	377	1.052	1	F	397	0.930
1	F	417	0.648	1	F	485	0.812
1	F	542	0.930	1	F	601	0.943
1	F	663	0.817	2	W	165	0.787
2	W	290	0.851	2	W	394	0.904
2	W	412	0.856	2	W	433	0.705
2	W	460	0.649	2	W	489	0.737
2	W	513	0.746	2	W	533	0.586
2	W	555	0.869	2	W	579	0.997
2	W	603	0.830	2	W	622	0.719
2	W	641	0.988	2	W	662	0.835
2	W	722	0.672	2	W	782	0.814
2	W	838	0.823	2	W	901	0.925
2	F	167	1.229	2	F	390	0.899
2	F	414	0.656	2	F	435	0.513
2	F	470	0.782	2	F	512	0.544
2	F	535	0.769	2	F	557	0.107
2	F	605	0.770	2	F	624	0.546
2	F	643	0.974	2	F	664	0.895
2	F	724	0.697	2	F	785	0.728
2	F	847	0.598	2	F	903	0.644
2	R	395	1.172	2	R	434	1.052
2	R	469	1.045	2	R	517	1.200
2	R	534	0.845	2	R	556	0.818
2	R	580	1.199	2	R	604	0.863
2	R	623	0.961	2	R	642	0.804
2	R	663	1.015	2	R	723	0.657
2	R	784	0.739	2	R	839	0.748
2	R	902	0.712	7	W	2183	1.054
7	W	2212	1.258	7	W	2242	1.028
7	W	2259	1.010	7	W	2286	0.966
7	W	2408	1.198	7	W	2454	1.167
7	W	2461	0.994	7	W	2476	0.843
7	W	2565	1.019	7	W	2583	1.027
7	W	2583	1.027	7	W	2988	1.127
7	W	3054	1.147	7	W	3184	1.192
7	W	3369	0.978	7	W	3426	0.920
7	W	3485	1.138	7	W	3547	1.221
7	W	3673	1.070	7	W	3733	0.965
7	W	3800	0.692	7	W	3862	0.744

7	W	3923	0.826	7	W	3985	0.643
7	W	4043	0.769	7	F	2184	1.247
7	F	2217	1.522	7	F	2244	1.290
7	F	2261	0.946	7	F	2283	1.476
7	F	2409	1.579	7	F	2455	0.971
7	F	2465	1.378	7	F	2564	0.923
7	F	2585	0.934	7	F	2989	0.886
7	F	3055	0.869	7	F	3186	1.732
7	F	3371	0.946	7	F	3428	0.883
7	F	3487	0.676	7	F	3549	1.961
7	F	3674	0.752	7	F	3735	2.160
7	F	3802	0.901	7	F	3864	2.817
7	F	3925	1.088	7	F	3987	0.632
7	F	4045	0.608	7	F	4223	0.738

APPENDIX B

PROGRAM LISTING FOR MICROMIXING MODEL

Some explanatory information on the computer program is provided here, and the program listing follows. This version represents the methods as described in chapter IV.

The first list below defines some of the major program variables. The second list gives brief descriptions of the general purpose of individual subroutine.

Integer Variables:

FINISH : ending time
ICNT : counter variable
INDEX : indicator variable, appeared in the
subroutine argument
INWET : current wetfall sample used as input
NF : number of throughfall sample collected
NT : number of tank (int(LAI)+1)
NW : number of throughfall sample collected
T : time variable
TANK : tank counter
THROUT : current throughfall sample used as output
TNK : tank variable
TTIME(40) : 40-element vector of throughfall collection
time

WTIME(40) :40-element vector of wetfall collector time

Logical Variable:

DONE : denotes the status for program termination
DRY(10) : a 10-element vector denoting wetting status of each tank
FINAL : denotes last tank status
MULTI : denotes cascade situation
OVER : denotes overflow
TERM : denotes early loop termination

Real Variables:

CA : calcium ion concentration in wetfall or throughfall sample
CL : chloride ion concentration in wetfall or throughfall sample
COAC(10): 10-element vector of calculated organic acid concentration in each tank
CPMASS(9): 9-element vector of cumulative predicted mass
CTMASS(9): 9-element vector of actual measured mass
CTP : calculated throughfall volume
CTVOLA(40):40-element vector of actual cumulative throughfall volume
CUMVOL(40):40-element vector of throughfall volume
CVS : throughfall volume collection
DD : temporary variable, transferring dry deposition to
DRYD(9) : 9-element vector of dry mass loading
HKMASS : mass retained in the tree for potassium ion
HSMASS : mass retained in the tree for sulfate ion

HOLDUP : maximum holdup volume of each tank

HVOL(10): 10-element vector of the current holdup in each tank

INMASS(9): 9-element vector of the mass introduced to a tank

INTCP : intercept from the throughfall as a function of wetfall curve, EQ(4.1)

INVOL : volume introduced to a tank

LAI : leaf area index

LC : temporary variable, transferring leaching coefficient to LEACH(ION)

LEACH(9): 9-element vector of leaching coefficients

MG : magnesium concentration in wetfall or throughfall

NA : sodium concentration in wetfall or throughfall sample

NEWCON(10,9)
: a 10*9 array of currently calculated concentrations, first subscript denotes the TANK, second denotes ionic species

NH4 : ammonium concentration in wetfall or throughfall

NO3 : nitrate concentration in wetfall or throughfall

OAC : amount of organic acid entering each tank

OACIN : the concentration of organic acids transferred from one compartment to the next

OLDCON(10,9)
: a 10*9 array of previously calculated concentrations, first subscript denotes the TANK, second denotes ionic species

OUTVOL : overflow volume for the current tank

PH : pH value in wetfall or throughfall sample

POT : potassium concentration in wetfall or throughfall

RATE : current rainfall intensity

SAMASS : calculated stemflow mass for sodium ion
SCMASS : calculated stemflow mass for calcium ion
SHMASS : calculated stemflow mass for hydrogen ion
SKMASS : calculated stemflow mass for potassium ion
SLMASS : calculated stemflow mass for chloride ion
SLOPE : a slope from the throughfall as a function
of wetfall curve, EQ (4.1)
SMASS : calculated stemflow mass for magnesium ion
SNHMAS : calculated stemflow mass for ammonium ion
SNMASS : calculated stemflow mass for nitrate ion
SO4 : sulfate concentration in wetfall or
throughfall
SSMASS : calculated stemflow mass for sulfate ion
SVOL : calculated stemflow volume
SVOLT : total stemflow volume
TCA : throughfall mass for calcium ion
TCL : throughfall mass for chloride ion
TCON(40,9)
: a 40*9 element vector of throughfall
concentrations, first subscript denotes sample
number, second denotes ionic species
MG : throughfall mass for magnesium ion
TNA : throughfall mass for sodium ion
TNH : throughfall mass for ammonium ion
TNO : throughfall mass for nitrate ion
TOTVOL : total volume in the tank
TPOT : throughfall mass for potassium ion
TSM : throughfall mass for sulfate ion
TV : total throughfall volume (measured)
TVOL(40): 40-element vector of throughfall collection

volume
 VOL : wetfall volume or throughfall volume (input)
 WCA : wetfall mass for calcium ion
 WCL : wetfall mass for chloride ion
 WCON(40,9)
 : a 40*9 vector of wetfall concentration, first
 subscript denotes sampling number, second
 denotes ionic species
 WMG : wetfall mass for magnesium ion
 WNA : wetfall mass for sodium ion
 WNH : wetfall mass for ammonium ion
 WNO : wetfall mass for nitrate ion
 WPOT : wetfall mass for potassium ion
 WSM : wetfall mass for sulfate ion
 WV : total wetfall volume vector
 WVOL(40): 40-element of wetfall collection volume

SUBROUTINE

General Purpose

CHECK The function of this subroutine is to
 check whether the variable TIME is
 equal to the variable FINISH; if the
 TIME is equal to FINISH, then the
 difference between the measured
 values and the predicted values will
 be calculated; if not then we will go
 back to the main program to get new
 input data

NAME This subroutine is used to give the
 ion name in printout

OUTPUT The function of this subroutine is to
 format the output whenever it is
 called

C THIS IS A PROGRAM TO SIMULATE THE ACID RAIN PASS THROUGH
 C THE TREE BY USING MIXING MODEL

C
 C AUTHOR: YUH-LING CHEN

C
 C DATE: APRIL 23, 1987

C
 C

```

REAL WCON(40,9),INMASS(9),OLDCON(10,9)
REAL HOLDUP,LAI,SLOPE,INTCP
REAL SVOL,SVOLT,CTP,OACIN,OACA,COAC(10)
REAL V,PH,SO4,NO3,CL,NH4,CA,MG,NA,POT,WSM,WNO
REAL WV,WCL,WNH,WMG,WCA,WNA,WPOT,TV,TSM,TNO,TCL,TNH,
REAL TMG,TNA,TPOT,LC,DD,RATE,OUTVOL,INVOL,TOTVOL
INTEGER NW,NF
INTEGER ICNT,INDEX
INTEGER TANK,TNT,NT,TNK,ION,INWET,THROUT,FINISH,TIME,T
LOGICAL MULTI,OVER,DONE,DRY(10),FINAL,TERM
COMMON/DATA1/HVOL(10),NEWCON(10,9),TCON(40,9),
&          CPMASS(9),CTMASS(9),CUMVOL(40),CTVOLA(40),
&          DRYD(9),LEACH(9)

```

```

COMMON/DATA2/HOLDUP,NT,WV,WSM,WPOT,SSMASS,SKMASS,
&          HKMASS,HMASS
COMMON/DATA3/CTP,TNT,CVS,SVOLT,ICNT
COMMON /DATA4/WVOL(40)
COMMON /DATA5/WTIME(40)
COMMON /DATA6/TTIME(40)
COMMON /DATA7/TVOL(40)
COMMON /DATA8/SHMASS,SNMASS,SLMASS,SNHMAS,SCMASS,
&          SMMASS,SAMASS
INTEGER WTIME,TTIME
REAL WVOL,TVOL
REAL HVOL,NEWCON
REAL TCON,CPMASS,CTMASS,CUMVOL,CTVOLA,DRYD,LEACH

```

C
 C READ IN PARAMETERS: HOLDUP, LAI, SLOPE AND INTCP

C
 C

```

OVER=.FALSE.
MULTI=.FALSE.
FINAL=.FALSE.
TERM=.FALSE.
DONE=.FALSE.

```

C

```

READ (5,*)HOLDUP, LAI, SLOPE, INTCP
WRITE(6,2)HOLDUP, LAI, SLOPE, INTCP
2  FORMAT('1','THE HOLDUP VOLUME IS',F10.4/ '0 THE LEAF
& AREA INDEX ', 'IS',F10.4/ '0 THE LINEAR RELATIONSHIP
& BETWEEN WETFALL VOLUME', ' AND THROUGHFALL VOLUME IS
& DETERMINED',// '0 THE SLOPE IS',F10.4/ '0 AND THE
& INTERCEPT IS',F10.4//)

```

C
 C

```

SLOPE=SLOPE/1000.
NT=IFIX(LAI)
TNT=NT+1
HOLDUP=HOLDUP/NT
C
C READ IN NUMBER OF WETFALL AND THROUGHFALL EVENT
C
      READ(5,*)NW,NF
C
C INPUT EXPERIMENTAL DATA, INCLUDING THE WETFALL VOLUME,
C CONCENTRATIONS
C INITIALIZE THE SUMMATION INDEXES
C
      WV=0
      WSM=0
      WNO=0
      WCL=0
      WNH=0
      WMG=0
      WCA=0
      WNA=0
      WPOT=0
      WRITE(6,4)
4      FORMAT('0 TIME VOL PH WSO WNO WCL WNH WCA
C      & ', 'WMG WNA WPOT')
C
      DO 100 I=1,NW
      READ(5,*)TIME,V,SO4,NO3,CL,NH4,CA,MG,NA,POT,PH
      WTIME(I)=TIME
      WVOL(I)=V
      WV=WV+V
      WCON(I,1)=1.E6*(10.**(-1*PH))
      WCON(I,2)=SO4
      WSM=WSM+SO4*V/1000.
      WCON(I,3)=NO3
      WNO=WNO+NO3*V/1000.
      WCON(I,4)=CL
      WCL=WCL+CL*V/1000.
      WCON(I,5)=NH4
      WNH=WNH+NH4*V/1000.
      WCON(I,6)=CA
      WCA=WCA+CA*V/1000.
      WCON(I,7)=MG
      WMG=WMG+MG*V/1000.
      WCON(I,8)=NA
      WNA=WNA+NA*V/1000.
      WCON(I,9)=POT
      WPOT=WPOT+POT*V/1000.
      WRITE(6,6)WTIME(I),V,PH,WSM,WNO,WCL,WNH,WCA,WMG,WNA,
C      & WPOT
6      FORAMT(3X,I4,1X,
C      & F4.0,2X,F3.1,2X,F5.1,2X,F5.1,6(2X,F4.1),1X,F6.4)
100     CONTINUE

```

```

C
C INPUT THROUGHFALL DATA, INCLUDING THROUGHFALL VOLUME,
C CONCENTRATIONS
C INITIALIZE THE SUMMATION INDEXES
C
      TV=0.
      TSM=0.
      TNO=0.
      TCL=0.
      TNH=0.
      TCA=0.
      TMG=0.
      TNA=0.
      TPOT=0.
      WRITE(6,8)
8      FORMAT('0 TIME VOL PH TSM TNO TCL TNH
C      & TCA ', 'TMG TNA TPOT')

      DO 200 I=1,NF
      READ(5,*)T,V,SO4,NO3,CL,NH4,CA,MG,NA,POT,PH
      TTIME(I)=T
      TVOL(I)=V
      TV=TV+V
      CTVOLA(I)=TV
      TCON(I,1)=1.E6*10**(-1*PH)
      TCON(I,2)=SO4
      TSM=TSM+SO4*V/1000.
      TCON(I,3)=NO3
      TNO=TNO+NO3*V/1000.
      TCON(I,4)=CL
      TCL=TCL+CL*V/1000.
      TCON(I,5)=NH4
      TNH=TNH+NH4*V/1000.
      TCON(I,6)=CA
      TCA=TCA+CA*V/1000.
      TCON(I,7)=MG
      TMG=TMG+MG*V/1000.
      TCON(I,8)=NA
      TNA=TNA+NA*V/1000.
      TCON(I,9)=POT
      TPOT=TPOT+POT*V/1000.
      CUMVOL(I)=0.
      WRITE(6,6)T,V,PH,TSM,TNO,TCL,TNH,TCA,TMG,TNA,TPOT
200     CONTINUE
C
C READ IN LEACHING COEFFICIENTS AND DRY DEPOSITION
C INITIALIZE ACCUMULATORS FOR CUMULATIVE MASS
C
      DO 250 ION=1,9
      READ(5,*)LC,DD
      LEACH(ION)=LC
      DRYD(ION)=DD
      CPMASS(ION)=0.
      CTMASS(ION)=0.

```

```
250    CONTINUE
C
C DETERMINE THE AMOUNT OF ORGANIC ACID ENTERING EACH TANK
C
      OAC=LEACH(6)+LEACH(7)+LEACH(8)+LEACH(9)
C
C
C INITIALIZE DRY STATUS AND HOLDUP VOLUME FOR EACH TANK
C
      DO 300 TANK=1,TNT
      DRY(TANK)=.TRUE.
      COAC(TANK)=0.
      HVOL(TANK)=0.0
      DO 300 ION=1,9
      OLDCON(TANK,ION)=0.
      NEWCON(TANK,ION)=0.
300    CONTINUE
C
C INITIALIZE COUNTER, RATE, AND ACCUMULATOR
C
      INWET=1
      THROUT=1
      TIME=0
      RATE=WVOL(1)/WTIME(1)
      FINISH=TTIME(NF)
      TNK=1
      SVOLT=0.
      SSMASS=0.0
      SKMASS=0.0
      CTP=0.
      SMP=0.
      PMP=0.
      CVS=0.
      ICNT=1
C
C START THE CALCULATIONS
C
450    CONTINUE
      IF (.NOT. OVER) THEN
      TIME=TIME+1
      FINAL=.FALSE.
      TERM=.FALSE.
      TNK=1
C
C SET OLD CONCENTRATION EQUAL TO NEW CONCENTRATIONS
C
      DO 700 TANK=1,TNT
      DO 700 ION=1,9
      OLDCON(TANK,ION)=NEWCON(TANK,ION)
700    CONTINUE
      END IF
C
C CHECK IF MORE THAN 1 TANK
C
```

```

550  CONTINUE
      IF (TNK .GT. 1) THEN
          MULTI=.TRUE.
          OVER=.TRUE.
      END IF
C
C CHECK FOR LAST TANK
C
      IF (TNK .EQ. TNT) THEN
          FINAL=.TRUE.
      END IF
C
C CALCULATE MASS OF EACH ION ENTERING TANK
C
      DO 800 ION=1,9
C
C FIRST TANK?
C
          IF (MULTI) THEN
              INMASS(ION)=(OUTVOL/1000.)*NEWCON(TNK-1,ION)
              OACIN=(OUTVOL/1000.)*COAC(TNK-1)
              INVOL=OUTVOL
          ELSE
C
C FIRST TANK!
C
              INMASS(ION)=(RATE/1000.)*WCON(INWET,ION)
              INVOL=RATE
              OACIN=0
          END IF
800  CONTINUE
C
      MULTI=.FALSE.
C
C COMPUTE TOTAL VOLUME IN TANK
C
      TOTVOL=INVOL+HVOL(TNK)
C
C CALCULATE NEW CONCENTRATIONS
C
      DO 900 ION=2,9
C
C CHECK FOR FINAL TANK FIRST, IF FINAL IS TRUE, THEN NO
C LEACHING OCCURS FOR FINAL TANK
C
          IF(FINAL) THEN
              A=0.
              OACA=0.
          ELSE
              A=LEACH(ION)
              OACA=OAC
          C
C IF TANK IS DRY, ADD DRY DEPOSITION AND CHANGE DRY STATUS
C FOR THAT TANK

```



```

C
      IF (DRY(TNK)) THEN
        A=A+DRYD(ION)
      IF (ION .EQ. 9) THEN
        DRY(TNK)=.FALSE.
      END IF
      END IF
      END IF
C
C DO CALCULATION OF THE NEW CONCENTRATIONS
C
      NEWCON(TNK,ION)=(A+INMASS(ION)+OLDCON(TNK,
& ION)*HVOL(TNK)/1000.)/(TOTVOL/1000.)
900 CONTINUE
C
C DO CALCULATION FOR ORGANIC AND CONCENTRATION,
C
      COAC(TNK)=(OACA+OACIN+(COAC(TNK)*HVOL(TNK)/1000.)
& )/(TOTVOL/1000.)
C
C DETERMINE HYDROGEN ION CONCENTRATION BY CHARGE BALANCE
C
      NEWCON(TNK,1)=NEWCON(TNK,2)+NEWCON(TNK,3)+
& NEWCON(TNK,4)+COAC(TNK)-NEWCON(TNK,5)-NEWCON(TNK,6)
& -NEWCON(TNK,7)-NEWCON(TNK,8)-NEWCON(TNK,9)
C
C CHECK FOR OVERFLOW CALCULATIONS
C
      IF (TOTVOL .GT. HOLDUP .AND. .NOT. FINAL) THEN
        HVOL(TNK)=HOLDUP
        OUTVOL=0.827395*(TOTVOL-HOLDUP)
C
C OUTVOL IS EQUAL TO THROUGHFALL VOLUME
C
C CALCULATE THE STEMFLOW VOLUME, SULFATE AND POTASSIUM MASS
C FOR CHECKING THE MATERIAL BALANCE
C
      SVOL=TOTVOL-HOLDUP-OUTVOL
      SSMASS=SSMASS+(SVOL*NEWCON(TNK,2)/1000.)
      SHMASS=SHMASS+(SVOL*NEWCON(TNK,1)/1000.)
      SNMASS=SNMASS+(SVOL*NEWCON(TNK,3)/1000.)
      SLMASS=SLMASS+(SVOL*NEWCON(TNK,4)/1000.)
      SNHMAS=SNHMAS+(SVOL*NEWCON(TNK,5)/1000.)
      SCMASS=SCMASS+(SVOL*NEWCON(TNK,6)/1000.)
      SMMASS=SMMASS+(SVOL*NEWCON(TNK,7)/1000.)
      SAMASS=SAMASS+(SVOL*NEWCON(TNK,8)/1000.)
      SKMASS=SKMASS+(SVOL*NEWCON(TNK,9)/1000.)
      SVOLT=SVOLT+SVOL
      ELSE
        HVOL(TNK)=TOTVOL
        TERM=.TRUE.
      END IF
C

```

```
C
      IF (.NOT. FINAL) THEN
          ICNT=ICNT+1
      END IF
C
C CHECK FOR EARLY TERMINATION
      IF (.NOT. TERM) THEN
          IF (TNK .NE. TNT) THEN
              OVER=.TRUE.
          END IF
      ELSE
          OVER=.FALSE.
      END IF
C
C
      IF (FINAL) THEN
          CALL CHECK(FINISH,TIME,INWET,THROUT,RATE,
&                   INDEX,DONE)
      ELSE
          IF (OVER) THEN
              TNK=TNK+1
              GO TO 550
          ELSE
              CALL CHECK(FINISH,TIME,INWET,THROUT,RATE,
&                   INDEX,DONE)
          END IF
      END IF
      IF (INDEX .EQ. 1) THEN
          GO TO 450
      ELSE
          GO TO 1000
      END IF
1000 STOP
      END
```

```
C THIS IS SUBROUTINE CHECK
C THE FUNCTION OF THIS SUBROUTINE IS TO CHECK WHETHER THE
C TIME IS EQUAL TO THE FINISH;
C IF THE TIME IS EQUAL TO THE FINISH, THEN WE ARE GOING TO
C CALCULATE THE DIFFERENCE BETWEEN THE MEASURED VALUES AND
C THE PREDICTED VALUES. ALSO, THE OUTPUT OF THESE
C DIFFERENCE IS PRINTED
      SUBROUTINE CHECK(FINSIH,TIME,INWET,THROUT,RATE,
&                      INDEX,DONE)
C
      LOGICAL DONE
      COMMON/DATA1/HVOL(10),NEWCON(10,9),TCON(40,9),
&      CPMASS(9),CUMVOL(40),CTVOLA(4),DRYD(9),CTMASS(9),
&      LEACH(9)
      COMMON/DATA2/HOLDUP,NT,WV,WSM,WPOT,SSMASS,
&      SKMASS,HKMASS,HSMASS
      COMMON/DATA8/SHMASS,SNMASS,SLMASS,
&      SNHMAS,SCMASS,SMASS,SAMASS
      COMMON/DATA3/CTP,TNT,CVS,SVOLT,ICNT
      COMMON/DATA4/WVOL(40)
      COMMON/DATA5/WTIME(40)
      COMMON/DATA6/TTIME(40)
      COMMON/DATA7/TVOL(40)
      INTEGER WTIME,TTIME
      INTEGER TIME,FINISH
      INTEGER TNT,NT,INWET,THROUT,INDEX
      REAL LEACH,NEWCON
C
      IF (TIME .EQ. FINISH) THEN
        DONE=.TRUE.
        CALL OUTPUT(DONE,TIME,THROUT)
        INDEX=2
      ELSE
        IF (TIME .EQ. WTIME(INWET)) THEN
          INWET=INWET+1
          RATE=WVOL(INWET)/(WTIME(INWET)-WTIME(INWET-1))
          IF (TIME .EQ. TTIME(THROUT)) THEN
            CALL OUTPUT(DONE,TIME,THROUT)
          END IF
          INDEX=1
        ELSE
          IF (TIME .EQ. TTIME(THROUT)) THEN
            CALL OUTPUT(DONE,TIME,THROUT)
            INDEX=1
          ELSE
C BACK TO MAIN PROGRAM CHECK OVERFLOW
            INDEX=1
          END IF
        END IF
      END IF
      RETURN
      END
```

```

C
C SUBROUTINE OUTPUT
C
C THE FUNCTION OF THIS SUBROUTINE IS TO PRINT THE DIFFERENCE
C BETWEEN THE CALCULATED VALUES AND THE MEASURED VALUES
C
C     SUBROUTINE OUTPUT(DONE,TIME,THROUT)
C
C
C     CHARACTER BUFFER(13)
C     LOGICAL DONE
C     INTEGER ION
C     COMMON/DATA1/HVOL(10),NEWCON(10,9),TCON(40,9),
C &         CPMASS(9),CTMASS(9),CUMVOL(40),DRYD(9),
C &         CTVOLA(40),LEACH(9)
C     COMMON/DATA2/HOLDUP,NT,WV,WSM,WPOT,SSMASS,
C &         SKMASS,HKMASS,HSMASS
C     COMMON/DATA3/CTP,TNT,CVS,SVOLT,ICNT
C     COMMON/DATA4/WVOL(40)
C     COMMON/DATA5/WTIME(40)
C     COMMON/DATA6/TTIME(40)
C     COMMON/DATA7/TVOL(40)
C     COMMON/DATA8/SHMASS,SNMASS,SLMASS,SNHMAS,SCMASS,
C &         SMMASS,SAMASS
C     REAL LEACH,NEWCON
C     INTEGER TIME,INDEX,THROUT,TNT,WTIME,TTIME,NT
C
C     WRITE(6,640)TIME
C     WRITE(6,650)
C     CTP=CTP+HVOL(TNT)
C
C C COMPARE THE DIFFERENCE BETWEEN PREDICTED CONCENTRATIONS AND
C C MEASURED CONCENTRATIONS
C
C     DO 100 ION=1,9
C     DIFF=NEWCON(TNT,ION)-TCON(THROUT,ION)
C     CALL NAME(ION,BUFFER)
C
C C CALCULATE THE PREDICTED MASS AND MEASURED MASS
C
C     CPMASS(ION)=CPMASS(ION)+(NEWCON(TNT,ION)*
C & HVOL(TNT)/1000.)
C     CTMASS(ION)=CTMASS(ION)+(TCON(THROUT,ION)*
C & TVOL(THROUT)/1000.)
C     WRITE(6,680) BUFFER,NEWCON(TNT,ION),TCON(THROUT,ION)
C     IF (DONE) THEN
C
C C CALCULATE THE MASS RETAINED IN TREE
C
C     HSMASS=0
C     HKMASS=0.
C
C
C     DO 200 I=1,NT

```

```

                HKMASS=HKMASS+(NEWCON(I,9)*HVOL(I)/1000.)
                HSMASS=HSMASS+(NEWCON(I,2)*HVOL(I)/1000.)
200          CONTINUE
                END IF
C
C RESET COLLECTION BUCKET
C
                NEWCON(TNT,ION)=0.
100          CONTINUE
C
640          FORMAT('1 PREDICTED CONCENTRATIONS AT TIME ',I4)
650          FORMAT('0 ION          PRED          ACTUAL          ')
680          FORMAT(1X,13A1,F6.1,5X,F6.1)
                WRITE(6,670)
                WRITE(6,650)
C
C COMPARISON OF PREDICTED TO ACTUAL MASS
C
                DO 300 ION=1,9
                DIFF=(CPMASS(ION)-CTMASS(ION))/CTMASS(ION)*100.
                CALL NAME(ION,BUFFER)
                BULK1=1000.*CPMASS(ION)/(CUMVOL(THROUT)+HVOL(TNT))
                BULK2=1000.*CTMASS(ION)/(CTVOLA(THROUT))
                WRITE(6,660)
                & BUFFER,CPMASS(ION),CTMASS(ION),DIFF,BULK1,BULK2
300          CONTINUE
C
C COMPARISON OF PREDICTED TO ACTUAL VOLUME
C
                CVS=CVS+HVOL(TNT)
                CUMVOL(THROUT)=CVS
C
                DIFF1=(HVOL(TNT)-TVOL(THROUT))/TVOL(THROUT)*100.
                DIFF2=(CUMVOL(THROUT)-
                & CTVOLA(THROUT))/CTVOLA(THROUT)*100.
                WRITE(6,690)
                & HVOL(TNT),TVOL(THROUT),DIFF1,CUMVOL(THROUT),
                & CTVOLA(THROUT),DIFF2
C
C RESET COLLECTOR VOLUME
C
                HVOL(TNT)=0.
                THROUT=THROUT+1
                IF (DONE) THEN
C
C COMPUTATION AND PRINTING OF FINAL MATERIAL BALANCE
C
                WRITE(6,700)
                TVT=HOLDUP*NT
                WRITE(6,710)WV
                WRITE(6,720)CUMVOL(THROUT-1),CTVOLA(THROUT-1)
                WRITE(6,730) SVOLT

```

```

WRITE(6,740) TVT
SUM= WV-TVT-SVOLT-CUMVOL(THROUT-1)
WRITE(6,750) SUM
WRITE(6,760)
WRITE(6,770) WSM,WPOT
DDTS=DRYD(2)*NT
DDTK=DRYD(9)*NT
WRITE(6,830) DDTS,DDTK
SLM=LEACH(2)*ICNT
PLM=LEACH(9)*ICNT
WRITE(6,810)SLM,PLM
WRITE(6,780) CPMASS(2),CPMASS(9)
WRITE(6,790) SSMASS,SKMASS
WRITE(6,800) HSMASS,HKMASS
SUMS=WSM+DDTS+SLM-HSMASS-SSMASS-CPMASS(2)
SUMK=WPOT+DDTK+PLM-HKMASS-SKMASS-CPMASS(9)
WRITE(6,820) SUMS,SUMK
END IF
660 FORMAT(3X,13A1,F9.1,2X,F9.1,2X,F6.1,5X,F6.1,3X,F6.1)
670 FORMAT('- CUMULATIVE MASS')
690 FORMAT('0 VOLUME, SAMPLE ',F8.3,3X,F8.3,3X,F6.1
& /11X, 'CUMUL',3X,F8.3,3X,F8.3,3X,F6.1)
700 FORMAT('1 FINAL MATERIAL BALANCES')
710 FORMAT('0 TOTAL INPUT VOLUME ',F6.1)
720 FORMAT('0 TOTAL THRUFULLL VOLUME PREDICTED ',F6.1,
& 'MEASURED ',F6.1)
730 FORMAT('0 TOTAL STEMFLOW VOLUME PREDICTED ',F6.1)
740 FORMAT('0 VOLUME RETAINED ',F6.1)
750 FORMAT('0 TOTAL INPUTS - OUTPUTS - HOLDUP ',F6.1)
760 FORMAT('- SULFATE POTASSIUM')
770 FORMAT('0 INPUT WET MASS ',F6.1,
& ',F6.1)
780 FORMAT('0 TOTAL THRUFULL MASS ',F6.1,
& ',F6.1)
790 FORMAT('0 TOTAL STEMFLOW MASS ',F6.1,
& ',F6.1)
800 FORMAT('0 TOTAL MASS RETAINED ',F6.1,
& ',F6.1)
810 FORMAT('0 TOTAL MASS LEACHED ',F6.1,
& ',F6.1)
820 FORMAT('0 TOTAL IN-OUT-HOLDUP ',F6.1,
& ',F6.1)
830 FORMAT('0 TOTAL DRY MASS ',F6.1,
& ',F6.1)
RETURN
END

```

C
C THIS SUBROUTINE NAME IS USED TO GIVE THE ION NAME IN OUTPUT
C
C

```
      SUBROUTINE NAME(I,BUFFER)
      CHARACTER*13 BUFFER,SULF,HYD,NIT,CHLOR,AMMON,CALC
      CHARACTER*13 MAGNES,SODIUM,POTASS
      INTEGER I
      SULF='SULFATE'
      HYD='HYDROGEN'
      CHLOR='CHLORIDES'
      NIT='NITRATE'
      MAGNES='MAGNESIUM'
      AMMON='AMMONIUMS'
      CALC='CALCIUM'
      SODIUM='SODIUM'
      POTASS='POTASSIUM'
      GO TO (10,30,50,70,90,110,130,150,170),I
10     CONTINUE
      BUFFER=HYD
      GO TO 190
30     CONTINUE
      BUFFER=SULF
      GO TO 190
50     CONTINUE
      BUFFER=NIT
      GO TO 190
70     CONTINUE
      BUFFER=CHLOR
      GO TO 190
90     CONTINUE
      BUFFER=AMMON
      GO TO 190
110    CONTINUE
      BUFFER=CALC
      GO TO 190
130    CONTINUE
      BUFFER=MAGNES
      GO TO 190
150    CONTINUE
      BUFFER=SODIUM
      GO TO 190
170    CONTINUE
      BUFFER=POTASS
      GO TO 190
190    CONTINUE
      RETURN
      END
```

APPENDIX C

ERROR ANALYSIS OF EXPERIMENTAL DATA

To determine the accuracy of the experimental data, the experimental data collected in Integrated Lake-Watershed Acidification Study has been analyzed by Johannes et. al. (1984). The results are summarized in the following tables.

TABLE XIX
SULFATE REPLICATE ANALYSES

Sample	No. of Replicates	Average Concentrations mg/L	Range of Concentrations mg/L	CV ¹
4186	4	0.26	0.20-0.30	0.16
5203	4	2.94	2.92-2.95	0.005
5247	4	1.54	1.52-1.56	0.011
6605	4	0.49	0.40-0.60	0.155
6834	4	0.58	0.52-0.65	0.089
7295	4	2.78	2.68-2.92	0.038
7299	4	1.79	1.60-1.92	0.066
8586	4	0.94	0.84-1.02	0.069
8962	4	0.64	0.60-0.68	0.044
9180	4	1.00	0.90-1.10	0.071
9255	4	0.40	0.39-0.41	0.021
9335	4	1.42	1.40-1.43	0.010
9389	4	0.79	0.73-0.83	0.048
9425	4	2.38	2.36-2.39	0.005
EPA-2	4	2.38	2.35-2.40	0.010
227	4	2.04	2.00-2.07	0.013
389	5	2.15	2.06-2.36	0.051
725	8	0.39	0.30-0.42	0.099
919	8	1.47	1.36-1.60	0.058
2296	5	2.90	2.58-3.05	0.058

CV¹ : coefficient of variation

TABLE XX
SULFATE ANALYSES OF EPA LABORATORY-PREPARED
STANDARD SOLUTIONS

Sample	Standard Solution Concentration mg/L S	Measured Concentration mg/L S	Percent Deviation	Method
EPA-2	7.2	7.50	4.1	AA [®]
EPA-2	7.2	7.39	2.6	AA
S-1.5	1.5	1.63	8.7	AA
S-3.0	3.0	2.93	2.3	AA
S-9.0	9.0	9.23	2.6	AA
S-15	15.0	16.4	9.3	AA
S-1	1.0	1.07	7.0	IC [#]
S-5	5.0	5.10	2.0	IC
S-10	10.0	10.4	4.0	IC

AA[®] : Autoabakzyzer

IC[#] : Ion Chromatograph

TABLE XXI

ANALYTICAL RESULTS FOR LABORATORY-PREPARED STANDARDS
AND U.S. EPA UNKNOWN SAMPLES

Parameters	Range of Concentrations in mg/L	Deviation in mg/L	Deviation, Percent
Laboratory Prepared Standards:			
pH (pH units)	4.0-5.0	0.04-0.06	1.0-1.5
SO ₄ ⁻² -S	1.5-15.0	0.07-1.4	2.3-9.3
NO ₃ ^{-N}	2.0-13.0	0.1-0.6	2.6-9.1
Cl ⁻	0.0175-0.095	0.01-0.09	2.3-6.3
NH ₄ ⁺ -N	0.90	0.07-0.08	7.8-8.9
Mg ⁺²	0.20	0.002-0.1	1.0-5.0
Na ⁺	0.20	0.001-0.1	0.5-5.0
K ⁺	1.0	0.01-0.03	1.0-3.0
EPA-Unknowns:			
pH (pH units)	7.7-8.6	0.04-0.16	0.5-1.8
SO ₄ ⁻² -S	7.2	0.19-0.30	2.6-4.2
NO ₃ ^{-N}	0.11-0.38	0-0.007	0.0-1.8
Cl ⁻	0.2-9.4	0.2-9.4	1.1-10.7
NH ₄ ⁺ -N	0.23-1.59	0.02-0.05	3.1-8.7

APPENDIX D

Mathematical Derivation of Equations (6.18) to (6.20)

Transformation

$$y = 1 - \frac{1-X}{1-R} \quad (6.17)$$

Clearly, the problem is transformed from a coordinate system (X,Z,T) to (y,Z,T) where the interface boundary is defined by the surface y=0.

$$\frac{\delta}{\delta X} = \frac{\delta y}{\delta X} \frac{\delta}{\delta y} + \frac{\delta Z}{\delta X} \frac{\delta}{\delta Z} + \frac{\delta T}{\delta X} \frac{\delta}{\delta T}$$

$$\frac{\delta}{\delta Z} = \frac{\delta y}{\delta Z} \frac{\delta}{\delta y} + \frac{\delta Z}{\delta Z} \frac{\delta}{\delta Z} + \frac{\delta T}{\delta Z} \frac{\delta}{\delta T}$$

$$\frac{\delta}{\delta T} = \frac{\delta y}{\delta T} \frac{\delta}{\delta y} + \frac{\delta Z}{\delta T} \frac{\delta}{\delta Z} + \frac{\delta T}{\delta T} \frac{\delta}{\delta T}$$

$$\frac{\delta y}{\delta Z} = \frac{\delta \left[1 - \frac{1-X}{1-R} \right]}{\delta Z} = - \frac{\delta \left[\frac{1-X}{1-R} \right]}{\delta Z} = \frac{\delta(1-X) \left(- \frac{\delta R}{\delta Z} \right)}{\delta(1-R)^2}$$

$$= \frac{y-1}{1-R} \frac{\delta R}{\delta Z}$$

$$\begin{aligned} \frac{\delta y}{\delta X} &= \frac{\delta \left[1 - \frac{(1-X)}{(1-R)} \right]}{\delta X} = \frac{-\delta \left[\frac{(1-X)}{(1-R)} \right]}{\delta X} = \frac{-1}{1-R} \frac{\delta(1-X)}{\delta X} \\ &= \frac{1}{1-R} \end{aligned}$$

$$\begin{aligned} \frac{\delta y}{\delta T} &= \frac{\delta \left[1 - \frac{(1-X)}{(1-R)} \right]}{\delta T} = \frac{-\delta \left[\frac{(1-X)}{(1-R)} \right]}{\delta T} = \frac{(1-X)}{(1-R)^2} \left(-\frac{\delta R}{\delta T} \right) \\ &= \frac{y-1}{1-R} \frac{\delta R}{\delta T} \end{aligned}$$

$$\frac{\delta C_1}{\delta T} = \frac{\delta y}{\delta T} * \frac{\delta C_1}{\delta y} + \frac{\delta C_1}{\delta T} = \frac{y-1}{1-R} \frac{\delta R}{\delta T} \frac{\delta C_1}{\delta y} + \frac{\delta C_1}{\delta T}$$

$$\frac{C_i}{Ni(T)} \frac{\delta Ni(T)}{\delta T} = \frac{C_i}{Ni(T)} \frac{dNi(T)}{dT}$$

$$\frac{\delta^2 C_1}{\delta X^2} = \frac{\delta}{\delta X} \left(\frac{\delta y}{\delta X} \frac{\delta C_1}{\delta y} \right) = \frac{\delta}{\delta X} \left(\frac{1}{1-R} \frac{\delta C_1}{\delta y} \right) = \frac{1}{(1-R)^2} \frac{\delta^2 C_1}{\delta y^2}$$

Equation (6.11)

$$\begin{aligned} &\frac{y-1}{1-R} \frac{\delta R}{\delta T} \frac{\delta C_1}{\delta y} + \frac{\delta C_1}{\delta T} + \frac{C_1}{Ni(T)} \frac{dNi(T)}{dT} + \frac{C_1}{Ni(T)} \frac{(y-1) \delta R}{(1-R) \delta T} \frac{\delta Ni(T)}{\delta y} \\ &= f_1 \frac{1}{(1-R)^2} \frac{\delta^2 C_1}{\delta y^2} - \frac{\delta C_1}{\delta Z} - \frac{y-1}{1-R} \frac{\delta R}{\delta Z} \frac{\delta C_1}{\delta y} \end{aligned}$$

$$\begin{aligned} \frac{dg_1}{dT} &= \frac{1}{R} \left\{ f_1 * N_1(T) \frac{\delta C_1}{\delta X_{x=R}} - g_1 \frac{\delta R}{\delta T_z} \right\} \\ &= \frac{1}{R} \left\{ f_1 * N_1(T) \frac{1}{1-R} \frac{\delta C_1}{\delta y_{y=0}} - g_1 \frac{\delta R}{\delta T_z} \right\} \quad (6.20) \end{aligned}$$

$$\begin{aligned} \frac{\delta R}{\delta T_z} &= \sum_{i=1}^N f_i * N_i(T) \frac{\delta C_1}{\delta X_{x=R}} \\ &= \sum_{i=1}^N f_i * N_i(T) \frac{1}{(1-R)} \frac{\delta C_1}{\delta y_{y=0}} \quad (6.19) \end{aligned}$$

$$\begin{aligned} \frac{\delta C_1}{\delta T} + \left\{ \frac{(y-1)}{(1-R)} \frac{\delta R}{\delta T} + \frac{(y-1)}{(1-R)} \frac{\delta R}{\delta Z} \right\} \frac{\delta C_1}{\delta y} + \frac{C_1}{N_1(T)} \frac{dN_1(T)}{dT} \\ = f_1 \frac{1}{(1-y)^2} \frac{\delta^2 C_1}{\delta y^2} - \frac{\delta C_1}{\delta Z} \end{aligned}$$

Rearrange the above equation, then

$$\begin{aligned} \frac{\delta C_1}{\delta T} + \frac{C_1}{N_1(T)} \frac{dN_1(T)}{dT} = f_1 \frac{1}{(1-R)^2} \frac{\delta^2 C_1}{\delta y^2} \\ + \frac{(1-y)}{(1-R)} \left\{ \frac{\delta R}{\delta T} + \frac{\delta R}{\delta Z} \right\} \frac{\delta C_1}{\delta y} - \frac{\delta C_1}{\delta Z} \quad (6.18) \end{aligned}$$

APPENDIX E

PROGRAM LISTING FOR DISSOLUTION MODEL

The variables declaration is given first, and the program listing follows. This version represents the methods as described in chapter VI.

The first list defines the variables used in the program, while the second half gives the brief description of the general purpose of individual subroutine.

Integer Variables:

IPATH : path indicator, IPATH=1, means the system
A*X=B is solved

JJ : number of mesh point in Z-direction

KK : number of mesh point in y-direction

JK : JJ*KK

N : number of components

Logical Variables:

CASE : if $0 < g_i < 1.0$, then case is TRUE
else CASE is set to FALSE

CONVER : if DRDT(J) less than 0.001 between two
successive iteration, then CONVER is TRUE,
else CONVER is set to FALSE

Real Variables:

A(N,JK,JK) : N*JK*JK dimension, containing the coefficient of the matrix
 ABD(JK,JK) : JK by JK matrix containing the coefficients of the linear system
 B(N) : dimensionless variable, Eq.(6.10g)
 C1(N) : inlet wetfall concentration
 CNEW(N,JK) : newly calculated concentrations
 DELT : difference scheme for time variable
 DELY : difference scheme for y-space variable
 DELZ : difference scheme for z-space variable
 DENSTY : mass density of the solid phase
 DGD(T(N)) : change of the mass fraction with respect to time
 DRDT(JJ) : change of the thickness with respect to time
 DRT(JJ) : previous values of DRDT(JJ)
 F(N) : relative diffusivity parameter to component 1
 FL(N,JK) : boundary condition at interface, $y=0$
 GNEW(N) : current value of mass fraction
 GOLD(N) : previous value of mass fraction
 H(N) : solubility parameter
 OLDCON(N,JK) : N*JK matrix, containing the concentrations in previous time step
 R(J) : temporage storage space for current value of thickness
 RHS(JK) : matrix containing right-hand-side of the equation $A*Z = RHS$
 RI(JJ) : initial values of thickness (at time=0)
 RNEW(JJ) : current value of thickness of solid layer at different location of Z

ROLD(JJ) : previous value of thickness of solid layer at
different location of Z

TIME : time variable

TOP(N,JJ): boundary condition at top, Z=0

Z(JK) : vector of length JK containing the solution to
the linear system, $A*Z=RHS$

SUBROUTINE	GENREAL PURPOSE
COEFF	Calculate the coefficients of matrix A and set the value to matrix ABD
COMNEW	Calculate the new mass fractio of component
IWKIN	Changing the amount of space allocated in the common area for storage of numeric data
LSARG	Solve a general system of linear equations with iterative refinement
MOVING	Calculate the new boundary position
RHSIDE	Compute the right-hand-side vector


```

INTEGER IPATH
PARAMETER (IPATH=1)
INTEGER JJ, KK, N, MU, ML
COMMON /GVALUE/ GOLD(4)
COMMON /CONC/ CNEW(4, 100)
COMMON /DIFF/ DELT, DELY, DTY2, DTY, DTZ, DELZ
COMMON /BOUND/ TOP(4, 10), FL(4, 10)
COMMON /CONST1/ JJ, KK, N, F(4), H(4), B(4)
COMMON /WORKSP/ RWKSP
REAL RWKSP(10359)
REAL DRDT(NEQ), DGDT(4), DRT(10)
LOGICAL CASE /.TRUE./
LOGICAL CONVER /.FALSE./
REAL Z(100), ABD(100, 100)
REAL A(4, 100, 100), OLDCON(4, 100), CNEW
REAL RNEW(10), ROLD(10), R(10), RI(10)
REAL RHS(100), FL, TOP, F, H, B
REAL C1(4), GOLD, GNEW(4), G(4)
REAL DELT, DELZ, DELY, DTY, DTZ, DTY2

C
C
C
COMMON /WORKSP/RWKSP
C
REAL RWKSP(10359)
C
CALL IWKIN(10359)
C
THESE THREE STATEMENT WERE USED TO CHANGE THE AMOUNT OF
C
SPACE ALLOCATED IN THE COMMON AREA
C
C
C
EXTERNAL LSARG
C
CALL ERRSET(207, 260, -1, 2, 0, 208)
CALL IWKIN(10359)
C
PRINT *, 'INPUT THE DIFFERENCE SCHEME FOR TIME (T)'
READ *, DELT
PRINT *, 'DELT = ', DELT

C
C
PRINT *, 'INPUT THE NUMBER OF COMPONENTS (N)'
READ *, N
PRINT *, 'N = ', N

C
PRINT *, 'INPUT THE DIFFERENCE SCHEME FOR SPACE Y AND Z'
READ *, JJ, KK
DELY = 1.0/KK
DELZ = 10.0/JJ

C
C *****
C COMPUTE DTZ, DTY2, DTY *
C *****
C
DTZ = DELT/DELZ
DTY2 = DELT/(DELY*DELY)

```

```

      DTY = DELT/2/DELY
C
C      INPUT THE PARAMETERS OF THE SYSTEM
C
C      *****
C      THE MASS DENSITY OF THE SOLID PHASE      *
C      *****
C
      PRINT *, 'THE MASS DENSITY OF THE SYSTEM'
      READ *, DENSTY
      PRINT *, 'DENSTY = ', DENSTY
C
C
      TIME = 0.0
C      *****
C      INITIAL THICKNESS OF SOLID LAYER      *
C      *****
C
      PRINT *, 'INITIAL THICKNESS OF SOLID LAYER'
      DO 1 J=1, JJ
          READ*, RI(J)
          ROLD(J)=RI(J)
1      CONTINUE
C
C      *****
C      INPUT COEFFICIENTS FOR MATRIX      *
C      INITIALLY SET ALL COEFFICIENTS TO ZEROES *
C      *****
C
      JK = KK*JJ
      DO 5 I = 1, N
          DO 5 J = 1, JK
              DO 5 K = 1, JK
                  A(I, J, K) = 0.0
5      CONTINUE
C
C      *****
C      INITIAL CONDITIONS AT TIME T=0      *
C      *****
C
      DO 6 I=1, N
          READ *, GOLD(I)
          PRINT *, 'THE INITIAL MASS FRACTION OF ', I, ' IS ', GOLD(I)
6      CONTINUE
C
C      THE INLET CONCENTRATION
C
      DO 2 I=1, N
          READ *, C1(I)
          PRINT *, 'THE INLET CONCENTRATION OF C(', I, ') IS : ', C1(I)
2      CONTINUE
C
C      *****
C      THE SOLUBILITY PARAMETER H(I)

```

```

C
DO 3 I=1,N
READ *,H(I)
PRINT *, 'THE SOLUBILITY FOR COMPONENT ',I,' IS :',H(I)
3 CONTINUE
C
C THE DIMENSIONLESS DIFFUSIVITY PARAMETER, F(I)
C
DO 4 I=1,N
READ *,F(I)
PRINT *, 'THE DIFFUSIVITY PARAMETER OF F(',I,') IS :',F(I)
4 CONTINUE
C
C THE INITIAL CONCENTRATION IN THE LIQUID PHASE
C
DO 7 I=1,N
B(I) = C1(I)/DENSTY
DO 8 M=1,JK
OLDCON(I,M) = -C1(I)/(H(I)*GOLD(I)-B(I))/DENSTY
PRINT *, 'OLDCON(',I,M,') = ',OLDCON(I,M)
8 CONTINUE
7 CONTINUE
C
C *****
C BOUNDARY VALUES AT INTERFACE, Y=0.0 *
C *****
C
DO 9 I=1,N
DO 10 J=1,JJ
FL(I,J) = 1.0
10 CONTINUE
9 CONTINUE
C
C *****
C BOUNDARY VALUES AT TOP Z=0 *
C *****
C
DO 11 I =1,N
DO 12 K =1,KK
TOP(I,K) = 0.0
12 CONTINUE
11 CONTINUE
C
IF (TIME .EQ. 0.0) THEN
DO 22 J=1,JJ
RNEW(J) = ROLD(J)
22 CONTINUE
DO 33 I=1,N
GNEW(I)=GOLD(I)
33 CONTINUE
END IF
C
C CALCULATE THE NEW POSITION OF THE BOUNDARY LAYER,
C AND THE CONCENTRATION DISTRIBUTIONS

```

```

C      INCREMENT TIME FIRST
C
      TIME= TIME+DELT
C
4444  DO 77 IEND=1, 10
      ICOUNT=0
      NCOUNT = 0
1999  IF (ROLD(1) .GT. 0) THEN
C
C      CALCULATE THE COEFFICIENTS OF THE A(I,JK,JK) MATRIX
C
55    DO 44 I=1,N
      CALL COEFF(I,JK,ROLD,RNEW,A,ABD)
C
C      CALCULATE THE RIGHT-HAND-SIDE OF THE EQUATIONS, A*Z=RHS
C
      CALL  RHSIDE(I,OLDCON,ROLD,RNEW,RHS,GNEW,GOLD)
C
C      COMPUTE THE Z VECTOR
C
      CALL  LSARG(JK,ABD,JK,RHS,IPATH,Z)
C
C      SET Z VECTOR TO NEW CONCENTRATION VALUES
C
      DO 9999 M=1,JK
          CNEW(I,M) = Z(M)
9999  CONTINUE
44    CONTINUE
C
C      USING THE NEW CONCENTRATION PROFILES, TO CALCULATE
C      THE NEW BOUNDARY POSITION
C
      CALL MOVING(DRDT,ROLD,RNEW,GNEW,GOLD)
      ICOUNT = ICOUNT+1
      PRINT *, 'ICOUNT = ', ICOUNT
C
C      FIRST ITERATION?
C
      IF (ICOUNT .LE. 1) THEN
C
C      COMPUTE NEW MASS FRACTION FOR MULTI-COMPONENT SYSTEM
C
      IF (N .GT. 1) THEN
          CALL COMNEW(GNEW,GOLD,DRDT,ROLD,DGDT,CASE)
C
C      IF ( 0<GI<1.0) THEN SET THE NEW POSITION AND NEW MASS
C      FRACTION TO TEMPORATY STORAGE VARIABLE
C      ELSE
C      STOP THE PRORAM
C
      IF (CASE) THEN
          DO 557 I=1,JJ
              R(I)=RNEW(I)
              DRT(I)=DRDT(I)

```

```

557 CONTINUE
C
DO 558 I=1,N
    G(I)=GNEW(I)
558 CONTINUE
GO TO 55
ELSE
C
C CASE IS FALSE
C
PRINT *, 'INVALID MASS FRACTION IS OBTAINED'
PRINT *, 'PROGRAM STOP'
GO TO 999
END IF
ELSE
C
C FOR SINGLE COMPONENT, WE DO NOT NEED TO CALCULATE THE
C NEW MASS FRACTION
C
DO 777 I=1,N
    GOLD(I)=GNEW(I)
777 CONTINUE
DO 888 J=1,J
    R(J)=RNEW(J)
    DRT(J)=DRDT(J)
888 CONTINUE
END IF
ELSE
C
C ICOUNT > 1, NOT FIRST ITERATION, WE NEED TO CHECK THE
C CONVERGENCE
C
IF (ICOUNT .GT. 1) THEN
DO 244 J=1,JJ
IF (ABS((DRT(J)-DRDT(J))/DRDT(J)) .LE. 1.0E-3) THEN
    NCOUNT = NCOUNT+1
ELSE
    CONVER=.FALSE.
    GO TO 911
END IF
244 CONTINUE
END IF
END IF
C234567
IF (NCOUNT .EQ. NEQ) THEN
    CONVER = .TRUE.
ELSE
    CONVER=.FALSE.
END IF
C
C IF CONVERGENCE IS TRUE, AND IF (RNEW(1) .GT.0), AND
C IF MULTICOMPONENT THEN
C CALL COMNEW TO CALCULATE THE MASS FRACTION
C PRINT OUT THE NEWLY CALCULATED RESULTS

```

```

C
911  IF (CONVER) THEN
      PRINT *, 'CONVERGENCE IS TRUE'
      PRINT *, 'TIME = ', TIME
      PRINT *, 'RNEW = ', RNEW
      IF (RNEW(1) .GT. 0.0) THEN
        IF (N .GT. 1) THEN
          CALL COMNEW(GNEW, GOLD, DRDT, ROLD, DGDT, CASE)
        ELSE
          GO TO 666
        END IF
      ELSE
        PRINT *, 'PROGRAM STOP'
        GO TO 999
      END IF
      IF (CASE) THEN
        PRINT *, 'GNEW = ', GNEW
      ELSE
        PRINT *, 'NEGATIVE VALUE IS OBTAINED FOR MASS FRACTION'
        PRINT *, 'PROGRAM STOP'
        GO TO 999
      END IF
END IF

C
C  REPLACE THE ROLD, GOLD, AND OLDCON, FROM THE NEWLY
C  CALCULATED VALUES FOR THE NEXT TIME INCREMENT
C
666  IF (ROLD(1) .GT. RNEW(1)) THEN
      DO 5555 I=1,N
      DO 6666 J=1,JJ
      DO 7777 K=1,KK
        M=(J-1)*KK+K
        PRINT *, 'CNEW( ', I, M, ') = ', CNEW(I, M)
        OLDCON(I, M)=CNEW(I, M)
7777  CONTINUE
      ROLD(J)=RNEW(J)
      R(I)=RNEW(I)
6666  CONTINUE
      GOLD(I)=GNEW(I)
      G(I)=GNEW(I)
5555  CONTINUE
C
C  TIME=TIME+DELT
      GO TO 4444
    ELSE
      PRINT *, 'THICKNESS IS GREATER THEN THE INITIAL VALUE'
      PRINT *, 'PRECIPITATION IS OCCURRED'
      GO TO 999
    END IF
C
C  ELSE
C
C  CONVERGENCE IS FALSE, WE NEED TO SET A NEW VALUE TO

```

```

C      REITERATE
C
      DO 99 J=1,JJ
          DRT(J)=DRDT(J)
          RNEW(J)=1/2*(RNEW(J)+R(J))
99     CONTINUE
        NCOUNT=0
        GO TO 55
        ELSE
        PRINT *, 'NEGATIVE RESULT IS OBTAINED'
        STOP
        END IF
        END IF
C
        ELSE
        GO TO 999
        END IF
77     CONTINUE
999    STOP
      END

C
C *****
C
C      SUBROUTINE COEFF(      )
C
C      CALCULATE THE COEFFICIENT OF MATRIX A AND SET THE VALUE TO *
C      ABD MATRIX
C
C *****
C
      SUBROUTINE COEFF(I,JK,ROLD,RNEW,A,ABD)
      COMMON /CONST1/JJ, KK, N, F(4), H(4), B(4)
      COMMON /DIFF/ DELT, DELY, DTY2, DTY, DTZ, DELZ
      REAL    ROLD(10), RNEW(10), A(4,100,100), ABD(100,100)
C
      DO 2  J=1,JJ
      DO 3  K=1, KK
      L = (J-1)*KK+K
        IF (J .LT. JJ) THEN
          L1= J*KK+K
          END IF
      A(I,L,L) = 1.0+F(I)*2*DTY2/(1.0-ROLD(J))**2
C
C      TOP ROW
C
      IF (J .EQ. 1) THEN
      CONST2 = DTY2/(1-ROLD(J))**2
      A(I,L1,L) = DTZ/2.0
      IF (K .EQ. 1) THEN
      CONST1= (1.0-K*DELY)/(1-ROLD(J))*(RNEW(J)-ROLD(J))
      &      /DELT*DTY

```

```

CONST2= DTY2/(1-ROLD(J))**2
  A(I,L+1,L) = -1.0*(CONST1 + F(I)*CONST2)
ELSE
  IF (K .GT. 1 .AND. K .LT. KK) THEN
    CONST1= (1.-K*DELY)/(1-ROLD(J))*(RNEW(J)-ROLD(J))
    & /DELT*DTY
    CONST2= DTY2/(1-ROLD(J))**2
    A(I,L+1,L) = -1.0*(CONST1+F(I)*CONST2)
    A(I,L-1,L) = CONST1-F(I)*CONST2
  ELSE
    IF (K .EQ. KK) THEN
      CONST2= DTY2/(1-ROLD(J))**2
      A(I,L-1,L) = -2.0*F(I)*CONST2
    END IF
  END IF
END IF

C
C
C
SECOND ROW TO NEXT TO LAST ROW

ELSE
  IF (J .GT. 1 .AND. J .LT. JJ) THEN
    CONST2= DTY2/(1.0-ROLD(J))**2
    CONST3= (RNEW(J)-ROLD(J))/DELT+(ROLD(J+1)-ROLD(J-1))/2
    & /DELZ
    L2 = (J-2)*KK+K
    A(I,L1,L) = DTZ/2.0
    A(I,L2,L) = -1.0*DTZ/2.0
    IF (K .EQ. 1) THEN
      CONST1= (1.-K*DELY)/(1.-ROLD(J))*CONST3*DTY
      A(I,L+1,L) = -1.0*(CONST1+F(I)*CONST2)
    ELSE
      IF (K .GT. 1 .AND. K .LT. KK) THEN
        CONST1= (1.0-K*DELY)/(1-ROLD(J))*CONST3*DTY
        A(I,L+1,L) = -1.0*(CONST1+F(I)*CONST2)
        A(I,L-1,L) = CONST1-F(I)*CONST2
      ELSE
        IF (K .EQ. KK) THEN
          A(I,L-1,L) = -2.0*F(I)*CONST2
        END IF
      END IF
    END IF
  END IF

C
C
C
BOTTOM ROW

ELSE
  IF (J .EQ. JJ) THEN
    L2=(J-2)*KK+K
    A(I,L,L) = A(I,L,L) + DTZ
    A(I,L2,L) = -DTZ
    CONST3= (RNEW(J)-ROLD(J))/DELT + (ROLD(J)-ROLD(J-1))
    & /DELZ
    CONST2= DTY2/(1.0-ROLD(J))**2
    IF (K .EQ. 1) THEN
      CONST1= (1.0-K*DELY)/(1-ROLD(J))

```



```

A(I,L+1,L) = -1.0*(CONST1*CONST3*DTY + F(I)*CONST2)
ELSE
  IF (K .GT. 1 .AND. K .LT. KK) THEN
    CONST1= (1.-K*DELY)/(1.-ROLD(J))
    A(I,L+1,L) = -1.0*(CONST1*CONST3*DTY + F(I)*CONST2)
    A(I,L-1,L) = CONST1*CONST3*DTY - F(I)*CONST2
  ELSE
    IF (K .EQ. KK) THEN
      A(I,L-1,L) = -2.0*F(I)*CONST2
    END IF
  END IF
END IF
END IF
END IF
END IF
END IF
CONTINUE
CONTINUE
C
C SET MATRIX A TO MATRIX ABD
C
DO 99 K=1,JK
DO 111 J=1,JK
ABD(K,J) = A(I,K,J)
111 CONTINUE
99 CONTINUE
C
C
RETURN
END

C
C *****
C
C SUBROUTINE RHSIDE( )
C
C CALCULATE THE RIGHT HAND SIDE VECTOR
C A*Z=RHS
C *****
C
SUBROUTINE RHSIDE(I,OLDCON,ROLD,RNEW,RHS,GNEW,GOLD)
C
C
COMMON /CONST1/ JJ, KK, N, F(4), H(4), B(4)
COMMON /DIFF/ DELT, DELY, DTY2, DTY, DTZ, DELZ
COMMON /BOUND/ TOP(4,10), FL(4,10)
C
C
REAL GNEW(4), GOLD(4), OLDCON(4,100)
REAL RHS(100)
REAL RNEW(10), ROLD(10)
C
C
C DEFINE THE FUNCTION VARG(I)

```

```

C
C
C
VARG(I) = H(I)*(GNEW(I)-GOLD(I))/(H(I)*GOLD(I)-B(I))
C
C
DO 12 J =1,JJ
DO 13 K =1,KK
L = (J-1)*KK+K
RHS(L) = (1.0-VARG(I))*OLDCON(I,L)
C
C
IF (J .EQ. 1) THEN
CONST2= DTY2/(1-ROLD(J))**2
CONST3= (RNEW(J)-ROLD(J))/DELT
RHS(L) = RHS(L)+DTZ/2.0*TOP(I,K)
IF (K .EQ. 1) THEN
CONST1= (1.0-K*DELY)/(1.0-ROLD(J))
RHS(L) = RHS(L)-(CONST1*CONST3*DTY-F(I)*CONST2)
& *FL(I,J)
END IF
ELSE
IF (J .GT. 1 .AND. J .LT. JJ) THEN
CONST2= DTY2/(1-ROLD(J))**2
CONST3= (RNEW(J)-ROLD(J))/DELT + (ROLD(J+1)-ROLD(J-1))
& /2/DELZ
IF (K .EQ. 1) THEN
CONST1= (1-K*DELY)/(1.0-ROLD(J))
RHS(L) = RHS(L) - (CONST1*CONST3*DTY-F(I)*CONST2)
& *FL(I,J)
END IF
ELSE
IF (J .EQ. JJ) THEN
CONST2= DTY2/(1.0-ROLD(J))**2
CONST3= (RNEW(J)-ROLD(J))/DELT + (ROLD(J)-ROLD(J-1))
& /DELZ
IF (K .EQ. 1) THEN
CONST1= (1.0-K*DELY)/(1.0-ROLD(J))
RHS(L) = RHS(L) -(CONST1*CONST3*DTY-F(I)*CONST2)*FL(I,J)
END IF
END IF
END IF
END IF
13 CONTINUE
12 CONTINUE
RETURN
END

C
C*****
C SUBROUTINE MOVING() *
C *
C CALCULATE THE NEW BOUNDARY POSITION BASED ON THE EQUATION *
C *
C *****

```

```

C
C   SUBROUTINE MOVING(DRDT,ROLD,RNEW,GNEW,GOLD)
C
C   COMMON /CONC/ CNEW(4,100)
C   COMMON /CONST1/ JJ, KK, N, F(4), H(4), B(4)
C   COMMON /DIFF/ DELT, DELY, DTY2, DTY, DTZ, DELZ
C   REAL   ROLD(10), DRDT(10), GNEW(4), GOLD(4), F, H, B, RNEW(10)
C
C   DO 1 J=1, JJ
C   DRDT(J)=0.0
C   M=(J-1)*KK+1
C   DO 2 I=1, N
C   DRDT(J)=DRDT(J)+F(I)*(H(I)*GOLD(I)-B(I))*
&      (CNEW(I,M)-1.0)/(1-ROLD(J))/DELY
2   CONTINUE
C   RNEW(J)=ROLD(J)+DRDT(J)*DELT
1   CONTINUE
C   RETURN
C   END

C
C *****
C
C SUBROUTINE COMNEW()
C
C   CALCULATE THE NEW COMPOSITION BASED ON THE EQUATION
C *****
C
C   SUBROUTINE COMNEW(GNEW, GOLD, DRDT, ROLD, DGDT, CASE)
C
C
C   COMMON /CONST1/ JJ, KK, N, F(4), H(4), B(4)
C   COMMON /CONC/ CNEW(4,100)
C   COMMON /DIFF/ DELT, DELY, DTY2, DTY, DTZ, DELZ
C   REAL DRDT(10), ROLD(10), DGDT(4), GNEW(4), GOLD(4)
C   LOGICAL CASE
C
C
C   SUMG=0
C   ICOUNT=0
C   N1=N-1
C   J=INT((1+JJ)/2)
C   M=J*KK+1
C   DO 30 I=1, N1
C   DGDT(I) = 1/ROLD(J)*(F(I)*(H(I)*GOLD(I)-B(I))/(1-ROLD(J))
1   *(CNEW(I,M)-1.0)/DELY - GOLD(I)*DRDT(J))
C   IF (I .LT. N) THEN
C   GNEW(I)=GOLD(I)+DGDT(I)*DELT
C   END IF
30  CONTINUE

```

C
C

```

IF (GNEW(1) .GE. 0 .AND. GNEW(1) .LE. 1.0) THEN
DO 40 I=2,N1
  IF (GNEW(I) .LT. 0) THEN
    PRINT*, 'NEGATIVE MASS FRACTION IS NOT ALLOWED'
    CASE = .FALSE.
    RETURN
  ELSE
    ICOUNT=ICOUNT+1
  END IF
40 CONTINUE
  ELSE
    IF (GNEW(1) .LT. 0) THEN
      PRINT *, 'GNEW(1) = ', GNEW(1)
      PRINT *, 'NEGATIVE RESULT IS WRONG'
      CASE=.FALSE.
      RETURN
    ELSE
      IF (GNEW(1) .GT. 1.0) THEN
        PRINT *, 'MASS FRACTION GREATER THAN 1.0 IS INVALID'
        CASE=.FALSE.
        RETURN
      END IF
    END IF
  END IF

C
C
  IF ((ICOUNT+1) .EQ. N1) THEN
    DO 7 I=1,N1
      SUMG=SUMG+GNEW(I)
7 CONTINUE
    GNEW(N)=1.0-SUMG
  ELSE
    CASE = .FALSE.
    RETURN
  END IF

C
RETURN
END

```

VITA ²

Yuh-Ling Chen

Candidate for the Degree of
Doctor of Philosophy

Thesis: ON THE USE OF TIME-DEPENDENT THROUGHFALL CHEMISTRY
DATA TO CALCULATE THE DRY DEPOSITION FLUX

Major Field: Chemical Engineering

Biographical:

Personal Data: Born in Taipei, Taiwan, Republic of
China, August 21, 1959, the daughter of Wen-Ru and
In-Hua Chen.

Education: Graduated from Taipei Chung-Sun Girls' High
School, Taipei, Taiwan, in June, 1976; received
Bachelor of Science Degree in Chemical Engineering
from National Cheng-Kung University in June, 1980;
received Master of Science Degree from University
of Iowa in December, 1984; completed requirements
for the Doctor of Philosophy Degree at Oklahoma
State University in December, 1988. Membership in
professional societies includes Omega Chi Epsilon
and Air Pollution Control Association.

Professional Experience: Piping Design Engineer,
Piping Design Engineering Department, Kaohsiung
Refinery, Chinese Petroleum Corporation, December,
1980 to June, 1982; Teaching Assistant, Chemical
and Material Engineering Department, University of
Iowa, January, 1983 to July, 1984; Research
Assistant, School of Chemical Engineering,
Oklahoma State University, August, 1985, to June,
1986; Teaching Assistant, School of Chemical
Engineering, Oklahoma State University, August,
1986 to present.